

## **INFORMATION TO USERS**

**This manuscript has been reproduced from the microfilm master. UMI films the text directly from the original or copy submitted. Thus, some thesis and dissertation copies are in typewriter face, while others may be from any type of computer printer.**

**The quality of this reproduction is dependent upon the quality of the copy submitted. Broken or indistinct print, colored or poor quality illustrations and photographs, print bleedthrough, substandard margins, and improper alignment can adversely affect reproduction.**

**In the unlikely event that the author did not send UMI a complete manuscript and there are missing pages, these will be noted. Also, if unauthorized copyright material had to be removed, a note will indicate the deletion.**

**Oversize materials (e.g., maps, drawings, charts) are reproduced by sectioning the original, beginning at the upper left-hand corner and continuing from left to right in equal sections with small overlaps.**

**ProQuest Information and Learning  
300 North Zeeb Road, Ann Arbor, MI 48106-1346 USA  
800-521-0600**

**UMI<sup>®</sup>**





**Université d'Ottawa • University of Ottawa**



**THE TREATMENT OF BILGE WATER USING A MF/UF HYBRID  
MEMBRANE SYSTEM: MEMBRANE FOULING, CLEANING AND THE  
EFFECT OF CONSTITUENTS ON FLUX DECLINE**

**By:**

**Hui Peng**

**A thesis submitted to the faculty of Graduate and Postdoctoral Studies  
in partial fulfillment of the requirements for the degree of  
MASTER OF APPLIED SCIENCE  
in the Department of Chemical Engineering  
University of Ottawa**

**June 20, 2002**



**National Library  
of Canada**

**Acquisitions and  
Bibliographic Services**

**395 Wellington Street  
Ottawa ON K1A 0N4  
Canada**

**Bibliothèque nationale  
du Canada**

**Acquisitions et  
services bibliographiques**

**395, rue Wellington  
Ottawa ON K1A 0N4  
Canada**

*Your file Votre référence*

*Our file Notre référence*

**The author has granted a non-exclusive licence allowing the National Library of Canada to reproduce, loan, distribute or sell copies of this thesis in microform, paper or electronic formats.**

**The author retains ownership of the copyright in this thesis. Neither the thesis nor substantial extracts from it may be printed or otherwise reproduced without the author's permission.**

**L'auteur a accordé une licence non exclusive permettant à la Bibliothèque nationale du Canada de reproduire, prêter, distribuer ou vendre des copies de cette thèse sous la forme de microfiche/film, de reproduction sur papier ou sur format électronique.**

**L'auteur conserve la propriété du droit d'auteur qui protège cette thèse. Ni la thèse ni des extraits substantiels de celle-ci ne doivent être imprimés ou autrement reproduits sans son autorisation.**

0-612-76623-3

**Canada**

## **ABSTRACT**

**Bilge water accumulates in recesses and bilges onboard ships. Depending on the type of design and age, ships can generate large volumes of bilge water. This wastewater is a mixture of fresh water and seawater containing various contaminants. Typical contaminants may include fuels, oils, greases, detergents, solvents, rusts, paints, insulation material and a wide variety of other substances. Bilge water is a very challenging wastewater to treat due to large variations in production rates and the complex nature of the wastes in solution. Bilge water contains a considerable amount of emulsified and free oil in solution. These oils are or can become surface active and cause serious damage to aquatic life. Ever increasing regulations are being imposed on the treatment and release of bilge water to the environment.**

**Membrane based Oily Water Separators (OWS) are being increasingly used throughout the world for the treatment of oily wastewater. This work focused on two areas of study: 1) Effects of selected components found in bilge water on membrane performance, and 2) Pilot scale testing using a Microfiltration/Ultrafiltration (MF/UF) hybrid system. The studies are aimed at determining suitable membrane materials and optimum operating conditions such as trans-membrane pressure (TMP) and backflushing for permeate flux enhancement.**

**In the first part of this study, the effect of selected components found in bilge water was studied using synthetic polymeric membranes of various pore sizes. Experimental results show that various components such as calcium and magnesium salts, and detergents, found in synthetic bilge water have a considerable effect on membrane performance.**

**In the second part of this study, experiments were performed to treat a synthetic bilge water mixture in a pilot scale MF/UF hybrid system. Large channel MF membranes were used as a pretreatment step and smaller pore size UF membranes were used as a final polishing step. The pilot system was equipped to perform the backflushing of the MF membranes and send permeate to the UF membranes for further treatment. Two MF**

membrane types were tested; carbon membranes (KOCH Membrane Systems, Ann Arbor, Michigan, USA) and ceramic membranes (TAMI Industries, Nyons, France). The best operating conditions to obtain maximum steady state permeate flux using permeate backflushing were determined. The best backflushing times were found to be 1% of the total filtration cycle. Backflushing pressure, trans-membrane pressure, type of membrane and different cleaning methods were also found to have considerable effect on permeate flux. It was found that backflushing of the carbon membrane was effective in increasing permeate flux while it had little effect on the ceramic membrane. Various pore size KOCH and TAMI membranes were tested. It was found that membranes with a 0.2 micron pore size are not suitable in this application due to the presence of 0.18 micron diameter particles in the synthetic bilge water mixture. TAMI Céram membranes with pore sizes below 0.07 micron had the best performance. Four different filtration mechanisms: complete blocking, intermediate blocking, pore constriction and cake filtration were used to interpret the permeate flux decline for these membranes.

In the third part of this work, oil and grease (O & G) concentration in permeate was determined using EPA Method 1664. It was found that the membranes tested had excellent oil rejection. It was also found that the oil and grease content of the feed solution did not affect permeate flux. The oil and grease content of the permeate was found to be proportional to the logarithm of the oil and grease content of the feed solution.

This work demonstrates that bilge water can be effectively treated in a MF/UF hybrid system using MF as pretreatment and UF as a post step treatment without chemical cleanings that produce wastes. By using a suitable membrane at suitable operating conditions, permeate flux can be maintained at a high level and system effectiveness can be improved.

## RÉSUMÉ

L'eau de cale s'accumule dans les cavités et dans le fond des navires. Selon leur type, conception et âge, les bateaux peuvent produire de grands volumes d'eau de cale. Cette eau usagée est un mélange d'eau douce et d'eau de mer contenant divers contaminants. Les contaminants typiques peuvent inclure des carburants, huiles, graisses, détergents, solvants, rouille, peinture, matériel isolant et une grande variété d'autres substances. L'eau de cale est une eau usagée très difficile à traiter en raison de la nature complexe des contaminants en solution de grandes variations dans les taux de production. L'eau de cale contient une quantité considérable d'émulsions et d'huiles libres en solution. Ces huiles sont ou peuvent devenir tensioactives et causer un dommage considérable à la vie aquatique. Des règlements toujours croissants sont imposés au traitement et au dégagement de l'eau de cale à l'environnement.

Des séparateurs d'eau huileuse à base de membranes sont de plus en plus utilisés dans le monde entier pour traiter ce genre de déchet. La présente étude vise à élucider certains phénomènes qui affectent la perméabilité de la membrane et l'opération d'un système membranaire. Elle comporte deux volets : 1) L'étude des effets de composants choisis que l'on trouve dans l'eau de cale sur la perméabilité des membranes. 2) Des essais à l'échelle pilote sur un système hybride microfiltration/ultrafiltration (MF/UF) pour le traitement de cette eau usagée. Les études visent à déterminer les matériaux appropriés pour la membrane et les conditions de fonctionnement optimales telles que la pression trans-membranaire et le lavage à contre-courant pour optimiser son flux.

Dans la première partie de cette étude, l'effet des composants choisis trouvés dans l'eau de cale a été étudié à l'aide des membranes polymères synthétiques de diverses tailles de pore. Les résultats expérimentaux prouvent que les composants tels que les sels de calcium et de magnésium, et les détergents, trouvés dans l'eau synthétique de cale ont un effet considérable sur le flux du perméat.

Dans la deuxième partie de cette étude, des essais ont été entrepris pour traiter un mélange synthétique d'eau de cale dans un système pilote hybride MF/UF. Des membranes micro filtrantes, à canaux multiples, ont été utilisées en prétraitement et des membranes ultra filtrantes à fibres creuses en étape de polissage final. Le système pilote était équipé pour permettre le lavage à contre-courant des membranes MF avec une partie du perméat de l'UF. Deux types de membranes de MF ont été examinés; membranes de carbone (systèmes de membrane de KOCH, Ann Arbor, Michigan, Etats-Unis) et membranes en céramique (industries de TAMI, Nyons, France). Les meilleurs modes de fonctionnement pour obtenir une production maximale de perméat ont été déterminés. Les meilleurs temps de lavage à contre-courant se sont avérés être 1% du cycle de filtration. La pression utilisée pour laver les membranes à contre-courant, la pression trans-membranaire (TMP), le type de membrane et les différentes méthodes de nettoyage ont un effet considérable sur le flux de perméat. On a constaté que le lavage à contre-courant de la membrane de carbone était efficace alors qu'il avait peu d'effet sur la membrane céramique.

L'effet de la grosseur des pores de la membrane a été examiné. On a constaté que les membranes ayant une taille de pore de 0.2 microns ne sont pas appropriées pour cette application due à la présence des particules de 0.18 microns de diamètre dans le mélange synthétique d'eau de cale. Les membranes de TAMI Céram avec des tailles de pore sous les 0.07 microns ont eu la meilleure performance. Quatre mécanismes de filtration: blocage complet, blocage intermédiaire, constriction des pores et la filtration de gâteau ont été employés pour interpréter le déclin du flux de perméat.

Dans la troisième partie de ces travaux, la concentration totale d'huile et de graisse dans le perméat a été déterminée par la méthode 1664 de l'EPA. Toutes les membranes UF et quelques membranes MF ont un excellent rejet d'huile et de graisse. La teneur en huiles et graisses de la solution d'alimentation n'a pas affecté le flux de perméat. La teneur en huile et graisse du perméat c'est cependant avéré proportionnelle a la concentration en huile et graisse de la solution d'alimentation.

**Ce travail démontre que l'eau de cale peut être traitée de façon efficace dans un système hybride MF/UF sans nettoyages chimiques qui produisent des eaux de lavage que l'on doit conserver à bord d'un navire. En utilisant une membrane céramique dont la taille des pores est inférieure à 70 nm, sous des conditions de fonctionnement appropriées, on peut produire de façon efficace une eau traitée qui surpasse les normes environnementales existantes.**

## **ACKNOWLEDGEMENTS**

I wish to express my sincere thanks to my supervisor, Dr. A.Y.Tremblay, for his guidance in the completion of this thesis. To Dr. Tremblay I thank you for your endless help and support throughout this work. Without your patience and day-to-day supervision, this study would not be possible. I will always remember and appreciate your generous assistance.

I am grateful to Mr. Dwight Vienot of the Defence Research Establishment Atlantic (DREA). Mr. Dwight's involvement in this project ensured that I received financial support to complete my Masters program.

I would like to thank Louis Tremblay, Gérard Nina and Franco Ziroldo for their assistance in the lab. I also wish to thank the Department's administrative and support staff for their help.

Finally, I wish to thank my wife, Huaiwen Chen, and our daughter, Xiaoshan Peng, for their love, support, encouragement and understanding throughout my studies here.

## NOMENCLATURE

$A$	= surface area of the membrane, $m^2$
$A_0$	= initial active filter membrane surface area, $m^2$
$c$	= concentration of feed, $kg/m^3$
$C_b$	= bulk concentration, $kg/m^3$
$d_p$	= mean diameter of the particles, m
$J_0$	= initial filtrate flux through the clean membrane, $L/ m^2/h$
$J_V$	= filtrate flux, $L/ m^2/h$
$J^*$	= effective velocity associated with the back mass transfer, $L/ m^2/h$
$m_{cake}$	= cake mass, kg
$N$	= pore density, $kg/m^3$
$N_0$	= initial pore density, $kg/m^3$
$K_{block}$	= constant in complete blocking model, $h^{-1}$
$K_{cake}$	= constant in cake filtration model, $h^{-1}$
$K_{constriction}$	= constant in pore constriction model, $h^{-1}$
$K_{inter}$	= constant in intermediate blocking model, $h^{-1}$
$R_c$	= hydraulic resistance of the particle cake, $m^{-1}$
$R_m$	= hydraulic resistance of the membrane, $m^{-1}$
$R_{inter}$	= filter resistance in intermediate blocking model, $m^{-1}$
$r_p$	= pore radius, m
$R_{total}$	= total resistance, $m^{-1}$
$t$	= filtration time, h
$V$	= cumulative filtration volume, $m^3$
$\Delta P$	= trans-membrane pressure, psig
$\sigma_0$	= membrane osmotic reflection coefficient
$\sigma_{inter}$	= blocked area per unit filtrate volume, $m^2/ m^3$
$\delta_m$	= cake thickness, m

$\Delta\Pi$	= osmotic pressure difference across the membrane, Pa (psig)
$\mu$	= viscosity of the solution, Pa s
$\alpha_{block}$	= pore blockage efficiency
$\alpha_{cake}$	= specific cake resistance, m/Kg
$\alpha_{pore}$	= pore constriction efficiency
$\varepsilon$	= void volume of the cake, m <sup>3</sup>
$\rho_p$	= density of the particles, kg/m <sup>3</sup>

## ACRONYMS

<b>BF</b>	= <b>Backflushing</b>
<b>BSA</b>	= <b>Bovine Serum Albumin</b>
<b>CSA</b>	= <b>Canada Shipping Act</b>
<b>DLS</b>	= <b>Dispersive Light Scattering</b>
<b>DND</b>	= <b>(Canadian) Department of National Defence</b>
<b>DREA</b>	= <b>Defense Research Establishment Atlantic</b>
<b>HP</b>	= <b>Horsepower</b>
<b>HSW</b>	= <b>Half Seawater</b>
<b>HEM</b>	= <b>Hexane Extractable Materials</b>
<b>ID</b>	= <b>Inside Diameter</b>
<b>LSI</b>	= <b>Langelier Saturation Index</b>
<b>MF</b>	= <b>Microfiltration</b>
<b>MSDS</b>	= <b>Material Safety Data Sheet</b>
<b>MWCO</b>	= <b>Molecular Weight Cut-Off</b>
<b>NATO</b>	= <b>North Atlantic Treaty Organisation</b>
<b>NF</b>	= <b>Nanofiltration</b>
<b>OD</b>	= <b>Outside Diameter</b>
<b>O &amp; G</b>	= <b>Oil and Grease</b>
<b>OWS</b>	= <b>Oily Water Separator</b>
<b>PAN</b>	= <b>Polyacrylonitrile</b>
<b>PVC</b>	= <b>Polyvinyl chloride</b>
<b>PVDF</b>	= <b>Polyvinylidene difluoride</b>
<b>ppm</b>	= <b>parts per million</b>
<b>RO</b>	= <b>Reverse Osmosis</b>
<b>RTD</b>	= <b>Resistance Temperature Detector</b>
<b>SW</b>	= <b>Seawater</b>
<b>TDS</b>	= <b>Total Dissolved Solids</b>
<b>TMP</b>	= <b>Transmembrane Pressure</b>
<b>TOG</b>	= <b>Total Oils and Greases</b>

**TSS** = **Total Suspended Solids**

**UF** = **Ultrafiltration**

## TABLE OF CONTENTS

<b>Abstract</b>		i
<b>Résumé</b>		iii
<b>Acknowledgements</b>		vi
<b>Nomenclature</b>		vii
<b>Acronyms</b>		ix
<b>Table of Contents</b>		xi
<b>List of Tables</b>		xiv
<b>List of Figures</b>		xviii
<b>1. Introduction</b>		1
1.1 Background		1
1.2 Objectives		3
<b>2. Literature review</b>		4
2.1 Conventional oily wastewater treatment methods		4
2.2 Membrane technology		5
2.2.1 Membrane materials		5
2.2.2 Module and process configurations		6
2.2.3 Fouling and its control		8
2.2.4 Research on bilge water treatment		11
<b>3. Theory</b>		13
3.1 Membrane filtration mechanisms and models		13
3.1.1 Complete blocking		13
3.1.2 Intermediate blocking		14
3.1.3 Pore constriction		15
3.1.4 Cake filtration		15
3.1.5 Cake resistance		17
3.2 Backflushing		20
<b>4. Experimental methodology</b>		22
4.1 Bilge water preparation		22
4.2 Flat sheet and hollow fiber UF membrane tests		24

4.2.1	Materials	24
4.2.2	Experimental set-up	25
4.2.3	Experimental procedure and analytical methods	28
4.3	MF/UF hybrid system tests	30
4.3.1	Materials	30
4.3.2	Experimental set-up	32
4.3.3	Experimental procedure and analytical methods	34
4.4	Oil and grease determination	36
<b>5.</b>	<b>Results and discussion</b>	<b>37</b>
5.1	Effect of bilge water components	37
5.1.1	Effect of carbonate on flat sheet membranes	37
5.1.2	Effect of CLEANBREAK and salts on flat sheet membranes	40
5.1.3	Effect of CLEANBREAK	46
5.1.3.1	Batch concentration run using hollow fiber membrane	46
5.1.3.2	Effect of CLEANBREAK concentration on hollow fiber membrane	47
5.1.3.3	Effect of CLEANBREAK and TMP on flat sheet Membranes	50
5.2	Pilot scale testing of operating parameters	52
5.2.1	Effect of trans-membrane pressure (TMP)	52
5.2.1.1	Effect of TMP on KOCH Carbo-cor membrane	52
5.2.1.2	Effect of TMP on the TAMI Céram multilumen membranes	56
5.2.2	Effect of backflushing on tubular membranes	58
5.2.2.1	Backflushing frequency	59
5.2.2.2	Backflushing pressure	61
5.2.2.3	Type of membrane	63
5.2.3	Membrane cleaning	65
5.2.3.1	Chemical cleaning	65
5.2.3.2	Non-chemical cleaning	66

5.3	Pore size of tubular membranes	71
5.3.1	KOCH Carbo-cor tubular membranes	71
5.3.2	TAMI Céram tubular membranes	73
5.4	Modeling and specific cake resistance	74
5.4.1	Modeling of filtration mechanisms	74
5.4.2	Specific cake resistance	84
5.5	Oil and grease content of the permeate	85
5.6	Effect of feed concentration on permeate flux and oil retention	87
<b>6.</b>	<b>Conclusions</b>	<b>90</b>
6.1	Effect of bilge water components	90
6.2	Effect of membrane pore size	90
6.3	Membrane cleaning	90
6.4	Effect of transmembrane pressure	91
6.5	Effect of backflushing	91
6.6	Cake vs. blocking	91
6.7	Oil and grease concentration	91
<b>7.</b>	<b>Recommendations</b>	<b>92</b>
<b>8.</b>	<b>References</b>	<b>93</b>
<b>Appendices</b>		
Appendix A - Langelier Saturation Index Calculation for Half Seawater Solution		
Appendix B - Raw Data and Sample Calculation of Flat Sheet Tests		
Appendix C - Raw Data and Sample Calculation of the KOCH XM50 Hollow Fiber Membrane Tests		
Appendix D - Raw Data and Sample Calculation of KOCH Carbo-cor Membranes Testing		
Appendix E - Calculation of Specific Cake Resistance for the KOCH Carbo-cor Membranes		
Appendix F - Oil and Grease Determination Using EPA Method 1664: Procedure and Standards		

## LIST OF TABLES

<u>Table Number</u>	<u>Table Title</u>	<u>Page Number</u>
3.1	Four different membrane filtration models	16
4.1	Concentration of various salts found in synthetic bilge water	23
4.2	Characteristics of membrane used in flat sheet tests	24
4.3	KOCH XM50 Hollow Fiber Membrane Characteristics	25
4.4	KOCH Carbo-cor Membrane Characteristics	30
4.5	TAMI Céram Membrane Characteristics	31
5.1	Langelier Saturation Index for seawater and a 50:50 mixture of fresh seawater	37
5.2	Salt make-up of feed solutions in flat sheet membrane testing	41
5.3	Specific cake resistance for different CLEANBREAK concentration run	50
5.4	Operating conditions and sum of square residual for the analysis of filtration mechanism described in Table 3.1	76
5.5	Operating conditions and different filtration constants for the analysis of various filtration mechanism described in Table 3.1	77
5.6	Calculated values of specific cake resistance $\alpha_{cake}$ and membrane resistance $R_m$ for various KOCH Carbo-cor and TAMI Céram membranes	84
5.7	Oil and grease recovery and rejection of the KOCH Carbo-cor 1.4 micron membrane in a MF/UF hybrid system	86
5.8	Oil and grease concentration in the permeate of various TAMI membranes after 1 hour in a permeation run at 4 g/l O & G feed concentration	88
A-1	Relationship between Langelier Saturation Index (LSI) and scale potential	A-1
B-1	QW, P707 & QX Membrane Run at 10 psig Experimental Data, Dated July 5, 2001	B-1

B-2	QW, P707 & QX Membrane Run at 20 psig Experimental Data, Dated July 6, 2001	B-3
B-3	QW, P707 & QX Membrane Run at 30 psig Experimental Data, Dated July 6, 2001	B-4
B-4	QW, P707 & QX Membrane Run at 30 psig Experimental Data, Dated July 6, 2001	B-5
B-5	GN, M100 & QW Membrane Experimental Data, Dated June 2-7, 2001	B-6
B-6	GN, M100 & QW Membrane Experimental Data, Dated May 26 - June1, 2001	B-7
B-7	GN, M100 & QW Membrane Experimental Data, Dated May 07-17, 2001	B-8
B-8	QW, P707 & QX Membrane Experimental Data, Dated June 16-18, 2001	B-9
B-9	QW, P707 & QX Membrane Experimental Data, Dated June 18-19, 2001	B-10
B-10	QW, P707 & QX Membrane Experimental Data, Dated June 19-20, 2001	B-11
B-11	QW, P707 & QX Membrane Experimental Data, Dated June 20-21, 2001	B-12
B-12	QW, P707 & QX Membrane Experimental Data, Dated June 21, 2001	B-13
B-13	GN, M100 & QW Membrane Experimental Data, Dated June 21-23, 2001	B-14
B-14	GN, M100 & QW Membrane Experimental Data, Dated June 23-24, 2001	B-15
B-15	GN, M100 & QW Membrane Experimental Data, Dated June 24-25, 2001	B-15
B-16	GN, M100 & QW Membrane Experimental Data, Dated June 25-26, 2001	B-16

<b>B-17</b>	<b>GN, M100 &amp; QW Membrane Experimental Data, Dated June 26, 2001</b>	<b>B-16</b>
<b>C-1</b>	<b>KOCH XM50 Hollow Fiber Membrane Experimental Data, Dated July 2-5, 2001</b>	<b>C-1</b>
<b>C-2</b>	<b>KOCH XM50 Hollow Fiber Membrane Experimental Data, Dated July 16, 2001</b>	<b>C-3</b>
<b>C-3</b>	<b>KOCH XM50 Hollow Fiber Membrane Experimental Data, Dated July 17, 2001</b>	<b>C-3</b>
<b>C-4</b>	<b>KOCH XM50 Hollow Fiber Membrane Experimental Data, Dated July 18, 2001</b>	<b>C-4</b>
<b>C-5</b>	<b>KOCH XM50 Hollow Fiber Membrane Experimental Data, Dated July 19, 2001</b>	<b>C-4</b>
<b>C-6</b>	<b>KOCH XM50 Hollow Fiber Membrane Experimental Data, Dated August 28, 2001</b>	<b>C-4</b>
<b>D-1</b>	<b>KOCH Carbo-cor 0.05 <math>\mu\text{m}</math> Experimental Data, Dated March 28, 2001</b>	<b>D-1</b>
<b>D-2</b>	<b>KOCH Carbo-cor 0.1 <math>\mu\text{m}</math> Experimental Data, Dated March 21-22, 2001</b>	<b>D-2</b>
<b>D-3</b>	<b>KOCH Carbo-cor 0.1 <math>\mu\text{m}</math> Experimental Data, Dated March 22-23, 2001</b>	<b>D-3</b>
<b>D-4</b>	<b>KOCH Carbo-cor 0.1 <math>\mu\text{m}</math> Experimental Data, Dated March 24-25, 2001</b>	<b>D-4</b>
<b>D-5</b>	<b>KOCH Carbo-cor 0.1 <math>\mu\text{m}</math> Experimental Data, Dated March 25-26, 2001</b>	<b>D-5</b>
<b>D-6</b>	<b>KOCH Carbo-cor 0.1 <math>\mu\text{m}</math> Experimental Data, Dated March 26-27, 2001</b>	<b>D-6</b>
<b>D-7</b>	<b>KOCH Carbo-cor 0.2 <math>\mu\text{m}</math> Experimental Data, Dated March 15-16, 2001</b>	<b>D-7</b>
<b>D-8</b>	<b>KOCH Carbo-cor 0.5 <math>\mu\text{m}</math> Experimental Data, Dated March 16-19, 2001</b>	<b>D-8</b>

D-9	KOCH Carbo-cor 0.8 $\mu\text{m}$ Experimental Data, Dated March 31, 2001	D-9
D-10	KOCH Carbo-cor 0.05 $\mu\text{m}$ Experimental Raw Data, Dated March 28, 2001	D-10
D-11	Permeate Tank Level Calibration Data, Dated March 05, 2001	D-11
E-1	KOCH Carbo-cor 0.05 $\mu\text{m}$ Experimental Data, dated August 21-25, 2001	E-1
E-2	Values of $Kp/2$ and $1/q_0$ determined from $t/V$ vs. $V$ plots for the KOCH Carbo-cor 0.05 micron membrane	E-4
F-1	Actual recovery values of different concentration Hexadecane and Stearic acid in 1 L of standard	F-2

## LIST OF FIGURES

<u>Figure Number</u>	<u>Figure Title</u>	<u>Page Number</u>
3.1	Schematic representation of the backflushing technique in crossflow filtration	21
4.1	Flowchart of three-cell UF membrane experimental set-up	27
4.2	Flow diagram of the MF/UF hybrid system	33
5.1	Plot of Flux vs. Time for the GN membrane (pore radius 3.7 nm, MWCO 10kD, operating pressure 50 psig, 25 °C)	39
5.2	Plot of Flux vs. Time for the M100 membrane (pore radius 5.2nm, MWCO 20kD, operating pressure 50 psig, 25 °C)	39
5.3	Plot of Flux vs. Time for the QW membrane (pore radius 6.4 nm, MWCO 30kD, operating pressure 50 psig, 25 °C)	40
5.4	Plot of Flux vs. Time for the QW, P707 & QX membranes (30psig, 25°C)	43
5.5	Plot of Flux vs. Time for the GN, M100 & QW membranes (50 psig, 25°C)	44
5.6	Plot of Flux vs. Time for the QW membrane at 30 and 50 psig operating pressure (25°C)	45
5.7	Plot of Flux vs. Time for KOCH XM50 membrane	47
5.8	Plot of Flux vs. Time for KOCH XM50 hollow fiber membrane (20 psig, 25°C)	47
5.9	Data from Figure 5.8 plotted as the Ratio of the actual flux/initial flux for the KOCH XM50 hollow fiber membrane (20 psig, 25°C)	48
5.10	Plot of specific cake resistance vs. CLEANBREAK concentration for the KOCH XM50 membrane (20 psig, 25°C)	50
5.11	Effect of trans-membrane pressure on steady-state flux for the P707, QW and QX membranes (25°C)	51

5.12	Flux vs. time for the larger pore size membranes as a function of transmembrane pressure (25°C)	52
5.13	Plot of Flux vs. Time for the KOCH Carbo-Cor 0.05 micron membrane at different TMP (25°C)	53
5.14	Plot of Flux vs. Time for the KOCH Carbo-Cor 0.1 micron membrane at different TMP (25°C)	54
5.15	Plot of Flux vs. Time for the KOCH Carbo-Cor 0.5 micron membrane at different TMP (25°C)	54
5.16	Plot of Flux vs. Time for the KOCH Carbo-Cor 0.8 micron membrane at TMP=10psig (25°C)	55
5.17	Plot of Flux vs. Time for the KOCH Carbo-Cor 1.4 micron membrane at different TMP (25°C)	55
5.18	Plot of flux vs. time for the TAMI 50 kD, 150 kD, 300 kD and 70nm membranes running at different TMP (35°C)	57
5.19	Plot of flux vs. time for the TAMI 0.8 micron membrane with different TMP (Backflushing 3secs/5min at 35 psi, 35°C)	57
5.20	Plot of flux vs. time for the TAMI 1.4 micron membrane with different TMP	58
5.21	Permeate production/m <sup>2</sup> /day vs. membrane pore diameter	59
5.22	Plot of flux vs. time for the KOCH Carbo-cor 1.4 micron membrane with different backflushing time (TMP=5psig, 35°C, backflushing pressure 35 psig)	60
5.23	Plot of flux vs. time for the KOCH Carbo-cor 0.8 micron membrane with different backflushing pressure (TMP=5psig, 25°, BT 297-3)	62
5.24	Plot of flux vs. time for the KOCH Carbo-cor 1.4 micron membrane with different backflushing pressure (TMP=5 psig, 25°C, BT 294-6)	62

5.25	Plot of flux vs. time for the KOCH Carbo-cor 1.4 micron and TAMI Céram 1.4 micron membrane with different TMPs (Backflushing 3secs/5min at 35 psig, 35°C)	63
5.26	Different support structure of the TAMI and KOCH membranes	64
5.27	Plot of Flux vs. Time for the KOCH Carbo-cor 0.1 micron membrane after cleaning (TMP=25 psig, 25°C)	66
5.28	Plot of permeate production vs. regeneration temperature for the KOCH Carbo-cor 1.4 micron membrane	67
5.29	Plot of permeate production vs. regeneration temperature including the runs with steam cleaning	68
5.30	Plot of the measured permeate flux vs. time in days	70
5.31	Plot of permeate flux vs. time for various KOCH Carbo-cor tubular membranes. (Operating pressure 35 psig, 25°C)	71
5.32	Particle size distribution for used oil	73
5.33	Plot of steady-state permeate flux vs. membrane pore size for the various TAMI and KOCH Carbo-cor membranes	74
5.34	Plot of flux vs. time for the KOCH Carbo-cor 0.05 micron membrane (TMP=5psig, 35°C)	78
5.35	Plot of flux vs. time for the KOCH Carbo-cor 0.1 micron membrane (TMP=5psig, 35°C)	78
5.36	Plot of flux vs. time for the KOCH Carbo-cor 0.2 micron membrane (TMP=35psig, 35°C)	79
5.37	Plot of flux vs. time for the KOCH Carbo-cor 0.5 micron membrane (TMP=10psig, 35°C)	79
5.38	Plot of flux vs. time for the KOCH Carbo-cor 0.8 micron membrane (TMP=10psig, 35°C)	80
5.39	Plot of flux vs. time for the KOCH Carbo-cor 1.4micron membrane (TMP=10psig, 35°C)	80
5.40	Plot of flux vs. time for the TAMI 50kD membrane (TMP=7.34psig, 35°C)	81

5.41	Plot of flux vs. time for the TAMI 150kD membrane (TMP=15psig, 35°C)	81
5.42	Plot of flux vs. time for the TAMI 300kD membrane (TMP=7.34psig, 35°C)	82
5.43	Plot of flux vs. time for the TAMI 70nm membrane (TMP=7.34psig, 35°C)	82
5.44	Plot of flux vs. time for the TAMI 0.8 micron membrane (TMP=15psig, 35°C)	83
5.45	Plot of flux vs. time for the TAMI 1.4 micron membrane (TMP=5psig, 35°C)	83
5.46	Plot of O & G concentration vs. membrane pore radius for the TAMI membranes	86
5.47	Plot of actual flux vs. O & G concentration in the feed loop for the TAMI membranes with different MWCOs. Operating temperature 35°C. TMP=1 barg (14.67 psig)	87
5.48	Plot of the O&G concentration in the permeate vs. the concentration of O & G in the feed solution. Operating temperature 35°C. TMP= 1 barg (14.67 psig)	89
D-1	Plot of Permeate tank level reading vs. Permeate volume	D-12
E-1	Plot of t/V vs. V for the KOCH Carbo-cor 0.05 micron membrane operating at TMP= 5psig	E-3
E-2	Plot of t/V vs. V for the KOCH Carbo-cor 0.05 micron membrane operating at TMP= 10psig	E-3
E-3	Plot of t/V vs. V for the KOCH Carbo-cor 0.05 micron membrane operating at TMP= 15psig	E-4
E-4	Plot of t/V vs. V for the KOCH Carbo-cor 0.05 micron membrane operating at TMP= 25psig	E-4
F-1	Calibration curve of n-Hexane liquid-liquid extraction for the determination of oil and grease	F-2

# **1. INTRODUCTION**

## **1.1 Background**

One of marine industry's primary environmental concern is the overboard discharge of liquid wastes. A major source of overboard discharge is bilge water, a wastewater that accumulates in the lowest internal part of a ship. Bilge water is an oily wastewater composed of a complex "cocktail" of mechanical and chemical emulsions, and contaminants. This oily wastewater differs from those found in the petrochemical and automotive industries or in domestic sewage operations. Bilge water is a mixture of fresh and seawater (SW). It contains a variety of salts and is very corrosive. Therefore, it is more appropriate to refer to bilge water as an oily brine. Bilge oil characteristics and generation rate depend on the type of ship and its operation mode (Bhattacharyya et al., 1979). Typical contaminants may include fuels, oils, detergents, greases, solvents, rusts, paints, insulation material and a wide variety of other substances. The varied nature and composition of bilge water poses a more difficult separation problem than the treatment of conventional oil in water emulsions.

In recent years, considerable attention has been focused on the discharge of oily wastewaters from ships. The discharge of oily wastewater must meet ever increasing waste-disposal regulations imposed by local, national and international authorities. Recently shipping companies have been severely fined for the release of this wastewater to the environment. Currently, overboard discharge regulations limit the total content of oil and grease to be no greater than 100 parts per million (ppm) oil beyond 12 nautical miles off shore, 15 ppm oil within 12 nautical miles off shore, and 5 ppm within coastal waters (Transport Canada, 2001).

There are two common strategies to manage the disposal of bilge water:

- i) Storing bilge water onboard a ship for on-shore treatment, analysis and disposal.
- ii) Treating bilge water onboard by a volume reduction technique, discharging treated effluent to sea and storing the concentrate for further treatment on-shore.

The first method limits the time a ship can spend at sea. The second method is preferable since storage space is limited onboard a ship. However, several considerations must be taken into account in selecting this method, such as; the proper treatment of the bilge water before discharge, the substantial volume reductions needed, the complexity of the technology and system automation to simplify its use.

Membrane technology in wastewater treatment has moved forward quickly in recent years because of the development of new technologies for the manufacture of membranes. Membrane ultrafiltration (UF) has been identified as a key technology in the treatment of oily wastewaters (Zeman and Zydney, 1996). Microfiltration (MF) membranes with a pore size of  $0.1\mu\text{m}$  were found to be effective in the separation of oily wastewaters and the recovery of surfactant in the feed (Cheryan and Rajagopalan, 1998). Several navies throughout the world are installing membrane based Oily Water Separators (OWS) to treat bilge waters. These systems are increasingly demonstrating the efficacy of this technology in this application.

Membrane fouling is present in most membrane applications. The key consideration in a membrane based treatment system is to maintain permeate flux by reducing fouling. The presence of excessive fouling in a system causes flux reductions and increases the labour associated with the operation of the system due to frequent filter changes and cleaning. Operating costs can be reduced by proper system design which reduces fouling and the control of operating parameters in the system.

Many problems related to the long-term efficacy of the membranes and issues related to the proper sizing of channels (lumens) within membrane modules remain. Therefore, a low-maintenance, long-lifetime and cost-effective bilge water treatment system, which can comply with stringent waste-disposal regulations needs to be studied and further developed.

## **1.2 Objectives**

In practice, membrane fouling can be reduced and the overall efficacy of membrane based oily water separators improved by proper membrane selection, system design and maintenance methods. This study will focus on the selection of membrane materials and porosity, membrane module type and operating conditions to obtain a maximum steady state permeate flux when backflushing a MF membrane with UF permeate.

A first objective was to study the effect of various components found in synthetic bilge water on permeate flux. This part of the work was performed with synthetic polymeric membranes. The major contribution of this part was the identification of the effects of components on membranes with different pore sizes.

The second objective was to design and assemble a membrane based oily bilge water treatment system and test different membranes in order to determine the most suitable membrane material and optimum operating parameters for the system. A MF/UF hybrid system was designed for the treatment of synthetic bilge water. A feed and bleed, crossflow tubular MF membrane was used as a pretreatment step. A second feed and bleed loop containing a UF hollow fiber membrane was used as a post treatment step. The MF membrane was backflushed with the UF permeate to reduce membrane fouling.

Wastewaters from membrane cleaning operations cannot be readily disposed of at sea. A third objective was to study membrane flux regeneration using different cleaning methods and to develop and validate an environmentally benign membrane cleaning method.

The fourth objective was to study the oil and grease concentration in the permeate from various commercially available membranes as a function of the molecular weight cut-off (MWCO) of the membrane. The effect of oil and grease (O & G) concentration on permeate flux and permeate concentration was also studied.

## **2. LITERATURE REVIEW**

### **2.1 Conventional oily wastewater treatment methods**

The most important consideration in oily wastewater treatment is the removal of oil and grease. Oily wastes can be grouped into three broad categories: free-floating oil, unstable oil/water emulsions, and highly stable oil/water emulsions (Cheryan, 1986). Stable oil/water emulsions are the most difficult to treat by conventional methods and the most amenable to treat by ultrafiltration (Porter, 1990). In a land based system, free oil is readily removed by mechanical gravity separation devices and unstable oil/water emulsions can be broken mechanically or chemically. In a ship-born application, the ship is in constant movement and the phase separation of sub-micron sized oil droplets suspended in water is difficult if not impossible. In some jurisdictions, phase separation agents cannot be readily added to the bilge water due to discharge regulations.

Conventional methods to treat oily wastewater have included gravity separation, de-emulsification, coagulation and flocculation. These approaches are effective in removing free oil; however, they are not effective in removing smaller oil droplets and emulsions. In land-based applications, emulsified oil in wastewater is usually pretreated chemically or physically to destabilize emulsions followed by gravity separation. Physical methods for breaking emulsions include centrifugation, heating, fiber beds, ultrafiltration, reverse osmosis and electrochemical methods (Cheryan and Rajagopalan, 1998). Centrifugation, heating and electrochemical methods all have limitations in ship-born applications while the membrane-based methods are quite amenable to integration and use onboard ships.

## **2.2 Membrane technology**

### **2.2.1 Membrane materials**

Early investigation in oily wastewater treatment using membrane separation technologies originated in the 1970s. Since then, many approaches have been conducted in this field. Membrane processes such as microfiltration and ultrafiltration have become the standard technology in oily wastewater treatment, because of their ability to remove stable emulsified oil from the wastewater. The UF and MF separation processes are based on their ability to physically remove or filter out micron and sub-micron sized particles from water. Ultrafiltration membranes are classified according to their ability to separate polydisperse solutes such as Dextran and Polyethylene glycol. They are rated according to a MWCO which is the molecular weight at which point the membrane exhibits 90% separation for a polydisperse solute. MF membranes are characterized by bubble point measurements according to the diameter of their pores (pore size). Most membrane companies recommend using membranes with molecular weight cut-offs of 20,000-50,000 Daltons for the treatment of oily wastewater (Cheryan, 1986). This can typically result in a permeate with less than 10-100 ppm of oil, unless high concentrations of a soluble surfactant or polar solvent are present (Cheryan, 1986).

Both polymeric and ceramic membrane materials are used in oily wastewater treatment. Membranes with improved oil resistance have been developed during the past two decades. Polymeric membranes are more economical than ceramic membranes but require more effort in membrane replacement and maintenance. The choice of ceramic membranes means a relatively expensive system but membrane life can extend to 10 years (Leon et al., 1992). Numerous studies have arrived at the conclusion that ceramic membranes are superior to polymeric membranes for oily water separation as they exhibited better properties such as chemical resistance, stability and wider range of pH values (Bhave, 1991).

Many works have been performed on oily wastewater treatment using different membrane materials. Pialipp et al. (1988) used polymeric membranes to investigate factors affecting both flux and rejection in the ultrafiltration of oil-water emulsions. They found that oil rejection was high (>99.9%) with less than 20ppm oil in the permeate. Hyun and Kim (1997) used ceramic microfiltration membranes synthesized by the reverse dip-drawing technique using an alumina/zirconia slurry to test oil-in-water emulsions. They concluded that the effective average pore sizes of alumina and zirconia top-layers were  $0.16\mu\text{m}$  and less than  $0.07\mu\text{m}$ , respectively; there was almost 100% removal of oil from o/w emulsion through the composite membranes. Mueller et al. (1997) used ceramic membranes to treat oily water containing various concentrations of heavy crude oil. They found that increased oil concentration in the feed decreased the steady state permeate flux while the addition of suspended solids increased the steady state permeate flux. They suggested that the suspended solids adsorb the oil, break up the oil layer, and act as a dynamic or secondary membrane which reduces fouling of the underlying primary membrane. Ting and Wu (1999) separated kerosene/water and n-dodecane/water emulsion systems using alumina anodisc membranes (Whatman, USA). The separation was found to be optimal at a trans-membrane pressure of 300 KPa and a feed rate of 6 ml/min with backflush using  $0.02\mu\text{m}$  membranes. The oil content was reduced from 2 wt% to 0.4 wt% achieving the separation factor of 5. Kong and Li (1999) investigated the separation of dilute oil-in water mixtures using flat sheet hydrophobic PVDF membranes with porosities of 0.72, 0.83 and 0.86 in an unstirred laboratory scale semi-batch experimental system operated at  $40^{\circ}\text{C}$ . They found that the percentage of oil removed could be achieved as high as 77% under normal experimental conditions.

### **2.2.2 Module and process configurations**

There are two major modes of operation in membrane filtration: dead-end and crossflow. In dead-ended filtration, the membrane is used in the traditional filtration mode where the entire feed solution is permeated through the membrane, leaving a cake at its surface. In crossflow filtration, pressure drives part of the feed through the

membrane; the remaining feed flows tangentially along the surface of the membrane. Particles moving towards the surface of the membrane can be swept away and sent back to the feed by crossflow. The advantage of this process over the traditional dead-ended filtration mode is a reduction in the accumulation of solutes and particulate matter at the surface of the membrane.

Four basic types of membrane module configurations are available: plate and frame, spiral, tubular and hollow fiber. Details of these configurations are available in many references (Matsuura, 1994; Zeman and Zydney, 1996 and Cheryan, 1986). The feed channels in the plate and frame, spiral and hollow fiber configurations are prone to plugging when feeds containing large amounts of particulate matter are treated. The tubular configuration is the most suitable for this application, due to the high concentration of suspended solids and oil in bilge water. The larger flow channels in this configuration limit the risk of channel blockage.

There are three basic process configurations used in commercial applications of crossflow ultrafiltration and microfiltration (Zeman and Zydney, 1996):

- i) **Single-pass** – In this case the operation is often run in a dead-end mode with the outlet retentate flow set equal to zero and all of the feed forced through the membrane into the permeate. It is not used extensively in most large-scale applications due to the difficulties involved in obtaining the desired permeate flow rate in a single pass.
- ii) **Batch** – The entire retentate stream is recycled back to a single large feed tank. This is probably the most common configuration for small-scale commercial operation. In this mode, higher fluxes can be obtained at the beginning of the run leading to a high average flux for the entire run.
- iii) **Feed and bleed** – Recycles only part of the retentate, with the remainder of the retentate continuously collected or fed to a subsequent processing step. This configuration is used in most large-scale commercial processes. Feed and bleed systems are often designed as multistage units which reduces membrane area requirements.

### **2.2.3 Fouling and its control**

During the treatment of wastewaters by membrane filtration processes, flux decreases as a result of concentration polarization and membrane fouling. Concentration polarization is defined as the accumulation of solute species in a solution phase near the surface of the membrane. Fouling refers to the deposition of particles, salts, colloids, etc. inside and on the surface of the membrane. Fouling is a very complex phenomenon and differs from one application to another and from one membrane to another (Mulder, 1991). Fouling consists of a number of different mechanisms, which can be classified as pore blockage, pore constriction and the formation of a dynamic cake layer on the surface of the membrane.

Approaches to reduce fouling and improve membrane performance can only be described very generally due to the complexity of fouling phenomenon. For a specific waste treatment system such as an oily bilge water treatment system, the following factors are considered to be important:

- i) Membrane material,
- ii) Module channel size and hydrodynamics,
- iii) Operating conditions, and
- iv) Membrane cleaning.

The selections of membrane material, membrane module and optimum operation conditions must be determined in a pilot or actual system. The cleaning method used for membrane regeneration is very important for a treatment system. For ship-born applications chemical cleaning must be mitigated since it will always create additional waste. Physical cleaning is preferred. Among the many available physical cleaning methods, sponge ball cleaning and ultrasonication can cause operational difficulties. The best solution to maintain flux is to periodically reverse the flow of the permeate to remove the filter cake accumulated on the surface of the membrane. This environmentally friendly cleaning method is known as backflushing and is widely used in industry.

Crossflow filtration is often helpful in slowing down membrane fouling but does not eliminate it (Bhave, 1991). Backflushing and backpulsing are effective processes to remove deposits from the surface of the membrane and improve the membrane productivity. Backflushing refers to low-frequency permeate flow reversal while backpulsing refers to high-frequency permeate flow reversal. In both processes, the trans-membrane pressure is periodically reversed. In rapid backpulsing, the reverse pressure pulses are applied for very short periods of time (typically less than 1 s) at a high frequency (typically 0.1-2 Hz). The combination of crossflow and backflushing will therefore be a more effective method for the reduction of fouling and the maintenance of flux. Many studies have focused on this technique.

Backflushing is a technically feasible and effective method in crossflow filtration for flux enhancement. Ramirez and Davis (1998) studied crossflow MF with rapid backpulsing for the treatment of aqueous clay suspensions of different concentration, as well as for a dilute crude oil-in-water dispersions. The backpulsing pressure duration (0.2 and 0.5s) and frequency (0.5, 1, 3, 5, 10, 20 and 50s) were varied for fixed values of the trans-membrane pressure (TMP) (20 psig) and crossflow velocity (2.6 m/s for clay and 3.5 m/s for oil). They reported that for clay, rapid backflushing can maintain the permeate flux at a level that is more than ten-fold over the steady-state flux in the absence of backpulsing; for oil-in-water dispersions, rapid backpulsing can increase the permeate flux by up to 25 times without any reduction in the permeate quality. Levesley and Hoare (1999) studied the effect of periodic backflushing on the microfiltration of yeast homogenate suspensions for the recovery of soluble proteins. They found that high frequency backflushing could increase the transmission of proteins during microfiltration of disrupted cell suspensions at high concentration, without significantly affecting the observed permeate flux. Up to six-fold increase in the mass flux of a target enzyme was obtained by backflushing.

Sondhi et al. (2000) conducted crossflow filtration experiments with  $\text{Cr}(\text{OH})_3$  suspension as synthetic electroplating wastewater using ceramic MF membranes of various pore sizes (0.2-5.0  $\mu\text{m}$ ). They concluded that backpulsing was effective in

reducing the fouling phenomenon resulting in up to a five-fold increase in the steady state permeate flux and 100% flux recovery compared to the conventional non backflushed case. A recent study by Kuberkar and Davis (2001) investigated crossflow microfiltration using yeast suspensions, bovine serum albumin (BSA) solutions, and mixtures of yeast and BSA with and without crossflushing or backflushing. They reported that both crossflushing and backflushing are more effective against yeast fouling than against BSA fouling, with backflushing being the more effective of the two methods.

Backflushing frequency is a topic being studied widely in many applications. Kim and Chang (1991) studied the effects of periodic backflushing hemoglobin and dextran ultrafiltration using hollow fiber membranes. They found that an optimum frequency of  $0.2 \text{ min}^{-1}$  existed for a pulse duration of 13.75 s which gave a maximum permeability while the retention of dextran decreased with increasing frequency. Rodgers and Sparks (1992) studied backpulsing of 10g/l protein solutions with ultrafiltration. They reported that for 0.05 s backflow at 0.5 s cycle, flux increased up to 100 times the unpulsed flux under laminar crossflow but no significant improvement in flux was observed in turbulent regime. Vigneswaran et al. (1996) reported results on the MF of filter backwash water from a wastewater treatment plant. They determined an optimum cycle of 1 min and backflushing duration of 1s. Kennedy et al. (1998) investigated intermittent crossflushing of hollow fiber ultrafiltration systems and reported that the efficiency for backflushing was more dependent on backflushing time than pressure. Srijaroonrat et al. (1999) used ceramic membranes to evaluate the treatment of an unstable secondary emulsion. They observed the contamination of the permeate with oil when using 0.5 micron MF membrane. They also found that, when applying backflushing, the optimum forward filtration and reverse filtration times were 1 min and 0.7 s, respectively.

Other studies focused on the effect of pressure, concentration of the feed solution and types of feed solution. Nakatsuka et al. (1996) studied the effect of backflushing in drinking water treatment using ultrafiltration hollow fiber membranes and concluded

that in order to maintain a constant high flux, the backflushing pressure should be more than twice the forward filtration pressure. Rodgers and Sparks (1993) studied backpulsing in protein solutions with ultrafiltration and reported on the effect of concentration. The backpulsing technique was efficient when the feed concentration was between 10 and 30 g/l while at 100g/l, the permeate flux did not increase. Héran and Elmaleh (2000) evaluated high frequency reverse filtration through a 0.2  $\mu\text{m}$  tubular ceramic membrane for a bentonite suspension, biologically treated wastewater and an activated sludge suspension. They concluded that the selection of membrane and suspension is the most important factor in high frequency reverse filtration and the ability to increase flux by crossflow is not the only criteria for choosing high frequency reverse flow filtration (Héran and Elmaleh, 2000).

These studies suggest that backflushing is a technically feasible and effective method to enhance crossflow filtration. However, the efficacy of backflushing seems to vary with frequency of backflushing, the solution being treated and membrane/particle interactions.

#### **2.2.4 Research on bilge water treatment**

A limited amount of information is available in the literature related to the application of membrane systems in bilge water treatment. Harris et al. (1976) studied oily bilge water treatment with a tubular ultrafiltration system using cellulosic and noncellulosic membranes and found that removal of oil from water to less than 15mg/l can be achieved. Bhattacharyya et al. (1979) conducted a series of ultrafiltration experiments to test the effects of detergent in a bilge water treatment system using noncellulosic, tubular membrane. Since these two works, few studies have been performed on the treatment of bilge water using membrane technologies. Resera (1992) studied various commercially available oily water separators and indicated that fouling is a primary obstacle to meet discharge requirements. On behalf of the Canadian Navy, Resera (1995) performed a bilge water characterization study and reported that contaminants found in bilge water include, but are not limited to, metal oxides (rust particles), asbestos, and other insulation particles, refrigerants and general wastes common to

municipal treatment facilities. The average composition of bilge water was determined to be (Resera, 1995):

- i) Total Oils and Greases (TOG) = 1,284 mg/L,
- ii) Total Suspended Solids (TSS) = 502 mg/L,
- iii) Total Dissolved Solids (TDS) = 17,735 mg/L, and
- iv) The remainder being water, which was an approximately equal mixture of seawater and potable water.

In a North Atlantic Treaty Organisation (NATO) expert workshop on Oily Water Separators held in 1999, many countries reported on the difficulties associated with pretreatment before oily water separators. These pretreatments were of the form of parallel plate separators, settling tanks or a hydrocyclone (Tremblay and Nottegar, 2000). A previous study performed for the Defense Research Establishment Atlantic (DREA) by Tremblay and Nottegar (2000) indicated that bilge water is a very challenging wastewater to treat due to the type and the size of particulate matter in solution. Particulates found in bilge water are formed from soot, emulsified oil and/or free oil and detergents. Three populations of particles having average radius of 3.5 nm, 90 nm and 1.2 microns were identified in the synthetic bilge water mixture used in the study. The study found that a membrane having a MWCO above 10,000 Daltons should be used in this application to allow for the passage of the 3.5 nm particles, which cause very high cake resistances. The larger 1.2 microns particles were easily treated as they were swept away from the surface of the membrane by the crossflow of fluid, provided that they do not adhere to the surface of the membrane. The study found that the 0.2 micron diameter particles have the lowest combined diffusivity for any sub-micron particle and are considered to be the most difficult particles to treat by crossflow membrane technologies.

### 3. THEORY

#### 3.1 Membrane filtration mechanisms and models

Membrane fouling occurs due to particle-particle and particle-membrane interactions. Fouling causes a decline in permeate flux and a change in membrane selectivity. Membrane fouling remains a poorly understood phenomenon. One of the major problems involved in developing a fundamental understanding of membrane fouling is the difficulty in identifying the actual foulant and in distinguishing between the symptoms of fouling and the effect of membrane compaction. There are two distinct types of fouling phenomena:

- 1) Macrosolute adsorption, which refers to specific intermolecular interactions between a macrosolute and the membrane that occur even in the absence of any filtration (i.e., in the absence of the hydrodynamic and body forces),
- 2) Filtration-induced macrosolute/particle deposition, which is over and above that observed in a static system.

In traditional dead-ended filtration, flux decline can be attributed to four mechanisms; complete pore blocking, intermediate pore blocking, pore constriction and cake filtration at the surface of the filter. Hermia (1982) reviewed and compared these different models for constant pressure filtration.

##### 3.1.1 Complete blocking

In the complete blocking model, it is assumed that each particle reaching the membrane seals the pores and the particles are not superimposed one upon the other. In this model, the rate of change in the number of open pores is assumed to be directly related to the rate of particle convection to the membrane surface (Hermia, 1982),

$$\frac{dN}{dt} = -\alpha_{block} A J_v C_b \quad (3.1)$$

where  $J_v$  is the filtrate flux,  $A$  is the surface area of the membrane,  $C_b$  is the bulk concentration, and  $\alpha_{block}$  provides a measure of the pore blockage efficiency. Cake formation is assumed to be negligible. Equation (3.1) can be integrated as:

$$\frac{J_v}{J_0} = \exp\left(-\frac{\alpha_{block} A J_0 C_b}{N_0} t\right) \quad (3.2)$$

where  $J_0$  is the initial filtrate flux through the clean membrane and  $N_0$  is the initial pore density.

### 3.1.2 Intermediate blocking

The intermediate blocking model is a less restrictive model. In this case, it is assumed that each particle would not block a pore; it is possible that the particles settle on other particles. It is assumed that the suspension is perfectly homogeneous, and the second particle layer has an equal probability to settle on the first layer as on the surface which was left free. The following equation can be obtained (Hermia, 1982),

$$J_v = \frac{J_0}{1 + (\sigma_{inter} \Delta P / \mu R_{inter}) t} \quad (3.3)$$

where  $\sigma_{inter}$  is blocked area per unit filtrate volume,  $\mu$  is the viscosity of the solution,  $R_{inter}$  is the filter resistance. Equation (3.3) can be put in the following form:

$$K_{inter} = \frac{1}{J_v} - \frac{1}{J_0} \quad (3.4)$$

where  $K_{inter}$  is equal to

$$\frac{\sigma_{inter} \Delta P}{\mu R_{inter} J_0} = \frac{\sigma_{inter}}{A_0} \quad (3.5)$$

where  $A_0$  is the initial active filter membrane surface area. Then from Equation (3.5) it is easy to deduce that

$$\frac{J_V}{J_0} = (1 + K_{inter} t)^{-1} \quad (3.6)$$

### 3.1.3 Pore constriction

In the pore constriction model, it is assumed that the pore volume decreases proportionally to filtrate volume due to the deposition of particles on the pore walls. The membrane filter is assumed to have a set of pores of constant diameter and length. In this model, the rate of change in the pore volume is assumed to be proportional to the rate of particle convection to the membrane (Hermia, 1982),

$$\frac{d}{dt}(\pi r_p^2 \delta_m) = -\alpha_{pore} A J_V C_b \quad (3.7)$$

yielding

$$\frac{J_V}{J_0} = \left( 1 + \frac{\alpha_{pore} A J_0 C_b}{\pi r_p^2 \delta_m} t \right)^{-2} \quad (3.8)$$

where  $\delta_m$  is cake thickness.

### 3.1.4 Cake filtration

If the particles are bigger than the pores, or if the pore becomes sufficiently clogged, the particles will deposit onto the membrane surface and form a filter cake. In the case of cake filtration, it is assumed that the flux decreases as cake thickness increases, and the cake thickness increase proportionally to filter volume. In this case, the hydraulic resistance provided by the particle cake is assumed to be proportional to the cake mass,  $m_{cake}$  (Hermia, 1982):

$$R_c = \left( \frac{\alpha_{cake}}{A} \right) m_{cake} \quad (3.9)$$

with the rate of particle deposition directly related to the rate of particle convection:

$$\frac{d m_{cake}}{dt} = A J_v C_b \quad (3.10)$$

Equations (3.9) and (3.10) can be combined and the following Equation can be obtained:

$$\frac{J_v}{J_0} = \left( 1 + \frac{2 \alpha_{cake} J_0 C_b}{R_m} t \right)^{-1/2} \quad (3.11)$$

The four different membrane filtration mechanisms for constant pressure filtration are summarized in Table 3.1 below.

Table 3.1: Four different membrane filtration models.

Model	Constant	Equation
Complete blocking	$K_{block} = \frac{\alpha_{block} A J_0 C_b}{N_0}$	$\frac{J_v}{J_0} = \exp(-K_{block} t)$
Intermediate blocking	$K_{inter} = \frac{\sigma_{inter} \Delta P}{\mu R_{inter} J_0}$	$\frac{J_v}{J_0} = (1 + K_{inter} t)^{-1}$
Pore constriction	$K_{constriction} = \frac{\alpha_{pore} A J_0 C_b}{\pi r_p^2 \delta_m}$	$\frac{J_v}{J_0} = (1 + K_{constriction} t)^{-2}$
Cake filtration	$K_{cake} = \frac{2 \alpha_{cake} J_0 C_b}{R_m}$	$\frac{J_v}{J_0} = (1 + K_{cake} t)^{-1/2}$

In order to extend these simple filtration equations to crossflow systems, it is necessary to account for the additional hydrodynamic and intermolecular forces on the particle and the effects that such forces have on the rate of particle deposition. Since the actual

analysis of the hydrodynamic and intermolecular forces can be quite complex, the typical approach is to simply rewrite the rate expressions, Equations (3.1), (3.4), (3.7) and (3.10), with an additional term to account for the rate of particle back transport. For example, in complete blocking model, the equation now becomes;

$$\frac{dN}{dt} = -\alpha_{block} A (J_v - J^*) C_b \quad (3.12)$$

where  $J^*$  is the effective velocity associated with the mass transfer back into the bulk solution.

In the early stages of a filtration run and until a steady state flux is reached,  $J_v \gg J^*$ . Particle deposition and clogging dominate membrane transport. In this situation, permeate flux decline can be modeled using the equations listed in Table 3.1. It is proposed in this work to identify the type of fouling mechanism affecting the treatment of bilge water using various membranes by fitting permeate flux decline curves to the four models identified in Table 3.1.

### 3.1.5 Cake resistance

In the case of flux decline associated with cake filtration, the effect of particulate fouling can be most easily understood using a D'Arcy's law formulation for the filtrate flux as modified to account for the osmotic effect (Zeman and Zydney, 1996):

$$J_v = \frac{\Delta P - \sigma_0 \Delta \Pi}{\mu (R_m + R_c)} \quad (3.13)$$

where  $\Delta P$  is the trans-membrane pressure drop,  $\sigma_0$  is the membrane osmotic reflection coefficient,  $\Delta \Pi$  is the osmotic pressure difference across the membrane,  $\mu$  is the viscosity of the solution, and  $R_m$  and  $R_c$  are the hydraulic resistance of the membrane and the particle cake (fouling layer) respectively. Membrane resistance can be estimated from its average pore size by the following relation (Zeman and Zydney, 1996):

$$R_m = \frac{8 \delta_m}{N \pi r_p^4} \quad (3.14)$$

where  $N$  is the number of pores per unit membrane area and  $r_p$  is the pore radius,  $r_p$  is the effective pore radius.

In MF and UF, the osmotic pressure term ( $\sigma_o \Delta \Pi$ ) in Equation (3.13) is assumed to be negligible due to the large pore size. The rate of particle transport back into the bulk suspension is assumed to be negligible due to the slow rate of Brownian particle diffusion and the absence of any shear-induced particle motion or inertial lift in the dead-end flow system. Long-range intermolecular interactions are also assumed to be negligible. Then equation (3.13) can be rewritten as

$$J_v = \frac{\Delta P}{\mu (R_m + R_c)} \quad (3.15)$$

The total resistance can be expressed as:

$$R_{total} = (R_m + R_c) \quad (3.16)$$

The specific cake resistance,  $\alpha_{cake}$ , can be estimated for cakes formed from uniform, spherical particles by the Carman-Kozeny relationship (Carman, 1938)

$$\alpha_{cake} = \frac{180 (1 - \varepsilon)}{\rho_p d_p^2 \varepsilon^3} \quad (3.17)$$

where  $\varepsilon$  is the void volume of the cake,  $\rho_p$  the density of the particles and  $d_p$  is the mean diameter of the particles. The Carman-Kozeny equation was formulated to describe the characteristics of a porous cake made up of solid, spherical particles. For

such a cake, the specific resistance would be expected to increase in proportion to the cake mass and as the inverse of the square of the particle size.

In dead-ended filtration studies, it is more convenient to measure the cumulative volume of filtrate  $V$  discharging from the filter, and convert  $V$  to a volume flow rate of filtrate  $dV/dt$  (Wakeman and Terleton, 1999). Filtrate flux and flow rate are related by:

$$J_v = \frac{1}{A} \frac{dV}{dt} \quad (3.18)$$

where  $A$  is the area of filter. Equations (3.13) and (3.15) can be combined as below (the osmotic pressure term in Equation (3.13) is assumed to be negligible):

$$\frac{dV}{dt} = AJ_v = A \frac{\Delta P}{\mu (R_c + R_m)} \quad (3.19)$$

The resistance of the cake is directly proportional to the mass of the dry solids deposited per unit area of filter, and the proportionality constant,  $\alpha_{\text{cake}}$ , provides a definition of the specific cake resistance:

$$R_c = \alpha_{\text{cake}} \frac{m_{\text{cake}}}{A} \quad (3.20)$$

The specific cake resistance,  $\alpha_{\text{cake}}$ , is used as a primary factor in scale up operations of filtration equipment. This is because the specific cake resistance remains relatively constant as the cake thickness increases (Wakeman and Terleton, 1999). When the TMP remains constant during filtration, Equation (3.19) can be integrated directly to give a relationship between filtration volume and time:

$$\frac{t}{V} = \left( \frac{K_p}{2} \right) V + \frac{1}{q_0} \quad (3.21)$$

where

$$K_p = \frac{\alpha_{cake} c \mu}{A^2 \Delta P} \quad (3.22)$$

and

$$\frac{1}{q_0} = \frac{\mu R_m}{A \Delta P} \quad (3.23)$$

where  $c$  is the concentration of feed. A plot of  $t/V$  versus  $V$  should yield a straight line with a slope equivalent to  $K_p/2$  and a y intercept equivalent to  $1/q_0$ . From Equation (3.22) the specific cake resistance can be determined as:

$$\alpha_{cake} = \frac{A^2 \Delta P K_p}{c \mu} \quad (3.24)$$

From equation (3.23) the resistance of membrane,  $R_m$ , can be determined as:

$$R_m = \frac{A \Delta P}{\mu q_0} \quad (3.25)$$

### 3.2 Backflushing

Backflushing is a method that can be used to reduce the concentration polarization and fouling effect on the membrane surface and improve the performance of crossflow filtration. Backflushing can be performed with air, water or permeate by applying higher pressure on the permeate side than on the feed side of the membrane. During the backflushing, the deposited filter cake may be removed from the membrane wall and swept away by the crossflow of the feed solution. Figure 3.1 below shows the backflushing process in crossflow filtration.

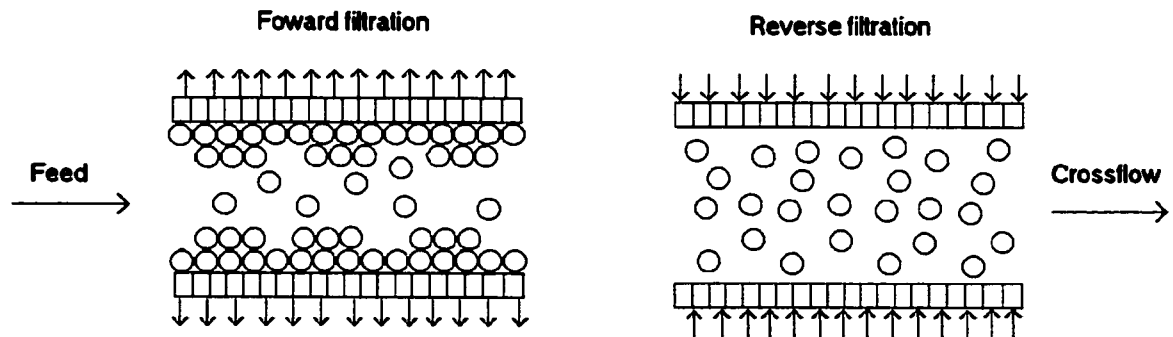


**Figure 3.1: Schematic representation of the backflushing technique in crossflow filtration.**

The optimal backflushing time and the time between backflushing must be determined experimentally because the ease of releasing the filter cake from the surface of the membrane is different for various types of wastes. Under normal operation, permeate flux declines with time and reaches a steady state value. Backflushing must occur before a steady state is reached. Backflushing at too high a frequency does not allow adequate permeate collection during forward filtration while too low a frequency results in significant flux decline due to cake formation. Therefore, the forward and reverse time need to be optimized experimentally in order to obtain a maximum permeate production.

## **4. EXPERIMENTAL METHODOLOGY**

### **4.1 Bilge water preparation**

Synthetic bilge water was made up from the components defined by the Canadian Navy (DND, 1996) as described below:

- i) 2000-ppm oils,
- ii) 500-ppm detergents and surfactants, and
- iii) 50/50 mixture of fresh water + seawater (approximately 99.75%).

This formed the basis for the makeup of the standard bilge water solution used in most tests. Tests using 4 g/L O & G concentration were also performed with wastewater containing twice the amount of oil and detergents/surfactants as in the standard bilge water composition described above.

#### **a) Oils, Detergents and Surfactants**

The oils were composed of the following Canadian Navy standard oils:

- i) 50% naval distillate (diesel fuel),
- ii) 40% used naval diesel engine lubricating oil, and
- iii) 10% hydraulic oil.

The detergents and surfactants were composed of the following Canadian Navy standard detergents and surfactants:

- i) 90% Canadian Navy standard oil and grease detergent (CLEANBREAK)
- ii) 10% Canadian Navy standard corrosion removal compound (OSTREM Rust Stain Remover).

## b) Composition of seawater

The salts being used to make synthetic ocean water in this work are listed in Table 4.1 according to “Standard Specification for Substitute Ocean Water”, ASTM D1141-90 (1992) as follows:

**Table 4.1: Concentration of various salts found in synthetic bilge water.**

Salt	Concentration in Bilge Water (mg/l)
NaCl	12267
MgCl <sub>2</sub> .6H <sub>2</sub> O	5556
Na <sub>2</sub> SO <sub>4</sub>	2047
CaCl <sub>2</sub>	579
KCl	347
NaHCO <sub>3</sub>	100.5
KBr	50.3
H <sub>3</sub> BO <sub>3</sub>	13.6
SrCl <sub>2</sub> .6H <sub>2</sub> O	2.1
NaF	1.5

Reverse Osmosis (RO) tap water was used as fresh water. In this study, synthetic bilge water containing twice the standard amount of oils, detergents and surfactants was prepared for each run. This solution offered a greater challenge to the membranes being tested, providing more realistic estimates of permeate flux.

### c) pH

As described in ASTM D1141-90 (1992), when making substitute ocean water, pH was adjusted to 8.2 with 0.1 N sodium hydroxide (NaOH) solution. Running at this slightly basic pH was necessary in order to maintain carbonates at their sparingly soluble limit. In all experiments the initial pH of the bilge water was adjusted to 8.2 before starting the run. In the case of flat sheet testing to determine the effects of various components found in bilge on membrane performance, the pH was adjusted at 8.2 for the entire run by adding NaOH.

## 4.2 Effect of the components found in bilge water on UF membrane performance

Flat sheet and hollow fiber membranes were tested to determine the effects of components found in bilge water on permeate flux.

### 4.2.1 Materials

#### A) Flat sheet tests

Five types of membranes with different pore size were employed. These membranes are summarized in Table 4.2 below.

Table 4.2: Characteristics of membrane used in flat sheet tests (Nottegar and Tremblay, 2000).

Membrane	GN	M100	QW	P707	QX
MWCO (kDaltons)	10	20	30	150	3,600
Estimated pore radius(nm)	3.7	5.2	6.4	14	70

The “G” and “Q” series membranes were manufactured by OSMONICS Inc. (Minnesota, USA) and the information about the composition of these membranes is proprietary. The M100 and P707 membranes were from KOCH Membrane Systems (Ann Arbor, Michigan, USA). They were made of polyvinylidene difluoride (PVDF).

## B) Hollow fiber tests

The KOCH XM50 membrane was employed in several experiments. The membrane is made of polyvinyl chloride/polyacrylonitrile (PVC/PAN) co-polymer. The characteristics of KOCH XM50 membrane are summarized in Table 4.3 below.

**Table 4.3: KOCH XM50 Hollow Fiber Membrane Characteristics**

Membrane Configuration	Hollow fiber
Composition	PVC/PAN (co-polymer)
Nominal MWCO	50,000 Daltons
Length	0.417m
Surface area	0.092416m <sup>2</sup> (1ft <sup>2</sup> )

### 4.2.2 Experimental set-up

#### A) Flat sheet tests

These tests were performed using the experimental set-up shown in Figure 4.1. In this system, a 200 litre feed tank provided feed solution to a 1½ horsepower (HP) multistage centrifugal pump (GRUNDFOS, ML90SAB-02, USA). A 100 micron, screen was placed before the pump to protect it from large debris that could accidentally be dropped into the tank. Three test cells were operated in crossflow. The permeate was either circulated back to the feed tank or discharged. The retentate stream was returned back to the feed tank. The circulation rate in the cells was 10 l/min. Two computers were used in this system. One computer added a standard 0.1N NaOH solution to control the feed solution's pH to  $8.2 \pm 0.1$  pH units. The other controlled the temperature of the feed tank to  $25.0 \pm 0.1$  °C. A computer running LABVIEW (National Instruments, Austin, Texas, USA) controlled an ON/OFF pneumatic valve that regulated the flow of cold tap water through a cooling coil inside the tank. Once the temperature in the system reached a set point, the system was able to maintain the temperature of the feed solution to within  $\pm 0.1$ °C.

Pressure gauges were placed at the inlet and outlet of the three cells. The operating pressure for each cell was estimated by assuming an equal pressure drop across each cell. The inlet pressure to all three cells was set to 3.45 barg (50 psig) for the GN, M100, QW (10, 20 and 30 kDalton) membranes and 2.07 barg (30 psig) for the QW, P707, QX (30, 150 and 3,600 kDalton) membranes.

The original circulation loop was constructed from stainless steel tubing. The extremely corrosive nature of seawater caused some rust within the system. During the early tests, rust was found at the surface of large pore membranes. In order to prevent iron fouling on these membranes, stainless piping in the system was replaced with PVC piping. This modification removed all traces of iron on the surface of the membranes.

#### **B) Hollow fiber tests**

The three cells in the loop were replaced by the KOCH XM50 membrane module described in Table 4.3. Other tubing and apparatus remained unchanged.

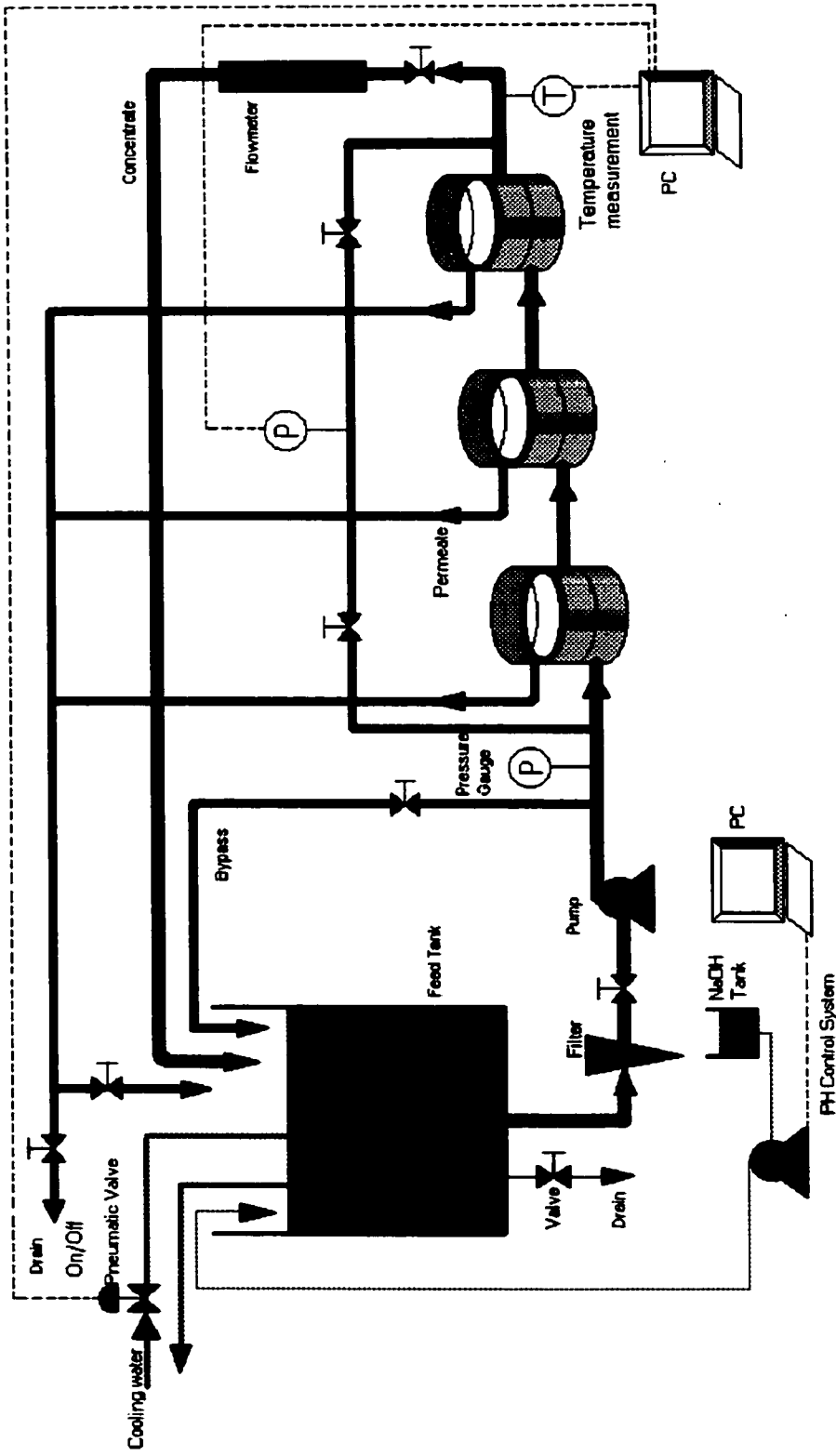


Figure 4.1: Flowchart of the three-cell UF membrane experimental set-up

### 4.2.3 Experimental procedure and analytical methods

#### A) Flat sheet tests

For each run, three kinds of membranes were put in the cells while 100 or 150 litres of feed solution was tested. The runs were usually carried out over a period of 5-6 days.

At the beginning of the experiment, pure water was permeated through the membranes until compaction caused the flux to reach a constant level. For pure water permeation, the permeate was circulated back to the feed tank. At this point, different feed solutions were made and tested and the pH of the feed solution was adjusted to 8.2.

For the 10, 20 and 30 kDalton membranes, the operating pressures at the inlet and outlet of the three cells were 3.45 and 3.03 barg (50 and 44 psig), respectively. An average pressure drop of 2 psig per cell was measured. The membrane flux recorded for each cell was normalized to a pressure of 50 psig by the following formula:

$$\text{Cell 1 flux @ 50psig} = (\text{flux measure for cell 1}) * 50/49$$

$$\text{Cell 2 flux @ 50psig} = (\text{flux measure for cell 2}) * 50/47$$

$$\text{Cell 3 flux @ 50psig} = (\text{flux measure for cell 3}) * 50/45$$

For the 30, 150 and 3,600 kDalton membranes, the operating pressures at the inlet and outlet of the three cells were 2.41 and 1.79 barg (35 and 26 psig), respectively. An average pressure drop of 3 psig per cell was measured at this inlet pressure. Membrane flux recorded for each cell was normalized to the 30 psig pressure by the following formula:

$$\text{Cell 1 flux @ 30psig} = (\text{flux measure for cell 1}) * 30/33.5$$

$$\text{Cell 2 flux @ 30psig} = (\text{flux measure for cell 2}) * 30/30.5$$

$$\text{Cell 3 flux @ 30psig} = (\text{flux measure for cell 3}) * 30/27.5$$

Permeate samples were collected in small vials and sample weights measured to  $\pm 1$  mg. The permeate flux was calculated using the following formula:

$$\text{Flux} = \frac{\text{permeate volume}}{\text{membrane area} * \text{sample time}} \text{ (l/m}^2\text{/h)} \quad (4.1)$$

The flux was corrected to 25°C in accordance with ASTM standard D5090-90: Standardizing Ultrafiltration Permeate Flow Performance.

$$\text{Flux at } 25^{\circ}\text{C} = (\text{Flux @ Temp.}) * (1 + (25 - \text{Temp.}) * 0.03) \quad (4.2)$$

The feed tank was cleaned with RO water after each run. The cleaning procedure was as follows:

- a) Add NaOH to the tank, adjust pH to 12, circulate for 15 minutes at 3.45 barg (50 psig);
- b) Add H<sub>2</sub>SO<sub>4</sub> to the tank, adjust pH to 2, circulate for 15 minutes at 3.45 barg (50 psig);
- c) Circulate with RO water for 15 minutes at 3.45 barg (50 psig).

#### B) Hollow fiber tests

The trans-membrane pressure used in this test was 1.38 barg (20 psig), while the feed flow rate was 13 l/min. The membrane module used in these tests was purchased from KOCH Membrane Systems (Ann Arbor, Michigan, USA). It was cleaned and reused in this work. The detergent used for cleaning the membrane was KLDII, a cleaner produced and recommended by KOCH Membrane Systems to clean this membrane when it is fouled by oil and grease. The module was cleaned with a water-KLDII solution. The cleaning solution makeup was 5 ml of KLDII added to 1 litre of water. Washes were conducted in a loop at high crossflow velocities and low pressure (3-5 psig). Permeate sample was collected and the sample weight measured. The methods for the calculation and the temperature correction of the permeate flux were the same as in the flat sheet tests.

### 4.3 MF/UF hybrid system tests

A MF/UF hybrid system was constructed out of one-inch diameter, schedule 40, 416 stainless steel tubing. All wetted parts in the MF system were constructed out of stainless steel and the parts in the UF system were assembled out of PVC and stainless steel. Both systems were solidly built to prevent any breakage during extended overnight runs. The MF loop was used for pretreatment while the UF loop was used as a post treatment step.

#### 4.3.1 Materials

Three types of commercially available membranes were selected for pilot scale tests. The characteristics of these membranes are described below.

##### A) KOCH Carbo-cor membranes

The KOCH Carbo-cor membrane (KOCH Membrane Systems, Ann Arbor, Michigan, USA) was made from scintered carbon. A thin carbon filtration layer constitutes the inside surface of a coarse asymmetrical support tube, made of composite carbon fiber. Carbo-cor membranes are made by mixing graphite with an organic binder and sintering the mixture at temperature of several hundred degrees. At these temperatures the organic binder is partially carbonized and holds the resulting graphite structure together. This type of membrane was used in the MF loop. The single tubes measure 6 mm ID x 8mm OD and are 1.2 m long.

Table 4.4: KOCH Carbo-cor Membrane Characteristics

Membrane configuration	Tubular (single channel)
Inside diameter, mm	6
Outside diameter, mm	8
Length, mm	1200
Membrane area, m <sup>2</sup>	0.022
Maximum operating pressure, psig	600
Maximum backpulsing pressure, psig	1500
Maximum operating temperature, °C	165
Pore size tested, µm	0.05, 0.1, 0.2, 0.5, 0.8, 1.4

## B) TAMI Céram membranes

TAMI Céram membranes (TAMI Industries, Nyons, France) are multi channel tubular ceramic membranes. They were used in the MF loop. These multilumen membranes were purchased as 25 mm OD x 1.2 m long tubes. The characteristics of the membranes tested are listed in Table 4.5. Five 6 mm channel multilumen membranes were selected for testing along with one 2.5 mm channel membrane. The pore sizes of the 6 mm channel membranes were 1.4, 0.8 and 0.07 microns (MF) and UF MWCOs of 300 and 150 kD. The 2.5 mm channel membrane had a cut-off of 50 kD. The manufacturer reports a maximum operating temperature of 150 °C, a pH range of 0 to 14, sterilizability, a bursting pressure > 90 barg, a good range of channel sizes and module packaging.

Table 4.5: TAMI Céram Membrane Characteristics

Name	Daisy	Dahlia
Membrane configuration	Tubular (8 channels)	Tubular (39 channels)
Inside diameter, mm	6	2.5
Outside diameter, mm	25	25
Number of channel	8	39
Surface area, m <sup>2</sup>	0.2	0.5
Length, ft	4	4
Membranes tested: Pore size (µm) or MWCO (kDaltons)	1.4, 0.8 & 0.07 micron and 300 & 150 kD	50 kD

## C) KOCH hollow fiber membrane

A KOCH XM50 hollow fiber membrane was employed in the UF loop. This membrane was used in the previous section and its characteristics are listed in Table 4.3 above.

### **4.3.2 Experimental set-up**

Membrane MF/UF pilot tests were performed in the system shown in Figure 4.2. There are two membrane circulation loops in this system, the MF loop served as pretreatment to the UF loop. During the experimental runs, MF permeate was sent to the UF loop while MF concentrate was circulated back to feed tank. Four pumps were employed in the system; one acted as a feed pump feeding bilge water to the MF loop, a second pump was used to circulate feed in the MF loop, a third pump circulated fluid in the UF loop and a pneumatic diaphragm pump, acted as a backflushing pump, drawing a suction from the permeate tank to backflush the MF membrane module. The contents of the feed tank were continually mixed to prevent the de-phasing of the bilge water.

Permeate from the UF loop was collected in a small 8 L permeate tank. The level in the tank was monitored to determine permeate flowrate. Liquid in the tank was used to backflush the membranes as needed. The permeate tank was linked to a pneumatic valve which served as a backflushing valve. The valve was computer-controlled. This valve was normally closed. During the backflushing operation the valve was opened and the permeate was backflushed through the MF membrane. The total operational cycle time and the backflushing times were set by the operator and controlled by the computer.

The temperature of the system was controlled by a water-cooled coil in the feed tank. A platinum RTD (Resistance Temperature Detector) probe placed in the MF loop provided an accurate measure of the feed temperature. A computer operated ON/OFF pneumatic valve controlled the flow of water through the coil in the tank. Once the temperature in the system reached its set point, the system was able to maintain the temperature of the feed solution within  $\pm 0.1^\circ\text{C}$  of the set point.

The temperature, pressure, flux of permeate and retentate were graphically displayed on the PC screen and recorded. LABVIEW software was used to control the system and acquire the data.

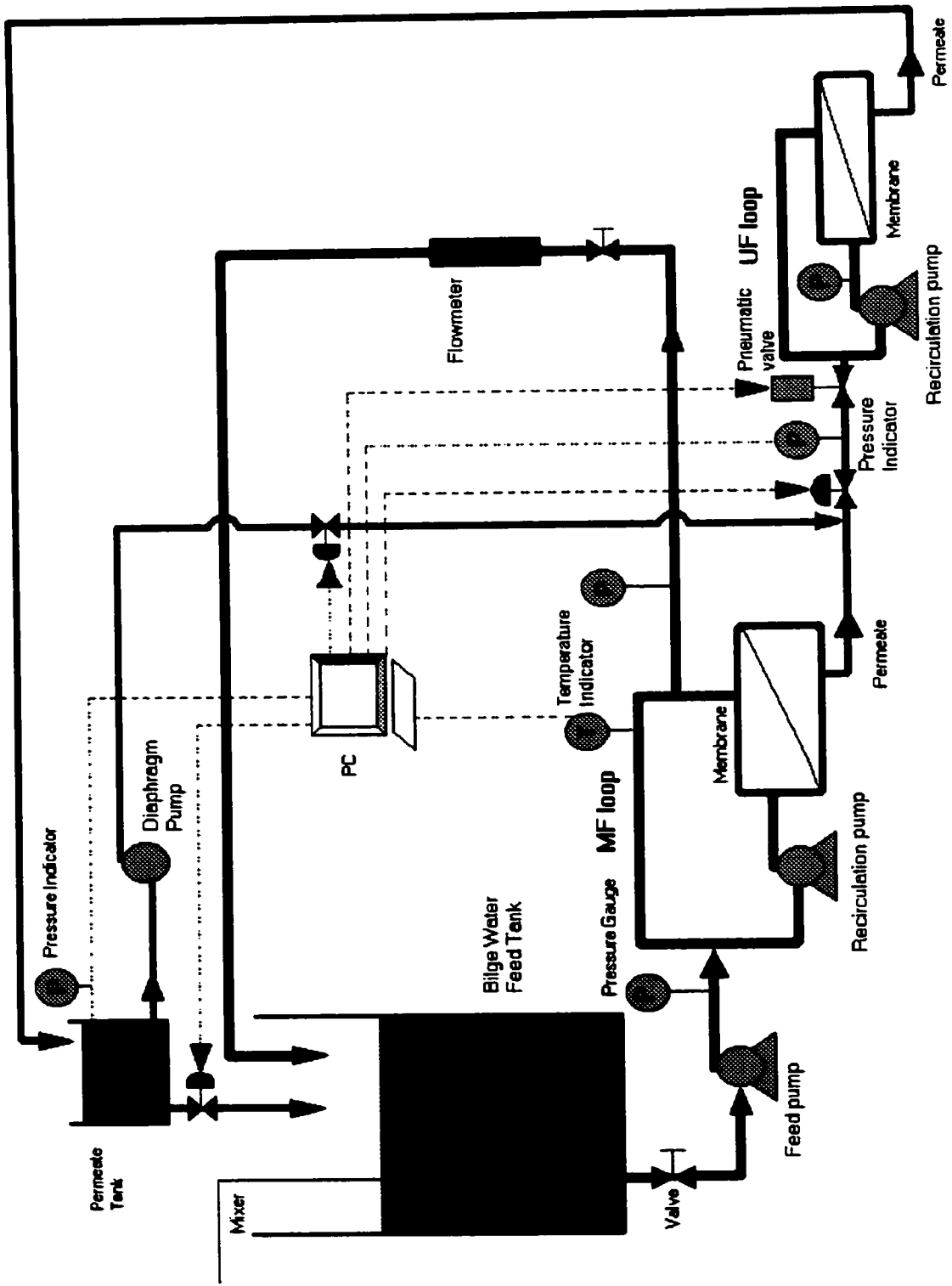


Figure 4.2: Flow diagram of the MF/UF hybrid system.

### **4.3.3 Experimental procedure and analytical methods**

All pilot scale runs were carried out at a crossflow rate of 5 to 6 m/s. A test volume of 100 L synthetic bilge water was prepared at room temperature and mixed in the feed tank for several hours before each run. Normally, a run lasted for 3 to 6 days. Prior to the tests, the KOCH Carbo-cor membranes were removed from the system and cleaned according to the following initial cleaning procedures recommended by KOCH Membrane Systems:

- 1) Flush the module with distilled water for 15 minutes at room temperature and a pressure of 2.07 barg (30 psig).
- 2) Alkaline cleaning. Flush with 1% NaOH and 150-ppm NaClO solution for 30 minutes at 60 °C at pressure 2.07 barg (30 psig).
- 3) Flush with distilled water to neutrality, same as step 1.
- 4) Acid cleaning. Flush with 2% HNO<sub>3</sub> solution for 30 minutes at 60 °C at pressure 2.07 barg (30 psig).
- 5) Flush with distilled water, same as step 1.

The new as received larger pore size TAMI membranes (0.8 and 1.4 micron) were rinsed with water and used directly in the tests. The smaller pore size TAMI membranes (50, 150 and 300 kD) were wet with isopropanol prior to use in order to displace any air present in membrane pores. This was followed by a rinse with RO water several times until all traces of isopropanol had disappeared.

After a run, the membrane was cleaned prior to the next run. For some of the runs using the Carbo-cor membranes, cleanings were performed using hot water, steam or air. For hot water cleaning, the membrane remained in the loop. Hot water at a given temperature was circulated in the MF loop for 1 hour and air backflushed through the membrane for 10 minutes. For the steam cleaning runs, pressurized steam (16-25 psig) was applied on the permeate side of the membrane for 20 minutes, followed by air backflushing for 10 minutes. For the TAMI membranes, cleanings were performed

three times with KLDII cleaner purchased from KOCH Membrane Systems Incorporated (Ann Arbor, Michigan, USA). The membranes were removed from the loop to prevent the contamination of the bilge water with the KLDII cleaning solution. All membranes were cleaned in a separate cleaning loop. The concentration of KLDII was 10 ml per litre of water. Washes were conducted at high crossflow velocities and low pressure (3-5 psig).

A flow meter was constructed out of a 10.2 cm x 0.5 m long PVC tube acting as a permeate tank, a pressure transducer (0-1 PSID, Cole-Parmer Instrument Company, Illinois, USA) and a pneumatic valve placed at the bottom of the tank. This type of flow meter was used due to the corrosive nature of the bilge water and the high level of particulates contained in the bilge water. The permeate tank was placed above the feed tank. At a low tank level set point, the discharge valve was closed, allowing for the permeate tank to fill. At a higher set point, the discharged valve opened and emptied the collected permeate back into the bilge water holding tank. The permeate tank level was converted to permeate volume by calibrating the relationship of the permeate tank volume and the corresponding tank level reading in the computer (See Appendix D for detailed calibration data). The volume of permeate collected over a given sampling period corresponding to the max change in tank level was used to determine permeate flowrate. The permeate flux was calculated using the following formula.

$$\text{Flux} = \frac{\text{permeate volume}}{\text{membrane area} * \text{sample time}} \text{ (l/m}^2\text{/h)} \quad (4.3)$$

The operating temperature was controlled to  $35 \pm 0.1^\circ\text{C}$ . For different runs, there was slight difference in temperature due to change of operating conditions such as room temperature and recovery within the MF loop which varied slightly throughout the runs. The results of permeate flux in this work were corrected to  $25^\circ\text{C}$  or  $35^\circ\text{C}$  in accordance with ASTM standard D5090-90: Standardizing Ultrafiltration Permeate Flow Performance. The following formulate was used:

$$\text{Flux at } 25^{\circ}\text{C} = (\text{Flux @ Temp.}) * (1 + (25 - \text{Temp.}) * 0.03)$$

$$\text{Flux at } 35^{\circ}\text{C} = (\text{Flux @ Temp.}) * (1 + (35 - \text{Temp.}) * 0.03)$$

#### **4.4 Oil and grease determination**

In this study, EPA Method 1664 (EPA, 1999) was used for the analysis of oil and grease. This method determines the amount of n-Hexane extractable material (HEM; oil and grease) using n-Hexane as extraction solvent. The procedure for n-Hexane extractable material (HEM; oil and grease) involves acidifying a 1 litre sample to a low pH followed by extraction with n-Hexane. (The detailed procedure and standardization for this method can be found in Appendix F).

## 5. RESULTS AND DISCUSSION

### 5.1 Effect of bilge water components

#### 5.1.1 Effect of carbonates on flat sheet membranes

Sparingly soluble salts present in bilge water such as calcium and magnesium carbonates are potential foulants in ultrafiltration. The effect of these salts on membrane flux was studied in this section. The solubility of carbonates in water is closely linked to pH, as shown in Table 5.1 below. The negative values of the Langelier Saturation Index (LSI) indicate that  $\text{CaCO}_3$  is soluble and positive values indicate that  $\text{CaCO}_3$  is insoluble.

Table 5.1: Langelier Saturation Index for seawater and a 50:50 mixture of fresh seawater. (See Appendix A for detailed calculation).

pH	Langelier Index for seawater	Langelier Index for half seawater
5	-1.72	-1.96
6	-0.72	-0.96
7	0.28	0.04
7.5	0.78	0.54
8	1.28	1.04
8.2	1.48	1.24
8.5	1.78	1.54
9	2.28	2.04

As seen in Table 5.1, the Langelier Saturation Index at a pH of 7 is 0.28 in seawater and 0.04 in half seawater (HSW) indicating that  $\text{CaCO}_3$  is sparingly soluble in both environments at this pH. At a pH of 8.2 or slightly above,  $\text{CaCO}_3$  is insoluble in both seawater and half seawater. As indicated in the experimental section, the precipitation of carbonates is closely linked to pH. A constant pH was maintained during the run by adding a 0.1N NaOH solution to the feed tank.

In order to determine the effect of carbonates on flux decline, tests were performed with normal and double concentration of  $\text{HCO}_3^-$  in seawater using the GN, M100 and QW flat sheet membranes. The characteristics of these membranes are given in Table 4.2. No oil and detergents were used in the preparation of feed solutions in this section. The permeate flux was normalized to 3.45 barg (50 psig) for the GN, M100 and QW membranes (See appendix B for raw data and detailed calculations), the temperature of feed solution was maintained at  $25.0 \pm 0.1$  °C. Results have been compiled and plotted in Figures 5.1 to 5.3 below. Data from previous runs performed on bilge water at 3.45 barg (50 psig), 25 °C were also included in these figures.

These results indicate that for the larger pore size membranes permeate flux decreased gradually during the 9-day run. For the smallest pore size tested (GN membrane, 8kD MWCO), the concentration of carbonate in seawater did not affect permeate flux, although a large amount of carbonate scale was found at the surface of this membrane. This suggested that the carbonate particles were larger than the 7.4 nm pore size (3.7 nm radius) for the GN membrane. However, the bilge water flux for this membrane is lower than the flux in both carbonate runs. The decrease is less pronounced in the case of the M100 and QW membranes. This would indicate that some compounds present in bilge water are adsorbing on the surface of the GN membrane reducing membrane flux for this membrane and to a lesser degree for the M100 and QW membranes. The results obtained for the M100 and QW membranes indicate that some very fine particulate matter is present in the carbonate test solutions and that its dimension is in between that of the pores in the GN and M100 membranes. This would imply that the diameter of the particulates is greater than 7.4 nm and less than 10.4 nm. These particles are also present in bilge water as evidenced by the similar flux seen in Figures 5.2 and 5.3 for the GN and M100 membranes respectively.

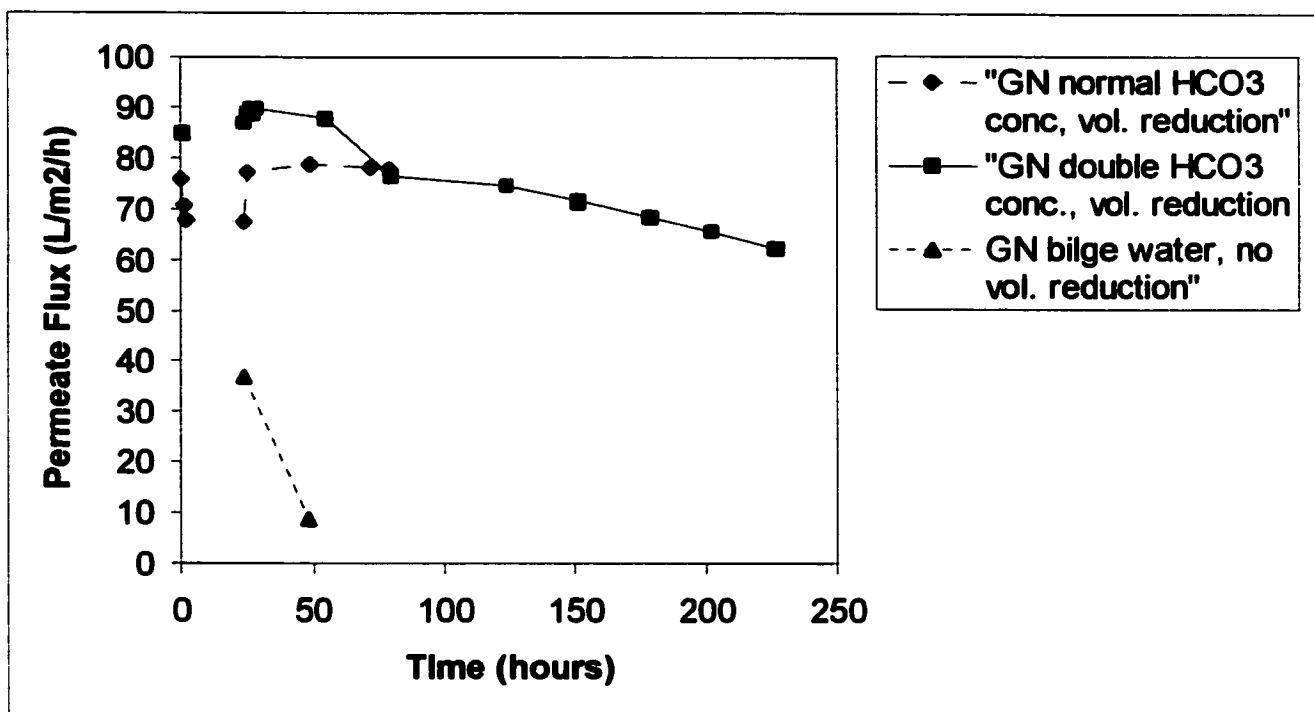


Figure 5.1: Plot of Flux vs. Time for the GN membrane (pore radius 3.7 nm, MWCO 10kD, operating pressure 50 psig, 25 °C). Pure water flux up to 24 hours at which point salt was added to the feed tank.

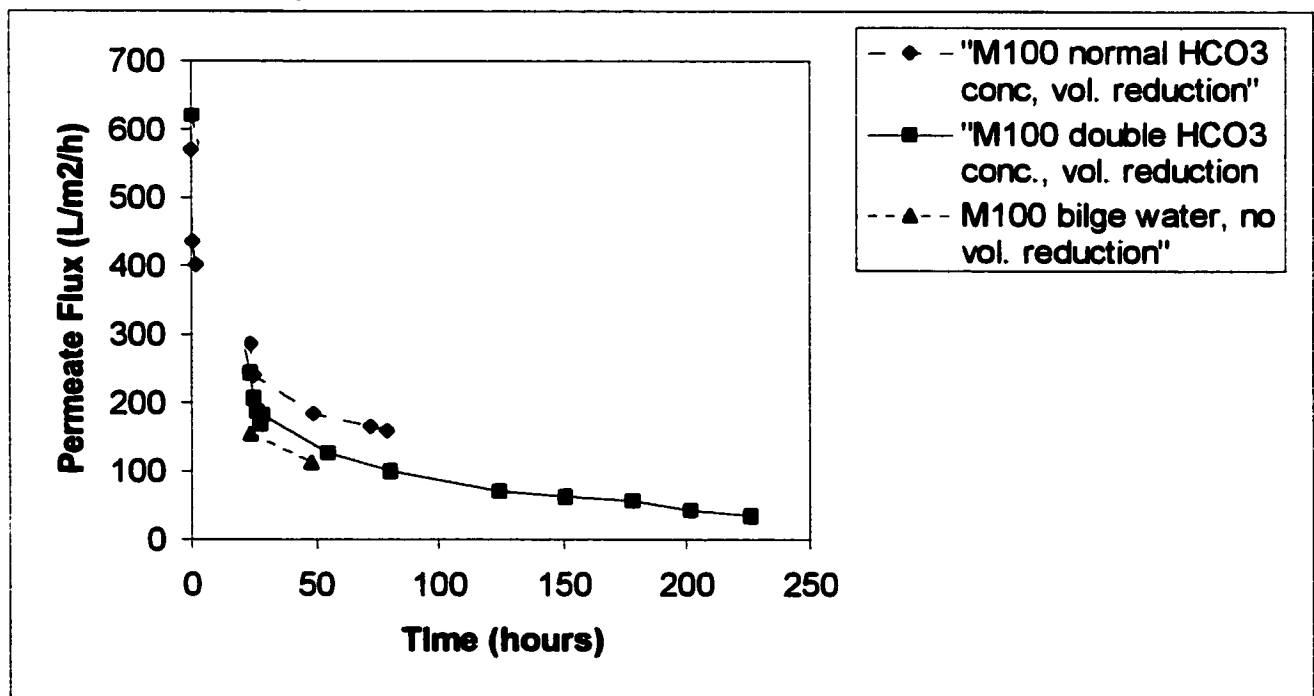


Figure 5.2: Plot of Flux vs. Time for the M100 membrane (pore radius 5.2nm, MWCO 20kD, operating pressure 50 psig, 25 °C). Pure water flux up to 24 hours at which point salt was added to the feed tank.

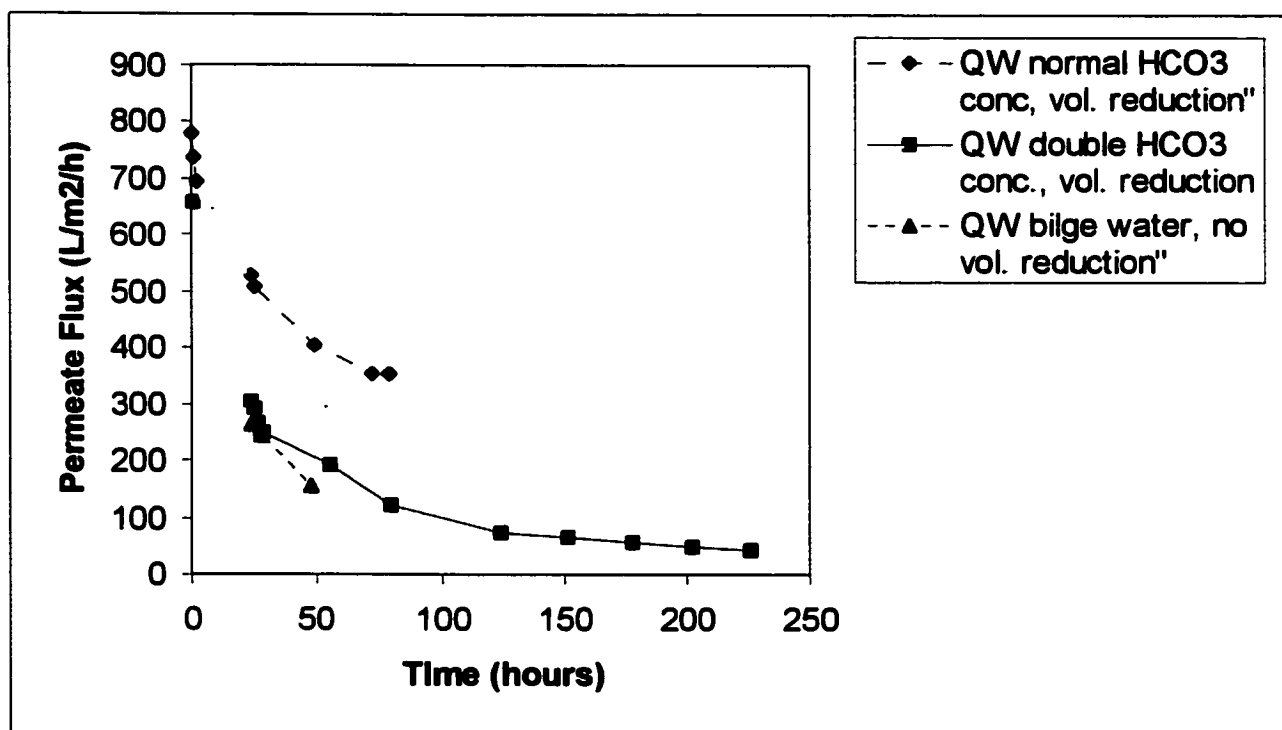


Figure 5.3: Plot of Flux vs. Time for the QW membrane (pore radius 6.4 nm, MWCO 30kD, operating pressure 50 psig, 25 °C). Pure water flux up to 24 hours at which point salt was added to the feed tank.

### 5.1.2 Effect of detergent and salts on flat sheet membranes

Flat sheet tests were performed to study the effects of a detergent and different salts present in bilge water. Five types of flat sheet membranes with different pore sizes were employed in these tests: GN, M100, QW, P707 and QX. No oil was used in the preparation of feed solutions in this section. These membranes were successively tested with a solution of CLEANBREAK and three salt mixtures. These mixtures contained the three major salt groups found in the makeup of seawater by ASTM method D1141-90 for the preparation of substitute seawater. The salt mixtures were dissolved in 1-2 litres of RO tap water prior to their addition to a 100 litre volume used in the permeation tests. Table 5.2 lists the three feed solutions tested. Each solution was tested for approximately 24 hours. The final solution (solution 3) had the composition of half seawater (HSW).

Table 5.2: Salt make-up of feed solutions in flat sheet membrane testing

Solution	Salt Mixture
Solution 1 (Salt group 1)	MgCl <sub>2</sub> 6H <sub>2</sub> O CaCl <sub>2</sub> SrCl <sub>2</sub> 6H <sub>2</sub> O Na <sub>2</sub> SO <sub>4</sub>
Solution 2 (Salt group 1 + 2)	Solution 1 + KCl NaHCO <sub>3</sub> KBr H <sub>3</sub> BO <sub>3</sub> NaF
Solution 3 (Salt group 1 + 2 + 3)	Solution 2 + NaCl

Five types of feed solutions were tested: pure water, CLEANBREAK, CLEANBREAK with Calcium and Magnesium salts (solution 1), CLEANBREAK with solution 2, CLEANBREAK with half seawater (solution 3).

Experimental results are shown in Figure 5.4 to 5.6 below. The permeate flux normalized to 2.07 barg (30 psig) for the QW, P707 and QX membranes and 3.45 barg (50 psig) for the GN, M100 and QW membranes can be observed in Figures 5.4 and 5.5 (See Appendix B for raw data and detailed calculations). The temperature of the feed solution was maintained at  $25 \pm 0.1$  °C.

In Figure 5.4, steep flux declines were observed after the introduction of CLEANBREAK into pure water. A second substantial drop occurred after the addition of salt group 1, containing calcium and magnesium. The addition of carbonate at half seawater concentrations (runs were performed without volume reduction) and sodium chloride had little effect on permeate flux.

The greatest flux reductions were observed for the membranes having the largest pore size. The flux of the membrane having the smallest pore size remained unchanged throughout the run. This indicates that the particle size formed by the CLEANBREAK

detergent is in the 0.05 to 0.14 micron range based on the pore diameter of the P707 and QX membranes found in Table 4.2.

The permeate flux for the QW membrane operated at 2.07 barg (30 psig) and 3.45 barg (50 psig) has been plotted in Figure 5.6. In this figure it is easily seen that the steep decline in flux is most pronounced at the lower operating pressures suggesting the possible deformation of these particles as they accumulate on the surface of the membrane and are permeated through membrane pores.

Although the exact composition of CLEANBREAK is not known, it contains various degreasing agents such as sulfonated hydrocarbons which are most often negatively charged. The results indicate that detergents and their behaviour in the extremely “hard” environment found in half seawater are a significant factor affecting membrane performance.

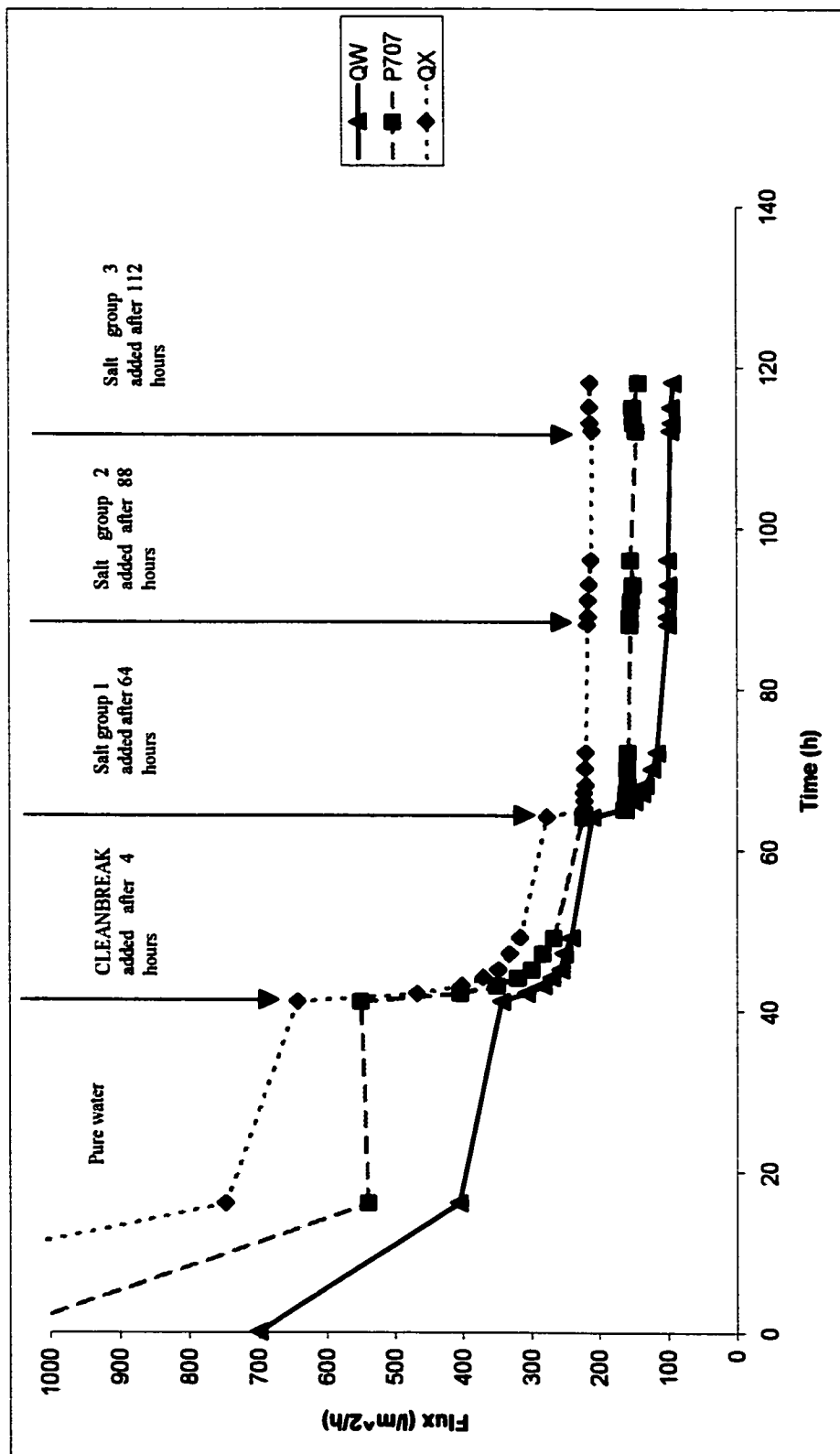


Figure 5.4: Plot of Flux vs. Time for the QW, P707 & QX membranes (30psig, 25°C)

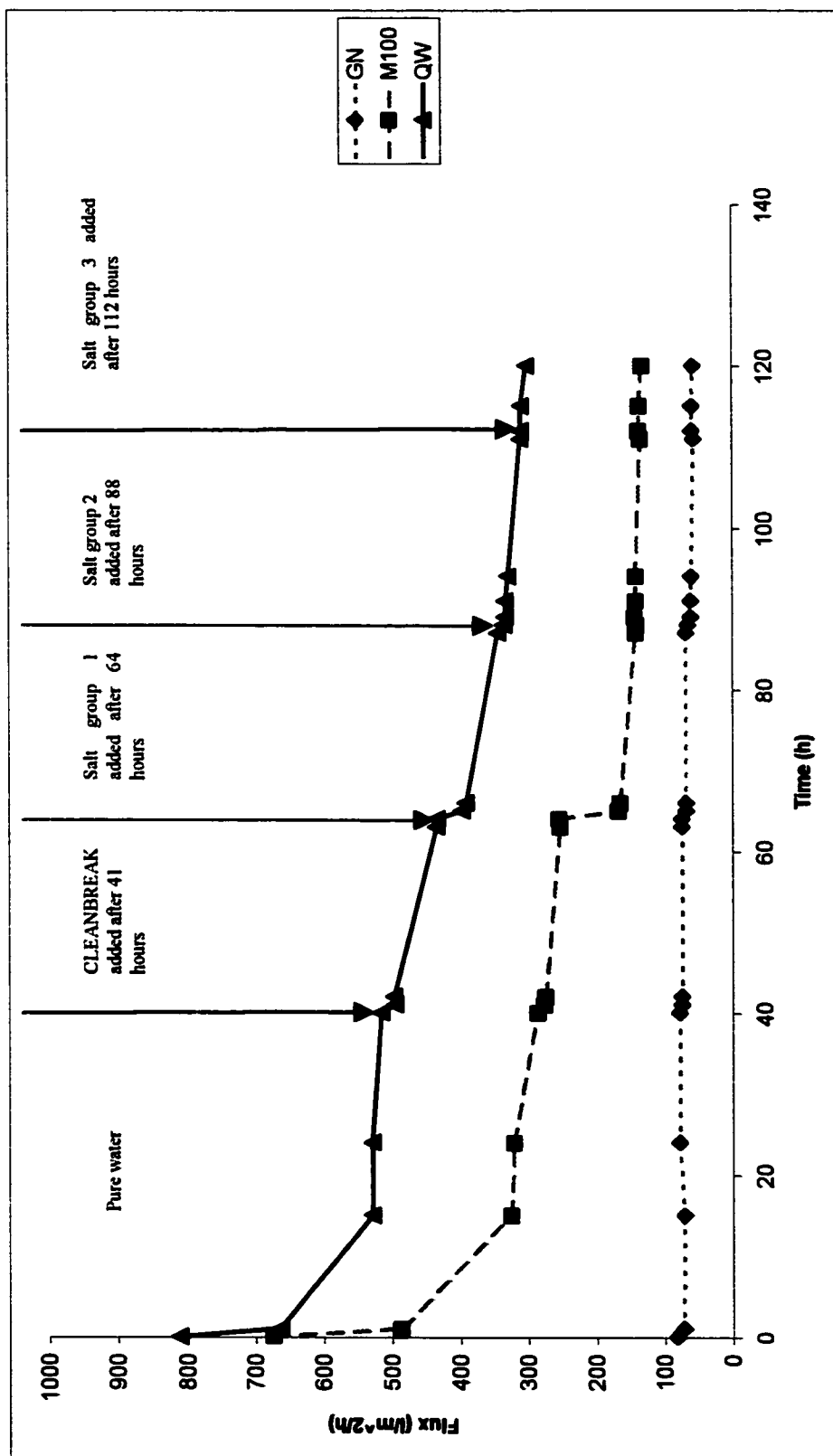


Figure 5.5: Plot of Flux vs. Time for the GN, M100 & QW membranes (50 psig, 25°C).

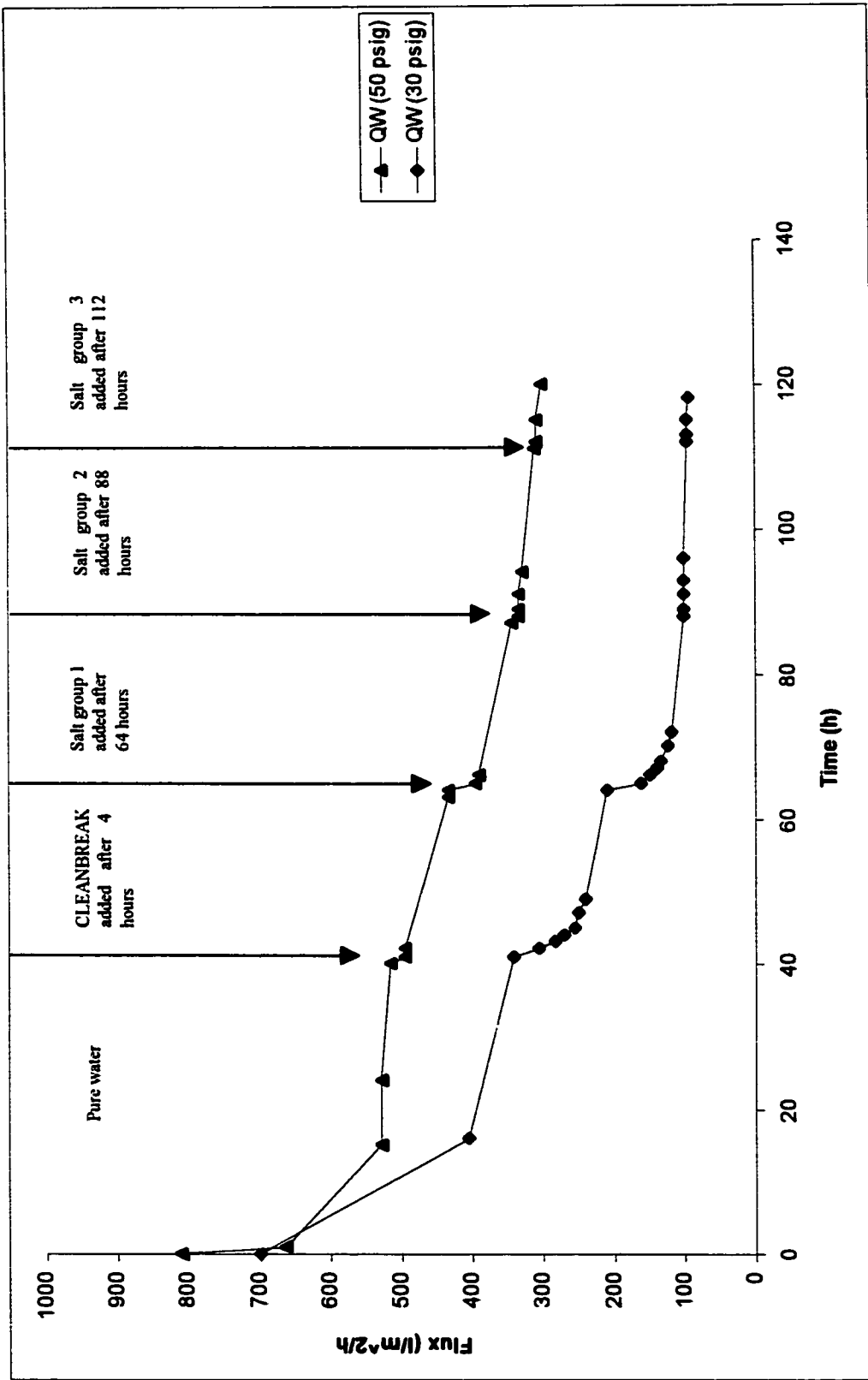


Figure 5.6: Plot of Flux vs. Time for the QW membrane at 30 and 50 psig operating pressure (25°C).

### **5.1.3 Effect of CLEANBREAK**

Further tests were performed to determine the effect of CLEANBREAK on membrane flux. CLEANBREAK is a degreasing agent that is specially formulated to promote phase separation after use. However, this particular formulation could increase the presence of colloidal matter in solution. The presence of considerable colloidal material is evidenced by the milky appearance of water containing CLEANBREAK. No oil was used in preparation of feed solutions in this section.

Section 5.1.3.1 reports on the study of a batch concentration run using KOCH XM50 hollow fiber membrane, section 5.1.3.2 is the study of the effect of CLEANBREAK concentration on KOCH XM50 hollow fiber membrane, section 5.1.3.3 is the study of effect of CLEANBREAK and TMP on flat sheet membranes.

#### **5.1.3.1 Batch concentration run using hollow fiber membrane**

Tests were also performed to study the effect of CLEANBREAK concentration on membrane flux using a KOCH XM50 (50kDalton MWCO) hollow fiber membrane module. The experiments were performed in a batch concentration mode where a total of 500 litres of HSW + CLEANBREAK (450 mg/L), was gradually reduced to 50 litres. Totally 225 g CLEANBREAK was added to the 500 litres HSW solution throughout the run. This experiment represents a ten-fold concentration of a solution originally containing 450 mg/L of CLEANBREAK. The TMP used in this experiment was 1.38 barg (20 psig) and the feed flow rate was 13 l/min.

Results are shown in Figure 5.7 below. They exhibit the typical flux decline found in cake filtration, indicating that CLEANBREAK was depositing on the surface of the membrane. The results have been labeled following the successive addition of fresh half seawater and CLEANBREAK solution.

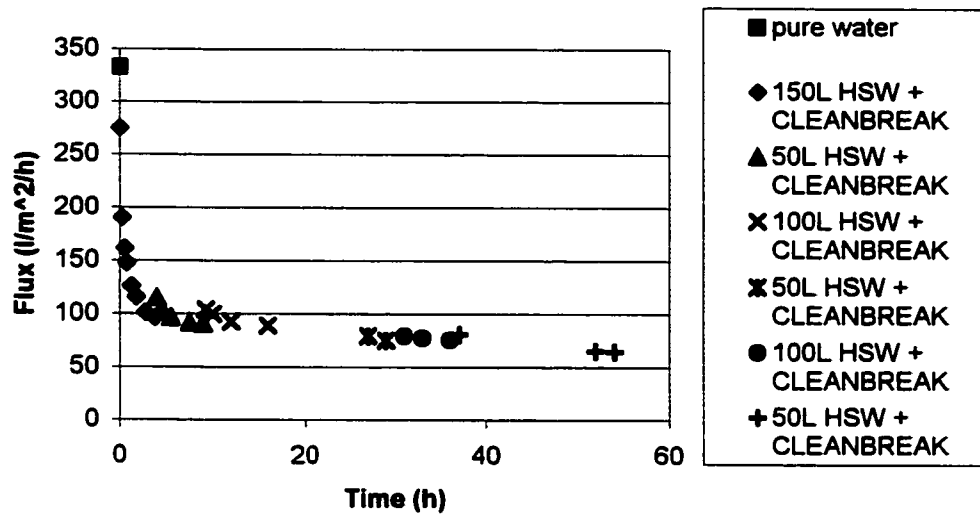


Figure 5.7: Plot of Flux vs. Time for KOCH XM50 membrane. Volume additions are for half seawater + CLEANBREAK (Operating pressure 20 psig, 25°C).

### 5.1.3.2 Effect of CLEANBREAK concentration on hollow fiber membrane

To further study the effect of CLEANBREAK, several runs were performed with different concentrations of CLEANBREAK, several runs were performed with different concentrations of CLEANBREAK in a 100L half seawater solution. The concentration of CLEANBREAK used in the runs was labelled as a factor of the concentration used in the makeup of synthetic bilge water. The concentration factors of 1, 2, 4, and 10 x correspond to 450, 900, 1800 and 4500 mg/L of CLEANBREAK, respectively. The membrane was cleaned using KOCH KLDII before each run. Results for the tests using pure water and half seawater are shown in Figure 5.8.

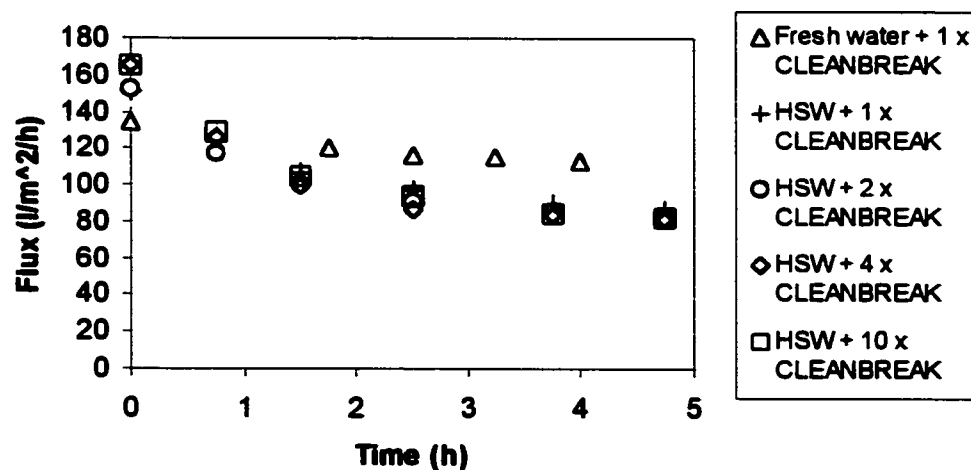


Figure 5.8: Plot of Flux vs. Time for KOCH XM50 hollow fiber membrane (20 psig, 25°C).

The results illustrate the effect of hardness on the UF of CLEANBREAK solutions. Plotting this data as a flux ratio de-couples initial flux variations from effects of cake formation and pore plugging. This is useful since it is impossible to obtain the same initial flux after each cleaning. Figure 5.9 is a plot of the data found in Figure 5.8 but replotted as a ratio of the actual flux at a given time in the run versus the initial flux. Flux ratios after 4 hours were 84 % for pure water + CLEANBREAK and 57, 53, 49 and 49 for 1, 2, 4, and 10 x half seawater + CLEANBREAK solutions respectively.

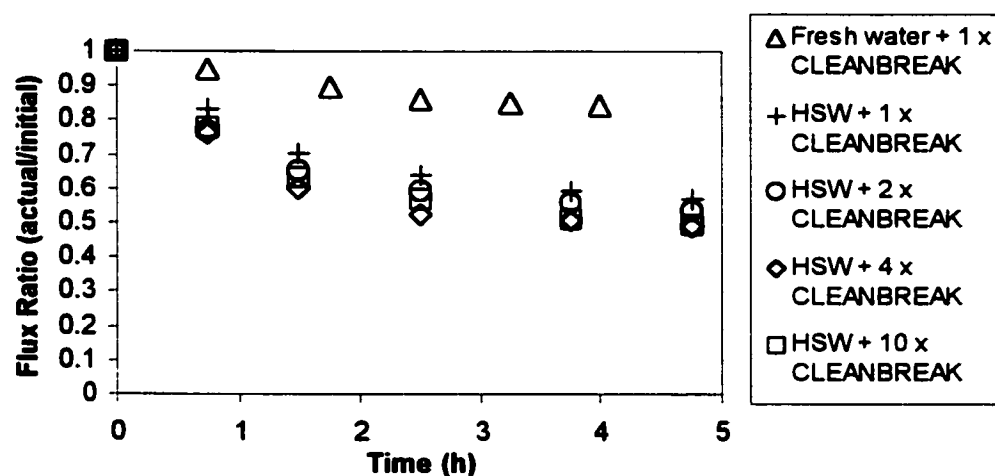


Figure 5.9: Data from Figure 5.8 plotted as the Ratio of the actual flux / initial flux for the KOCH XM50 hollow fiber membrane (20 psig, 25°C).

The flux for the pure water solution was observed to be 50% greater than that of the 1x half seawater solution. This can be attributed to the presence of Ca and Mg in half seawater, leading to the precipitation of detergents present in CLEANBREAK. These colloidal precipitates accumulate on the surface of the membrane forming a cake layer. The amount of colloidal material in solution will be greater in “hard” water. The result is a decrease in flux for the runs containing half seawater.

It is rather difficult to model this flux decline without knowing the composition of CLEANBREAK. The Material Safety Data Sheet (MSDS) for CLEANBREAK does state that it is not soluble in water, has a specific gravity of 0.786, a boiling point of 195 °C and a flash point of 66 °C. A search on the composition of degreasers revealed that

most contain; sulfonated hydrocarbons, kerosene, various alcohols, and surfactants that are most often negatively charged. Increasing the concentration of CLEANBREAK in a solution will eventually cause most of the free  $\text{Ca}^{2+}$  and  $\text{Mg}^{2+}$  ions to bind with detergent molecules. Increasing this concentration beyond a saturation point would not cause appreciable flux decline beyond that observed for pure water. For half seawater with different detergent concentrations, the flux after 5 hours was found to be independent of CLEANBREAK concentration, indicating that the saturation level had already been reached at the 450 mg/L CLEANBREAK concentration. Excessive concentrations of CLEANBREAK had little effect on the performance of the membrane.

The results also illustrate that adsorption effects onto the membrane material were minimal. In both cases, membrane flux would have declined to a greater extent in the presence of absorption. They also indicate that the KOCH membrane material is resistant to the components found in the commercial degreasing agent CLEANBREAK.

Table 5.3 below shows the specific cake resistance for each run. Data in Table 5.3 were plotted as shown in Figure 5.10. It can be found that for 1 x CLEANBREAK solutions, the specific cake resistance in pure water solution is much lower than that in half seawater solution. The specific cake resistance decreased with the increasing of CLEANBREAK concentration. The possible explanation is that CLEANBREAK binds the calcium and magnesium ions which softens the half seawater solution. Given the concentration of CLEANBREAK in Table 5.3, there would be sufficient CLEANBREAK to considerably soften the half seawater solution and decrease the specific cake resistance.

Table 5.3: Specific cake resistance for different CLEANBREAK concentration run

Solution	CLEANBREAK concentration (mg/L)	Specific cake resistance, $\alpha_{cake}$ (m/Kg)
Fresh water + 1 x CB	450	4.48E+12
HSW + 1 x CB	450	1.76E+13
HSW + 2 x CB	900	8.82E+12
HSW + 4 x CB	1800	5.88E+12
HSW + 10 x CB	4500	1.76E+12

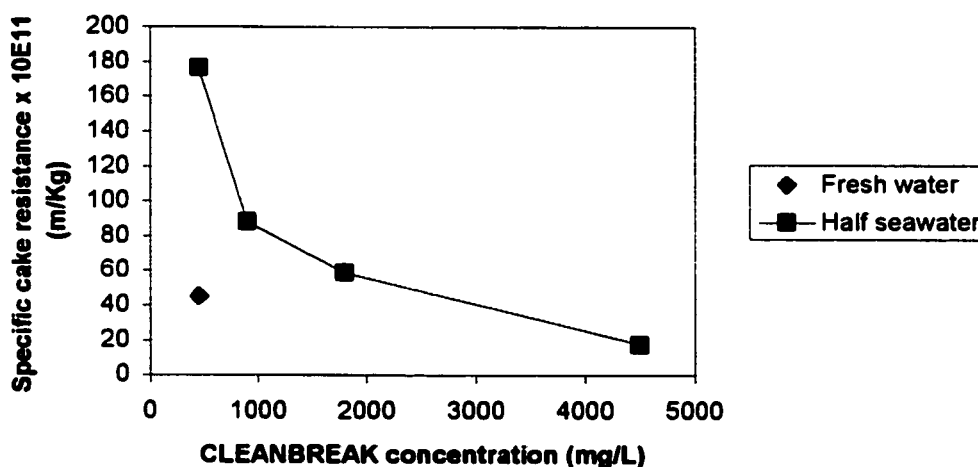


Figure 5.10: Plot of specific cake resistance vs. CLEANBREAK concentration for the KOCH XM50 membrane (20 psig, 25°C).

### 5.1.3.3 Effect of CLEANBREAK and TMP on flat sheet membranes

Increasing TMP has a significant effect on permeate flux during membrane separations. A run was conducted to determine the effect of TMP on the larger pore size membranes used in this study: QW, P707 & QX. The feed solution challenging the membranes was from a previous volume reduction run from 500 L to 50 L HSW + CLEANBREAK. Experiments were performed at TMPs of 0.69, 1.38, 2.07 and 2.76 barg (10, 20, 30 and 40 psig) with feed flow rate at 10 l/min. The steady-state flux after 1 day of operation

was plotted in Figure 5.11 below. Figure 5.12 shows permeate flux decline of P707, QW and QX membranes at various pressure.

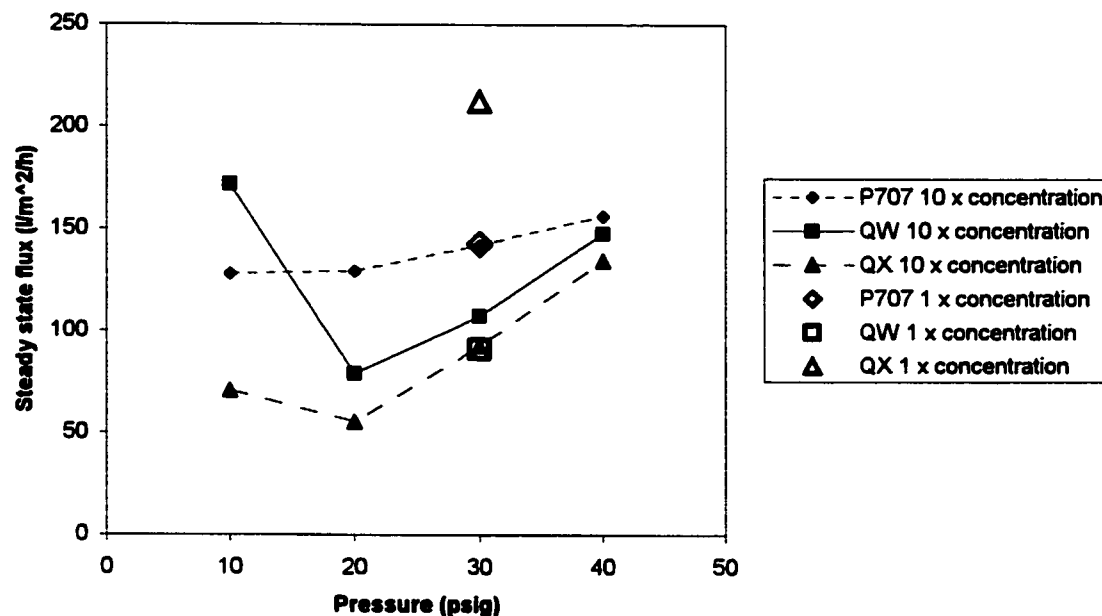


Figure 5.11: Effect of trans-membrane pressure on steady-state flux for the P707, QW and QX membranes (25°C).

The results indicate that at pressure above 1.38 barg (20 psig), the steady-state flux increases with pressure. The 14nm pore radius membrane P707 has the highest flux while the 70nm pore radius membrane QX had the lowest flux. The steady-state flux for these membranes for half seawater with normal CLEANBREAK concentrations are also shown in Figure 5.11. For the P707 membrane, the flux of half seawater with normal concentration (142.4 l/m<sup>2</sup>/h) is almost the same as with ten times concentration (141.9 l/m<sup>2</sup>/h). For the QW membrane, the fluxes are slightly different. However, the fluxes for the largest pore size membrane are quite different. The flux of the ten times concentration solution was much lower than the normal concentration for the QX membrane.

The flux results are almost the same at a TMP of 2.76 barg (40 psig) as shown in Figure 5.12 below. This indicates that once the cake is formed and pore plugging in the QX membrane has stopped, the separation is more likely to be controlled by the new

dynamically formed membrane. In pure cake filtration, flux should decrease with increasing pressure which is clearly not happening here and indicates some deformation of the CLEANBREAK particles.

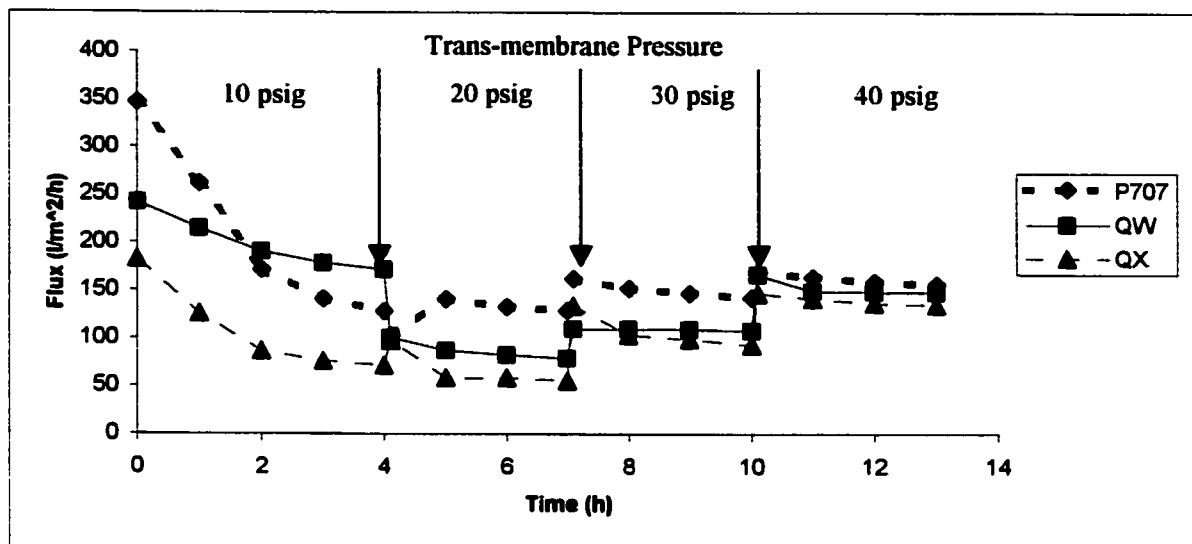


Figure 5.12: Flux vs. time for the larger pore size membranes as a function of trans- membrane pressure (25°C).

## 5.2 Pilot scale testing of operating parameters

Section 5.2.1 reports on the effect of trans-membrane pressure, section 5.2.2 is the study of the effect of backflushing on tubular membranes, section 5.2.3 is the study of different membrane cleaning methods.

### 5.2.1 Effect of trans-membrane pressure (TMP)

#### 5.2.1.1 Effect of TMP on KOCH Carbo-cor membrane

Tests were performed to study the effect of TMP on the permeate flux of the Carbo-cor membranes. The TMP was increased from 0.34 barg (5 psig) to 1.72 barg (25 psig) during the runs. The actual membrane flux vs. time was plotted in Figures 5.13 to 5.17. No backflushing pressure was applied for these runs.

The results indicate that for smaller pore size membranes, the change of TMP affected the permeate flux significantly. The flux increased with the increase of pressure from 0.34 barg (5 psig) to 1.72 barg (25 psig). However, for the larger pore sized membranes, increasing pressure had very little effect on permeate flux.

This gradual decrease in flux with time after a change in pressure in the system, observed for the smaller pore membranes, is indicative of cake filtration. In the case of pore plugging, the flux should decrease from the onset of the run without the characteristic flux decline on increasing pressure found in cake filtration. Cake filtration was observed for the 0.05 and 0.1 micron membranes. The fouling mechanism for the 1.4 micron pore size was not cake filtration as further increase in pressure greatly reduced permeate flux. At the higher pressure of 20 psig the membrane was completely plugged as seen in Figure 5.17.

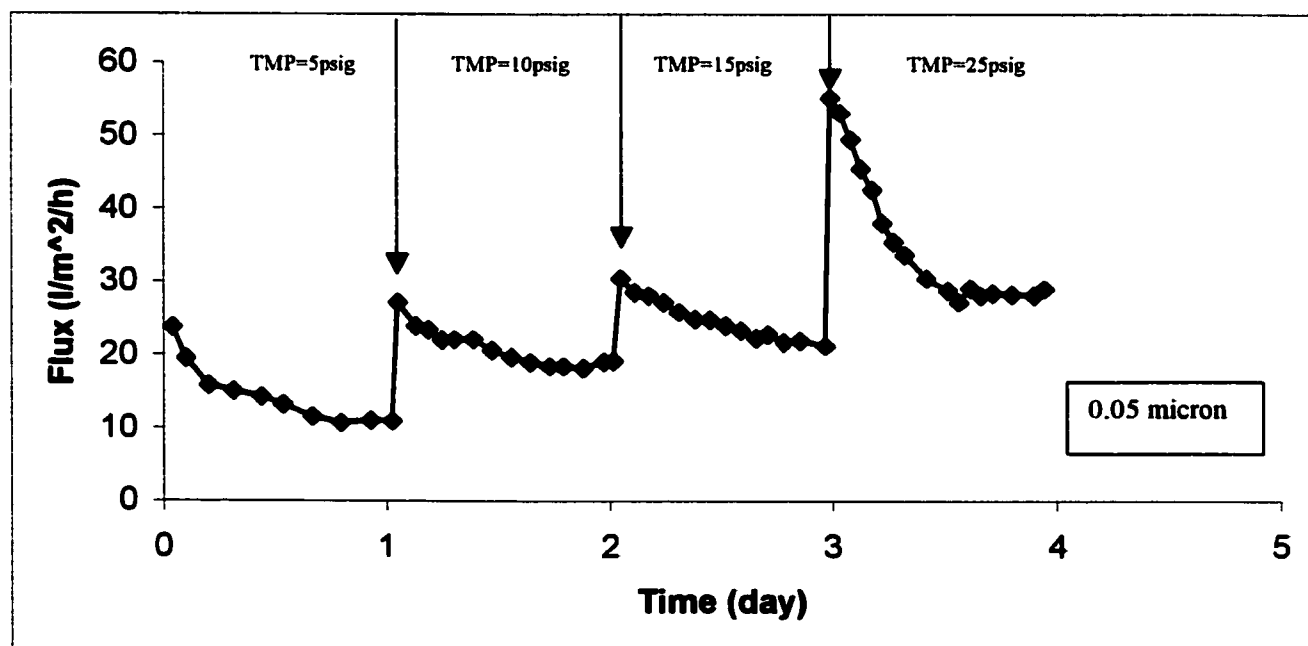


Figure 5.13: Plot of Flux vs. Time for the KOCH Carbo-Cor 0.05 micron membrane at different TMP (25°C).

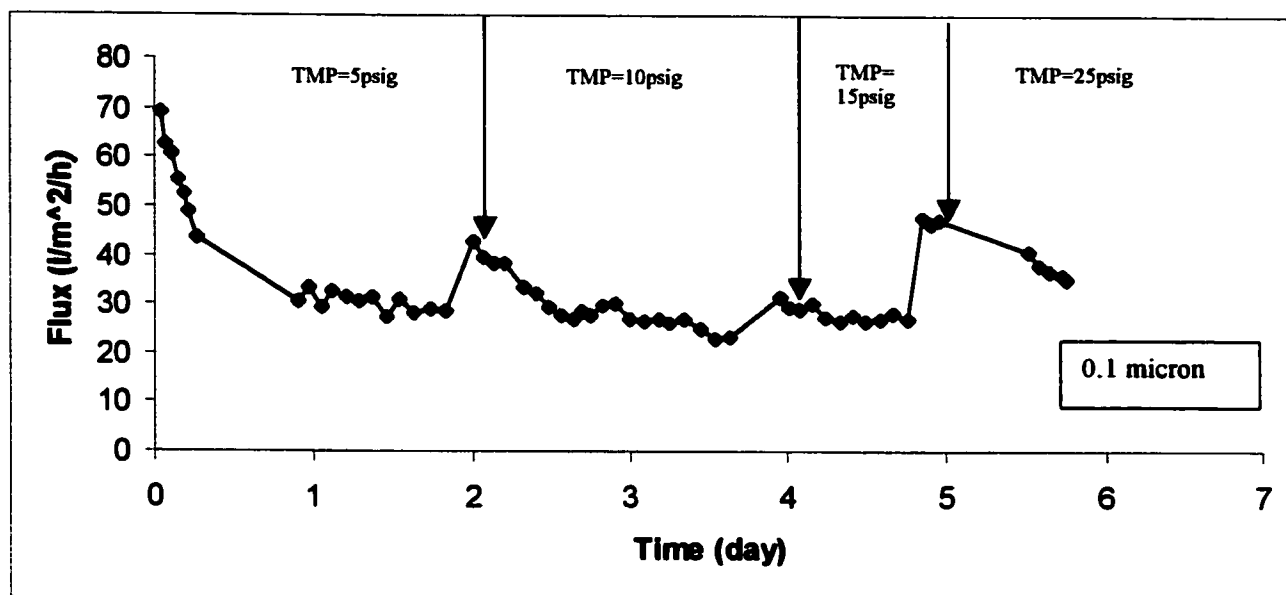


Figure 5.14: Plot of Flux vs. Time for the KOCH Carbo-Cor 0.1 micron membrane at different TMP (25°C).

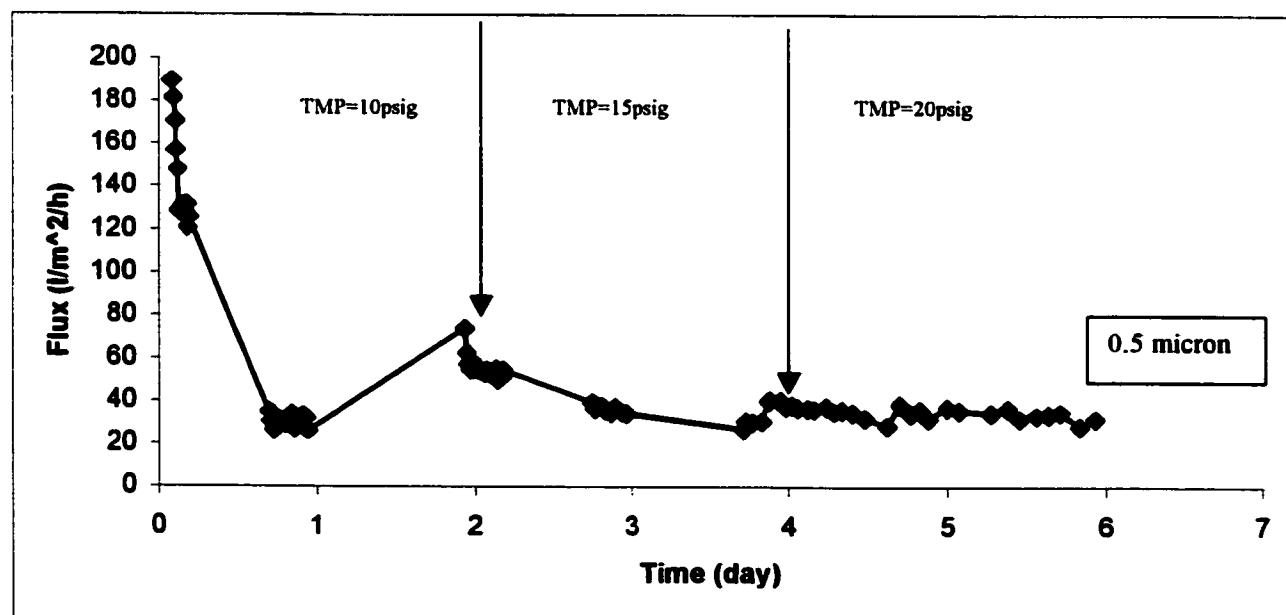


Figure 5.15: Plot of Flux vs. Time for the KOCH Carbo-Cor 0.5 micron membrane at different TMP (25°C).

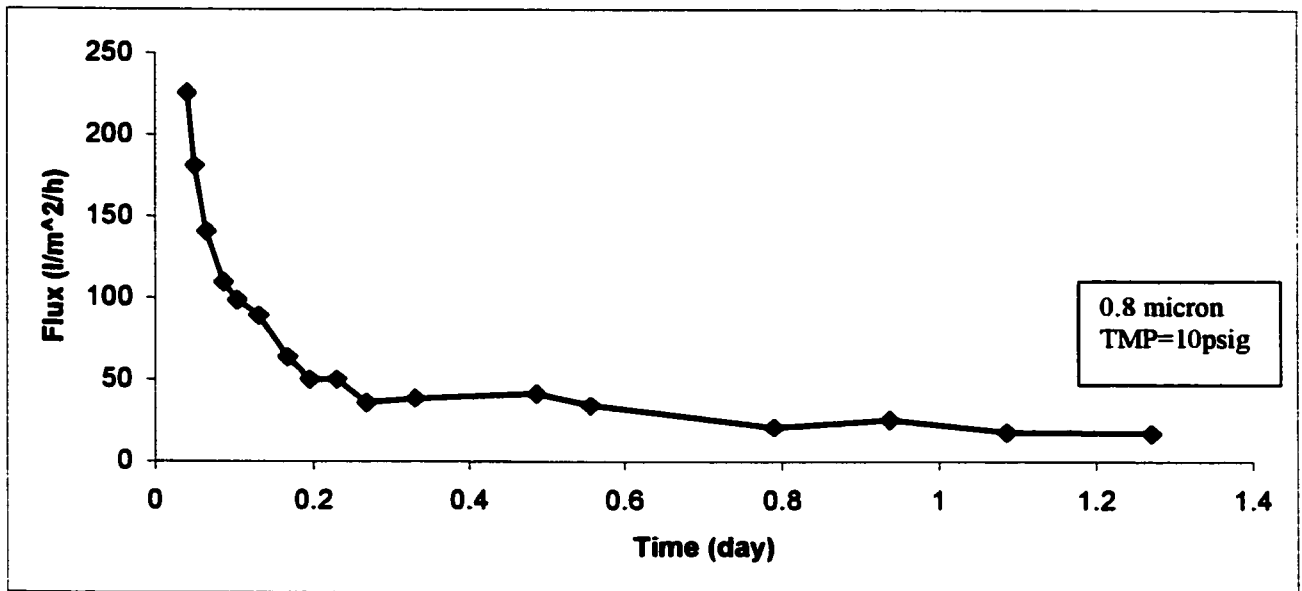


Figure 5.16: Plot of Flux vs. Time for the KOCH Carbo-Cor 0.8 micron membrane at TMP=10psig (25°C).

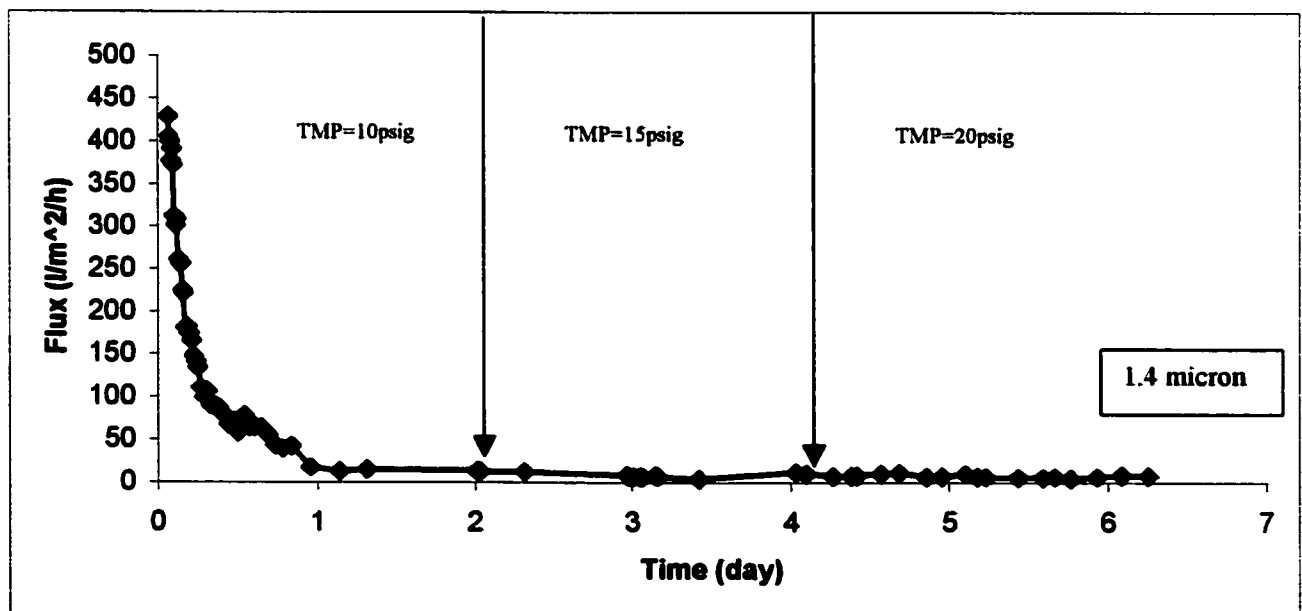


Figure 5.17: Plot of Flux vs. Time for the KOCH Carbo-Cor 1.4 micron membrane at different TMP (25°C).

### **5.2.1.2 Effect of TMP on the TAMI Céram multilumen membranes**

For the smaller pore size membranes (50 kD, 150 kD, 300 kD & 70nm), tests were performed by changing the TMP from 0.5 barg (7.34 psig) to 1 barg (14.67 psig). These membranes were tested without backflushing. Different TMPs were also applied to the larger pore size membranes (0.8 and 1.4 micron) but with backflushing as this was clearly needed from the results obtained with the Carbo-cor membranes, see section 5.2.1.1 above.

Experimental results have been plotted in Figures 5.18 to 5.20 below. As seen in Figure 5.18, for the TAMI 50 kD, 150 kD, 300 kD and 70nm membranes, increasing of TMP from 0.5 barg (7.34 psig) to 1 barg (14.67 psig) resulted in an increasing permeate flux. The flux of the smallest pore size membrane (50 kD) only increased about 10% while the other membranes increased significantly. The results of the TAMI 0.8 micron membrane is different. It is found that flux could not be increased by increasing the TMP although flux was maintained at approximately 100 l/m<sup>2</sup>/h over the four days run. Test results for TAMI 1.4 micron membrane have been plotted in Figure 5.20. A steep decline in permeate flux occurred during the first hour of operation and backflushing (3secs/5min at 35 psig) did not bring the permeate flux back to an acceptable level. The membrane was then cleaned with KLDII solution. A new run was performed at higher backflushing pressure (55 psig) after cleaning. However, increasing the backflushing pressure to 3.79 barg (55 psig) offered little benefit for this membrane.

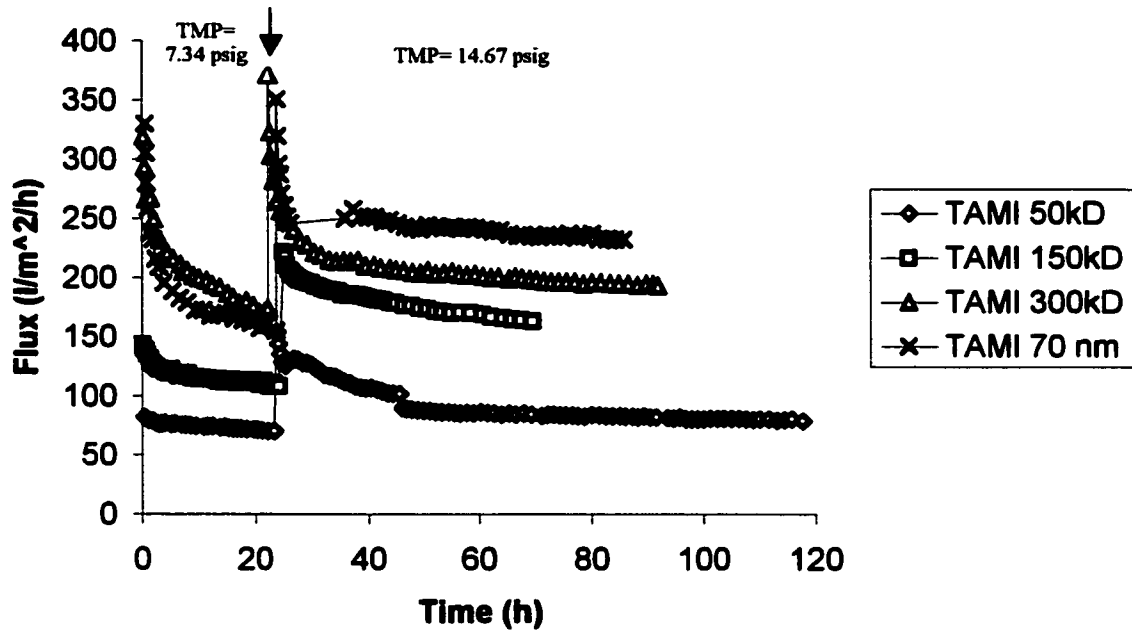


Figure 5.18: Plot of flux vs. time for the TAMI 50 kD, 150 kD, 300 kD and 70nm membranes running at different TMP (35°C).

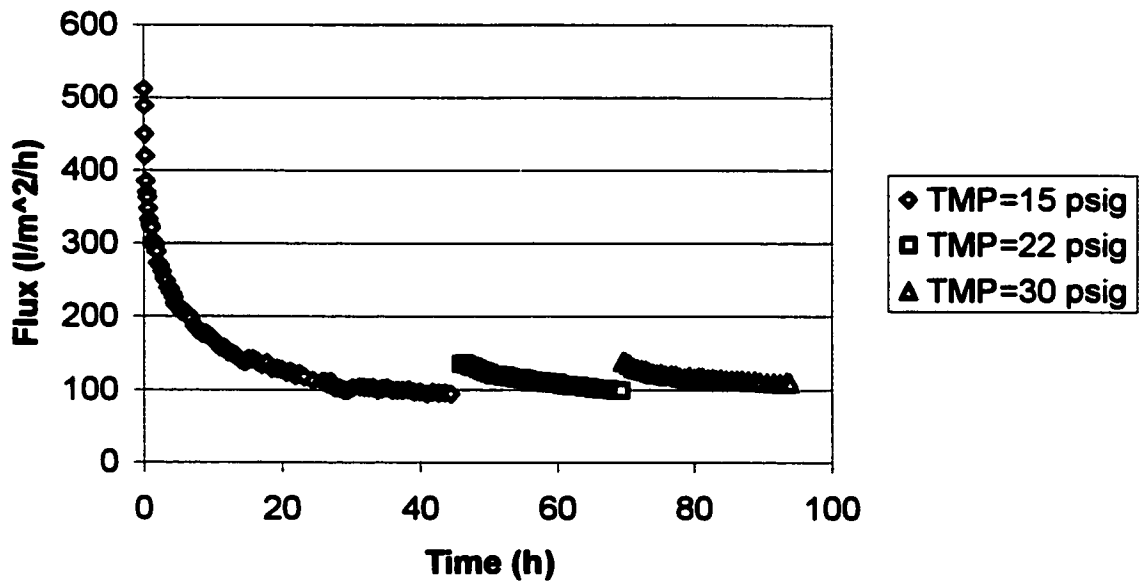


Figure 5.19: Plot of flux vs. time for the TAMI 0.8 micron membrane with different TMP (Backflushing 3secs/5min at 35 psig, 35°C).

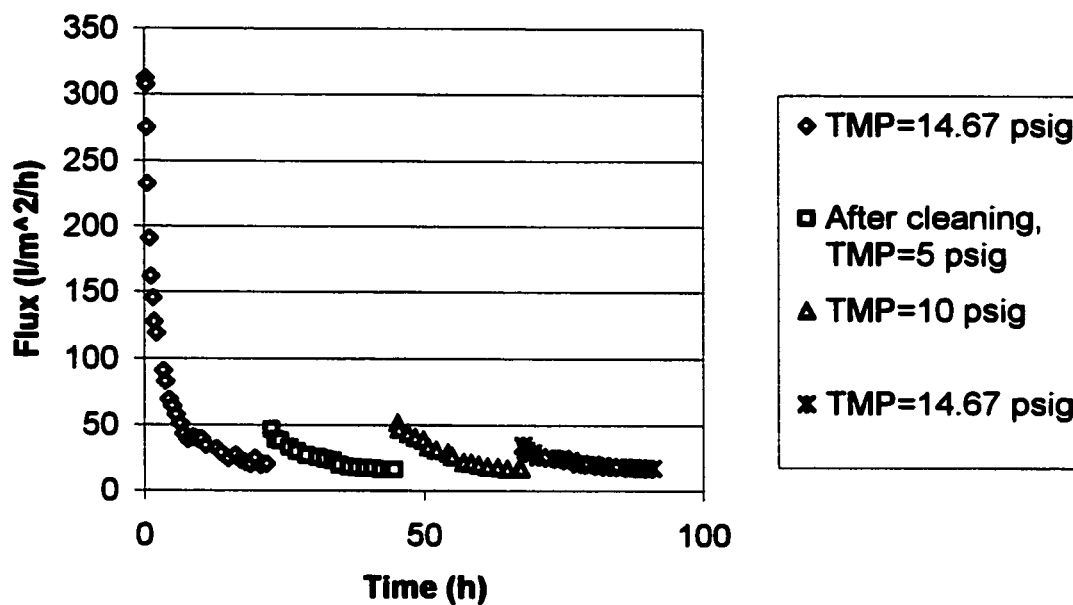


Figure 5.20: Plot of flux vs. time for the TAMI 1.4 micron membrane with different TMP (Backflushing 3secs/5min at 35 psig for the first 22 hours of operation. Backflushing 3secs/5min at 55 psig for the remainder of operation, 35°C).

### 5.2.2 Effect of backflushing on tubular membranes

As described in the literature review section, by using backflushing, a ten-fold increase in permeate flux for treatment of aqueous clay suspensions was reported (Ramirez and Davis, 1998) and up to six-fold increase in the mass flux of a target enzyme was obtained for the treatment of yeast homogenate suspensions (Levesley and Hoare, 1999). Comparative tests using the KOCH Carbo-cor membranes with backflushing and without backflushing were performed. Permeate production was calculated by integrating the flux vs. time curve over a 24 hour period. Results are shown in Figure 5.21 below. Results for the 0.05 and 0.1 micron membranes were obtained at a TMP of 1.72 barg (25 psig) while those for the 0.8 and 1.4 micron membranes were produced at a TMP of 0.34 barg (5 psig). As seen in Figure 5.21, with backflushing, the permeate production was 5-8 times more than that without backflushing. The results also indicate that in the absence of backflushing, membrane productivity is relatively independent of pore size.

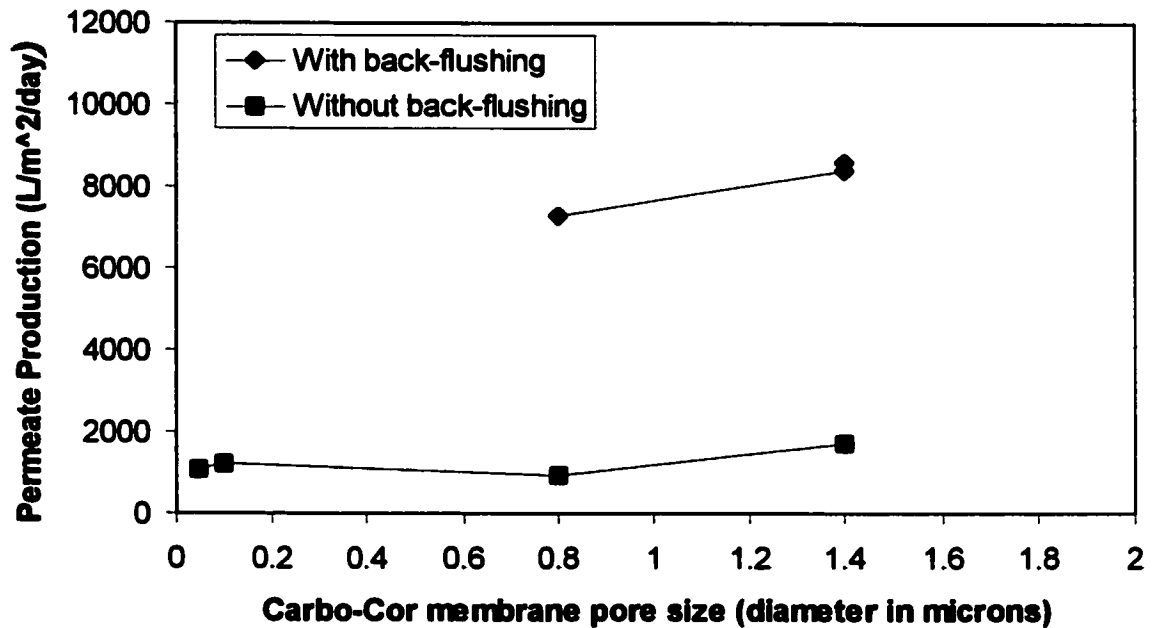


Figure 5.21: Permeate production/m<sup>2</sup>/day vs. membrane pore diameter. Back-flushing runs were performed using the MF/UF hybrid system (Back-flush using UF permeate, effective back-flushing TMP=2.41 barg (35 psig), for 3 sec/ 5 min, based on newly prepared bilge water containing 4 g/l of O & G + detergents).

### 5.2.2.1 Backflushing frequency

Backflushing frequency is an important factor affecting membrane performance when using backflushing technology. Srijaroonrat et al. (1999) used ceramic membranes to evaluate the treatment of an unstable secondary emulsion and found that, when applying backflushing, the optimum forward filtration and reverse filtration times were 1 min and 0.7 s, respectively. An optimum backflushing frequency of 1 min and duration of 1s was found by Vigneswaran and co-workers (1996) using membrane microfiltration of filter backwash water from a wastewater treatment plant. Three different backflush times were tested using the Carbo-cor 1.4 micron pore size membrane to investigate the influence of backflushing frequency for the treatment of synthetic bilge water:

- i) BT 297-3 (Backflushing Tests with forward filtration 297 seconds, then reverse filtration 3 seconds), backflushing time 1% of the full cycle;
- ii) BT 294-6 (Backflushing Tests with forward filtration 294 seconds, then reverse filtration 6 seconds), backflushing time 2% of the full cycle; and
- iii) BT 895-5 (Backflushing Tests with forward filtration 895 seconds, then reverse filtration 5 seconds), backflushing time 0.56% of the full cycle.

Results are shown in Figure 5.22 below. A steep flux decline was found when the backflushing time was 895-5. This indicates that the forward filtration time is too long or the reverse filtration time is too short for the permeate to remove the particles accumulated on and within the membrane. With a backflushing time of 1% and 2% of the full cycle, flux declined gradually to higher steady-state levels. Forward filtration 297 seconds, then reverse filtration 3 seconds was found to be the best backflushing cycle for the treatment of bilge water.

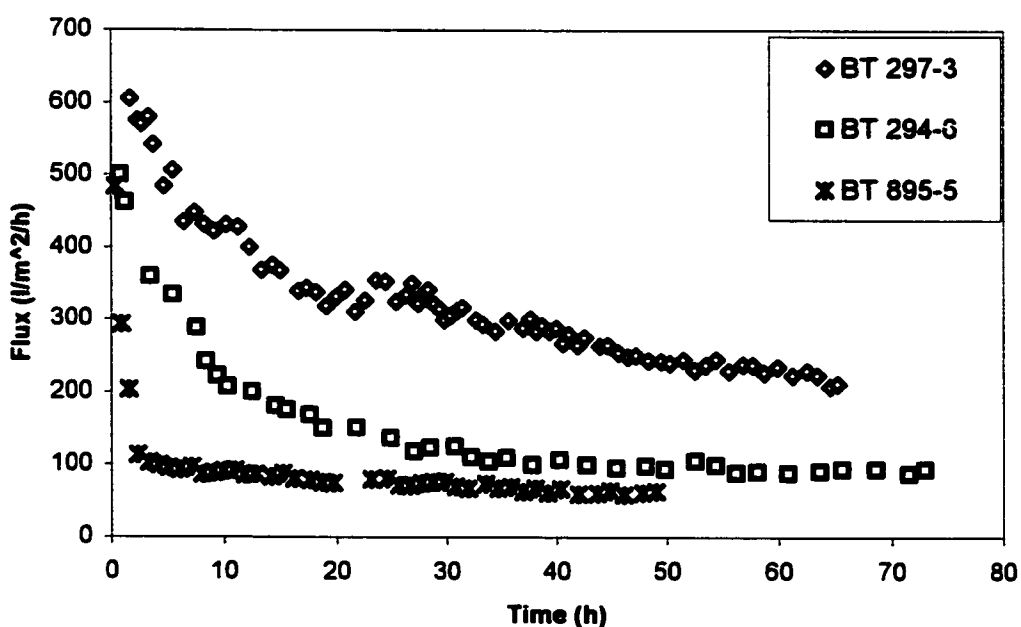


Figure 5.22: Plot of flux vs. time for the KOCH Carbo-cor 1.4 micron membrane with different backflushing time (TMP=5 psig, 35°C, backflushing pressure 35 psig).

### **5.2.2.2 Backflushing pressure**

The effect of backflushing pressure on membrane performance was studied in this section. Tests using various backflushing pressures (20, 25, 35 and 45 psig) were conducted on the KOCH Carbo-cor 0.8 and 1.4 micron membranes at TMP of 0.34 barg (5 psig). Experimental results are shown in Figures 5.23 and 5.24. They indicate that higher pressures are beneficial in this application. The permeate flux increases with the increasing of the backflushing pressure.

For the KOCH Carbo-cor 0.8 micron membrane, flux was maintained at 200 l/m<sup>2</sup>/h when applying a 35 psig backflushing pressure. For the KOCH Carbo-cor 1.4 micron membrane, the flux increased about 50% at the higher backflushing pressure. However, the 3.1 barg (45 psig) backflushing pressure had to be reduced because 3.1 barg (45 psig) differential was considered to be somewhat high for these membranes. At this backflushing pressure, 4.82 barg (70 psig) was applied to the permeate while the feed remained at its operating pressure of 1.72 barg (25 psig) within the loop. The Carbo-cor membranes are rated at a maximum TMP of 3.4 barg (58 psig). If the feed pressure were to drop to zero, a 4.82 barg (70 psig) would be applied across the membrane. This would exceed the safe forward operating pressure. These membranes were made by coating a carbon tube with a selective layer of scintered carbon particles. Backflushing could detach this layer from the support tube. A backflushing pressure of 2.41 barg (35 psig) was considered to be a safe limit in order to prevent the release of the selective layer.

The effect of backflushing pressure can also be found in the literature. Nakatsuka et al. (1996) studied effect of backflushing in drinking water treatment using ultrafiltration hollow fiber membrane and concluded that in order to maintain a constant high flux, the backflushing pressure should be more than twice the forward filtration pressure.

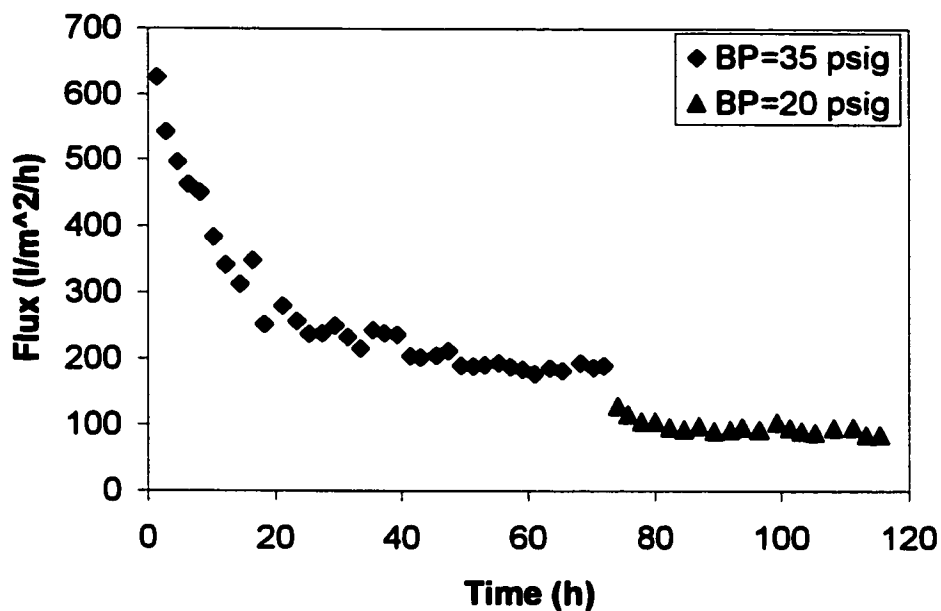


Figure 5.23: Plot of flux vs. time for the KOCH Carbo-cor 0.8 micron membrane with different backflushing pressure (TMP=5 psig, 25°C, BT 297-3).

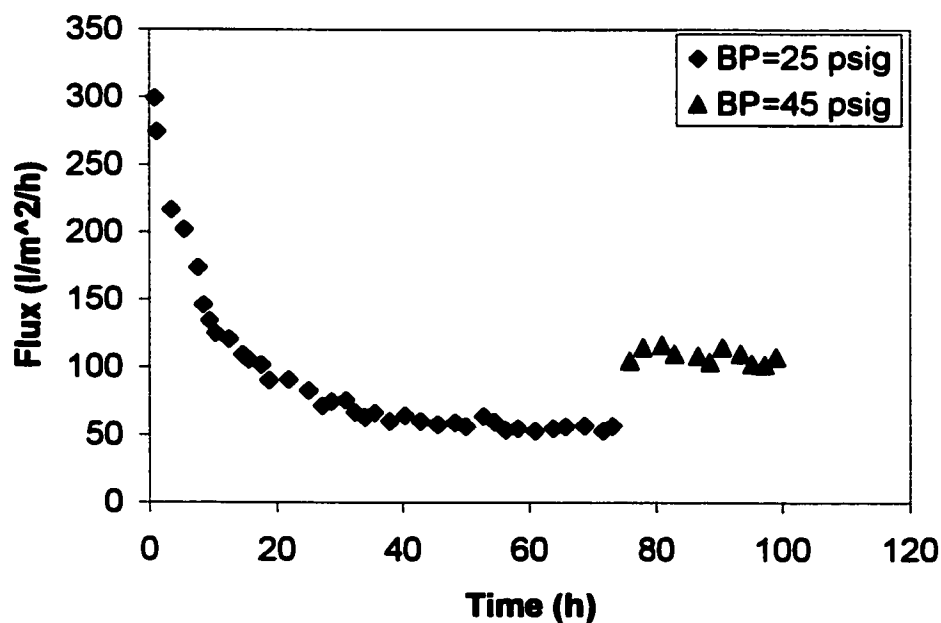


Figure 5.24: Plot of flux vs. time for the KOCH Carbo-cor 1.4 micron membrane with different backflushing pressure (TMP=5 psig, 25°C, BT 294-6).

### 5.2.2.3 Type of membrane

In order to compare the performance of KOCH and TAMI membranes when applying backflushing, two runs were conducted using the TAMI 1.4 micron membrane and the KOCH Carbo-cor 1.4 micron membrane under the same operating conditions. Experimental results from these runs have been plotted in Figure 5.25 below. The results clearly show that the effect of backflushing and TMP are different for different types of membranes. Increasing the TMP had little effect on the performance of TAMI 1.4 micron Céram membrane but had a significant effect on the KOCH Carbo-cor 1.4 micron membrane. By increasing TMP, the permeate flux of the KOCH Carbo-cor 1.4 micron membrane increased dramatically and could be easily maintained at 150 l/m<sup>2</sup>/h or higher.

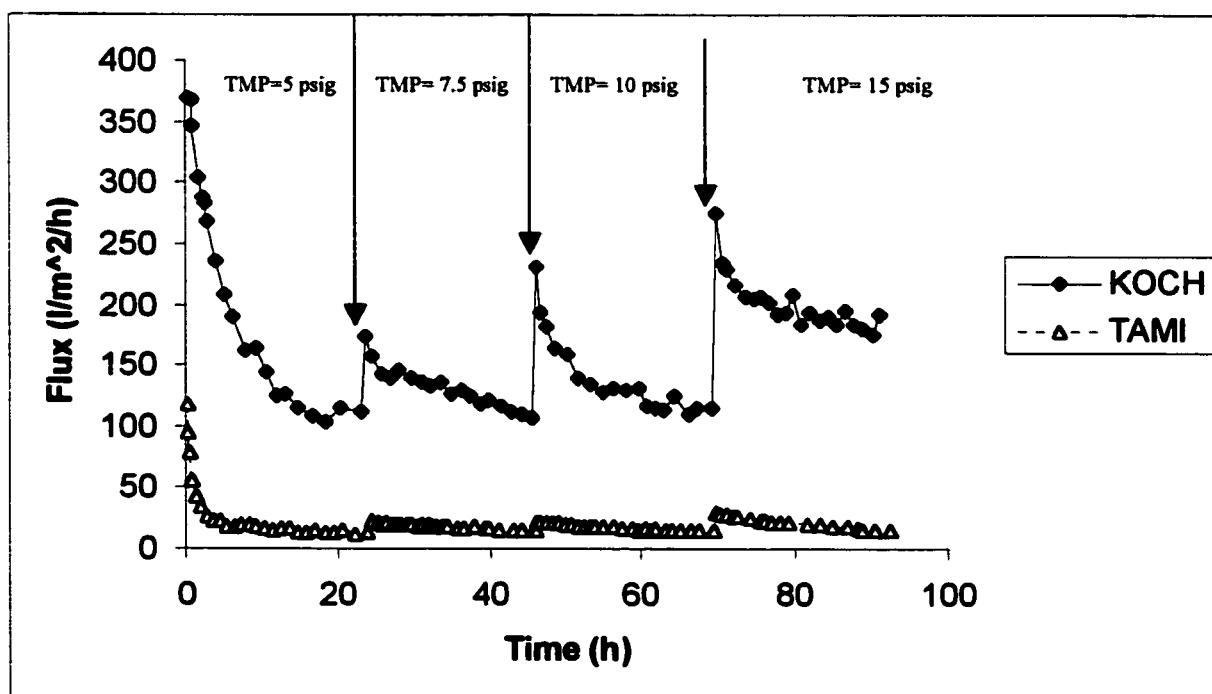


Figure 5.25: Plot of flux vs. time for the KOCH Carbo-cor 1.4 micron and TAMI Céram 1.4 micron membrane for different TMPs (Both membranes were backflushed for 3 seconds out of a 5 minutes cycle at 35 psig, 35°C).

The results indicate that these major differences that can be attributed to the support structure of these membranes. The different support structures of the two membranes are shown in Figure 5.26 below. Both membranes are reported to have 1.4 micron pore size but their support structures are different. The KOCH Carbo-cor membrane is layered inside a single porous carbon tube having a 10 to 14 micron pore size. This construction provides excellent clearance, as particles entering the support layer must travel a short distance before exiting. The TAMI membrane is a multilumen membrane with a complex support. The pore size of the support is not known. The clearance for this membrane is lower than the Carbo-cor membrane. Sub 1.4 micron particles passing through the selective layer of the membrane must travel through the supporting bridges of the star shaped tube before leaving the membrane. This leads to a substantial accumulation of the particles in the support and reduces the permeate flux. The arrows in Figure 5.26 indicate paths for the particles during the permeation run. Only the outer circular area of the membrane offers good clearance while clearance for the remaining area is rather poor. The construction used in the multilumen membrane would not be recommended in a backflushing operation to treat this wastewater.

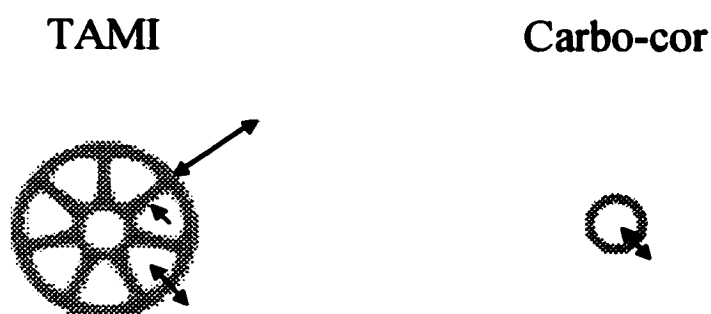


Figure 5.26: Different support structure of the TAMI Céram and KOCH Carbo-cor membranes.

### **5.2.3 Membrane cleaning**

#### **5.2.3.1 Chemical cleaning**

Proper cleaning is very important in membrane flux regeneration. Three different cleaning methods were conducted for the KOCH Carbo-cor 0.1 micron membranes after a 6 day permeation run. These are as follows;

1. Clean with KLDII solution for 30 minutes with concentration 10 mL/L at 2.07 barg (30 psig, from feed side), 40 °C then rinse with RO water.
2. Clean with 1% NaOH solution at 2.07 barg (30 psig, from feed side), 40 °C, for 30 minutes, rinse with RO water, then backflush with air for 5 minutes at 2.07 barg (30 psig, from feed side).
3. Clean with 1% NaOH solution at 2.07 barg (30 psig, from feed side), 40 °C, for 30 minutes then rinse with RO water.

Caustic solutions are often used to clean inorganic membranes. They are sparingly used to clean polymeric membranes as repeated use leads to polymer degradation and reduced membrane life. Figure 5.27 shows the regenerated flux for the KOCH Carbo-cor 0.1 micron membrane for the three different cleaning methods described above.

Cleaning methods 2 and 3 regenerated the membrane to a greater extent than the first method. KLDII was recommended by the membrane manufacturer but was not as effective as NaOH. Cleaning with 1% NaOH and backflushing with air gave the highest flux. The results suggest that the cleaning mechanisms for KLDII and NaOH are very different. KLDII relies on the solubilisation of oil and grease by the formation of miscelles, while NaOH degrades most greases and detergents. Treating these membranes with NaOH and then backflushing with air would produce a cleaning solution that could be neutralized and further processed through an OWS eliminating the need for a cleaning solution holding tank. This cleaner would be inexpensive and environmentally benign. It would however require the handling of strong acids and

bases onboard a ship. Handling acids and bases onboard a ship is to be avoided, as spills are difficult to clean and remain a major safety concern.

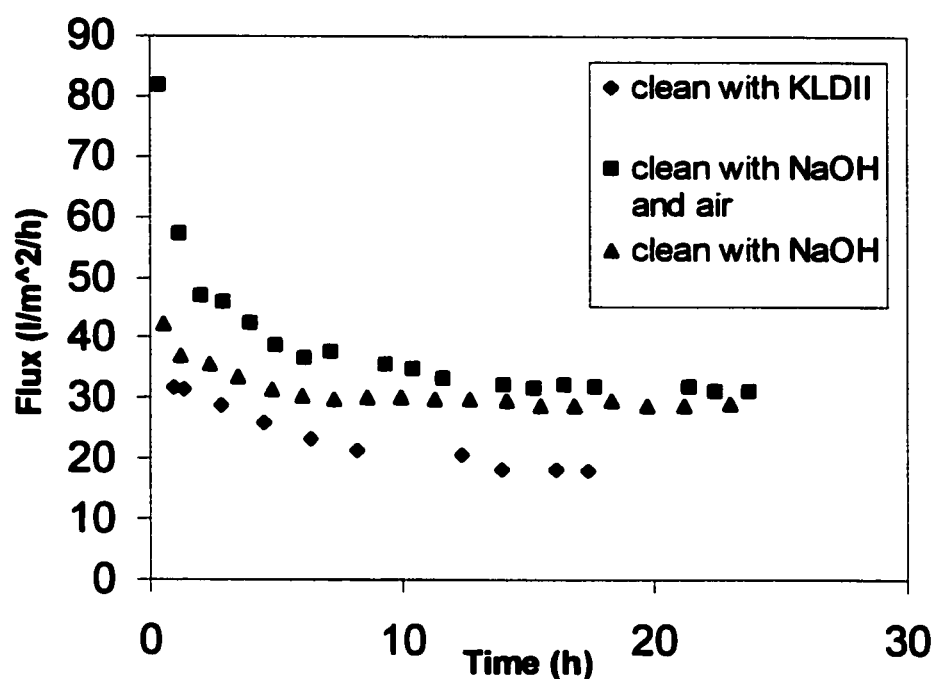


Figure 5.27: Plot of Flux vs. Time for the KOCH Carbo-cor 0.1 micron membrane after cleaning (TMP=25 psig, 25°C).

### 5.2.3.2 Non-chemical cleaning

In order to further study environmentally friendly cleaning methods for membrane flux regeneration, hot water, air and pressured steam were used to clean the KOCH Carbo-cor 1.4 micron membrane. During the permeate run, small particles and oil emulsions present in synthetic bilge water can penetrate inside the 1.4 micron membrane pores. Visual observations indicate that free oil is also present in bilge water. Should these smaller particles enter the pores of the membrane, they can coalesce and block the pores.

Air backflushing is a simple technology that can be used to flush oil out of membrane pores. Heating the membrane should further enhance the removal of oil. Heat will reduce the viscosity of the free/emulsified oil blocking the membrane pores. The

temperature of the membrane prior to air backflushing will affect the removal of oil. Higher temperatures will produce a membrane having a greater number of open pores. Hot water cleaning was done by emptying the feed loop and circulating hot water on the permeate side of the MF membrane for 10 minutes. The membrane was then backflushed with air at 4.13 barg (60 psig) for 10 minutes. It was then back-flushed with 100 to 200 mls of UF permeate at 4.13 barg (60 psig). Steam at 2.41 barg (35 psig, 126 °C) was also used to regenerate the membrane. The KOCH Carbo-cor membranes with fitted O-rings are rated, for continuous operation, at 165 °C and can easily withstand these temperatures. In this procedure, pressurized steam was applied on the permeate side of the membrane and allowed to flow for 2 to 20 minutes. The membrane was then backflushed with air followed by UF permeate as described in the hot water cleaning method.

The results of these tests using different cleaning methods are summarized in Figure 5.28 below. The results for steam cleaning can be found in Figure 5.29.

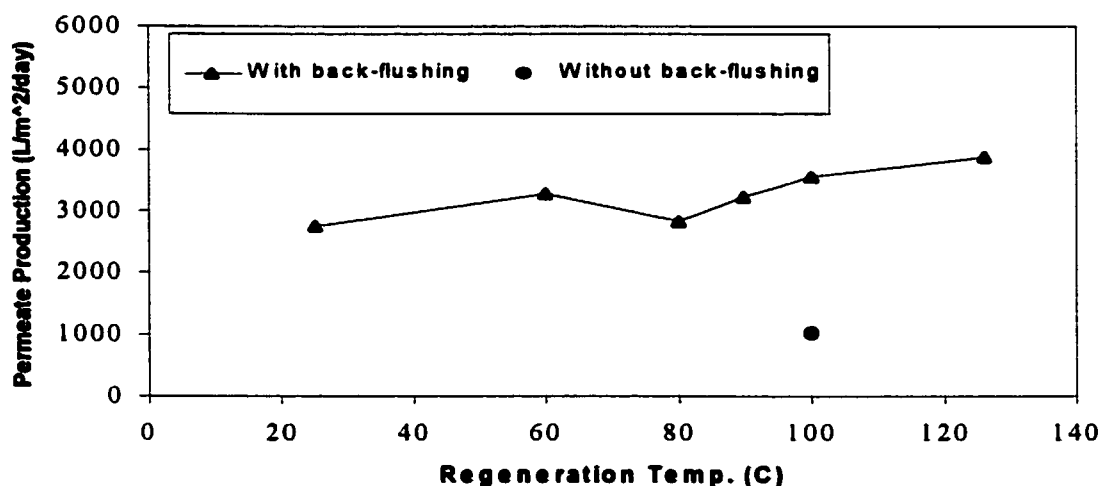


Figure 5.28: Plot of permeate production vs. regeneration temperature for the KOCH Carbo-cor 1.4 micron membrane. Data as measured for a 6 to 8 g/l O & G + detergent bilge water concentration. (TMP=5 psig, backflushing pressure 35 psig).

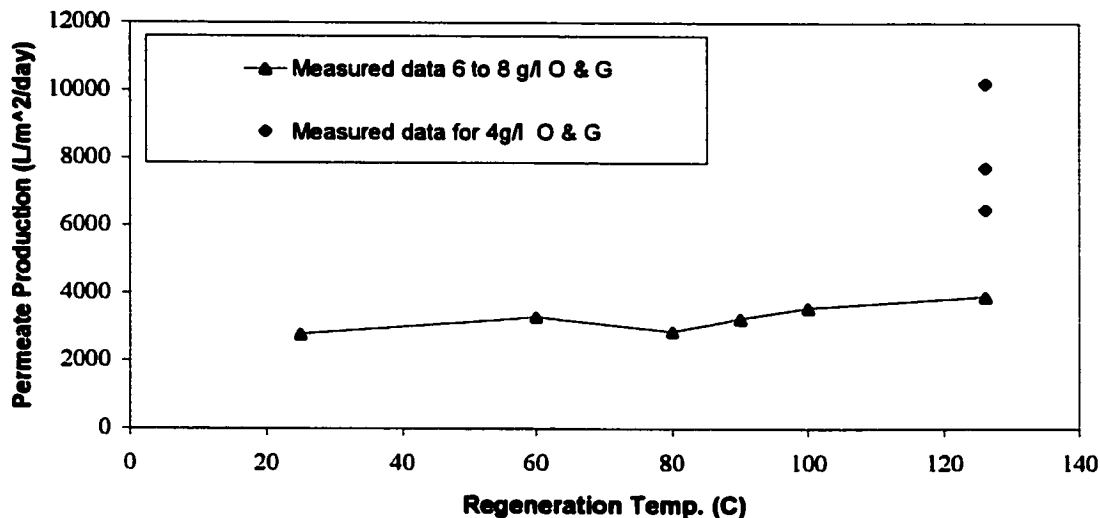


Figure 5.29: Plot of permeate production vs. regeneration temperature including the runs with steam cleaning. Measured flux is for a bilge conc. of 6 to 8 g/l O & G + detergent. (TMP=5 psig, backflushing pressure 35 psig).

The results in Figure 5.28 clearly illustrate the necessity for backflushing for the 1.4 micron membrane. They also indicate a gradual increase in permeate production with the regeneration temperature. The O & G concentration for fresh bilge water was 4g/l, it increased over the course of the experiments due to evaporation and permeate losses when the UF system was cleaned. The results in Figure 5.29 indicate that the greatest benefits are for regenerations performed at the higher temperatures of 100 and 126 °C. This indicates that the particles present in membrane pores were most likely coalesced free oil or large miscelles. Used free oil is rather viscous and is more easily flushed out of membrane pores at higher temperatures. The procedure involving steam, air backflushing followed by UF permeate was very effective in removing coalesced oil from these membranes pores. This was also evidenced by visual observations of the Carbo-cor tube before and after steam cleaning. The exterior of the tube was covered in a layer of sooty oil, that had a characteristic used oil smell. The cleaned membrane had little if any smell and a grey, mat appearance as observed with the new “as received” Carbo-cor tubes.

A series of runs were performed after these cleaning tests. The results of these runs have been plotted in Figure 5.30 below. They demonstrate the ease of regeneration for the 1.4 micron MF membrane and its ability to consistently provide average permeate fluxes above 100 l/m<sup>2</sup>/h for bilge water containing 6 to 8 g/l O & G + detergent. The first 5 runs all produced average flux rates above 100 l/m<sup>2</sup>/h. Back-flushing pressure was not applied to the permeate for the 6<sup>th</sup> run. This rapidly produced much lower flux rates. At the end of the run, the flux was 39 l/m<sup>2</sup>/h. The fouled membrane was easily regenerated with hot water at 100 °C. The 7<sup>th</sup> run produced excellent results. For the 8<sup>th</sup> run, the MF membrane was back-flushed with MF permeate instead of UF permeate. This leads to a final flux of 72 l/m<sup>2</sup>/h which is much lower than the flux of 96-110 l/m<sup>2</sup>/h obtained from runs backflushed with UF permeate. The membrane was then treated with steam for 5 minutes and then flushed with air on both sides to remove any particles that had accumulated in the back-flushing process. The 9<sup>th</sup> run in Figure 5.30 was excellent starting at 368 l/m<sup>2</sup>/h and ending, after 23 hours, at 110 l/m<sup>2</sup>/h, producing 3883 l/m<sup>2</sup>/day at the 8 g/l feed concentration.

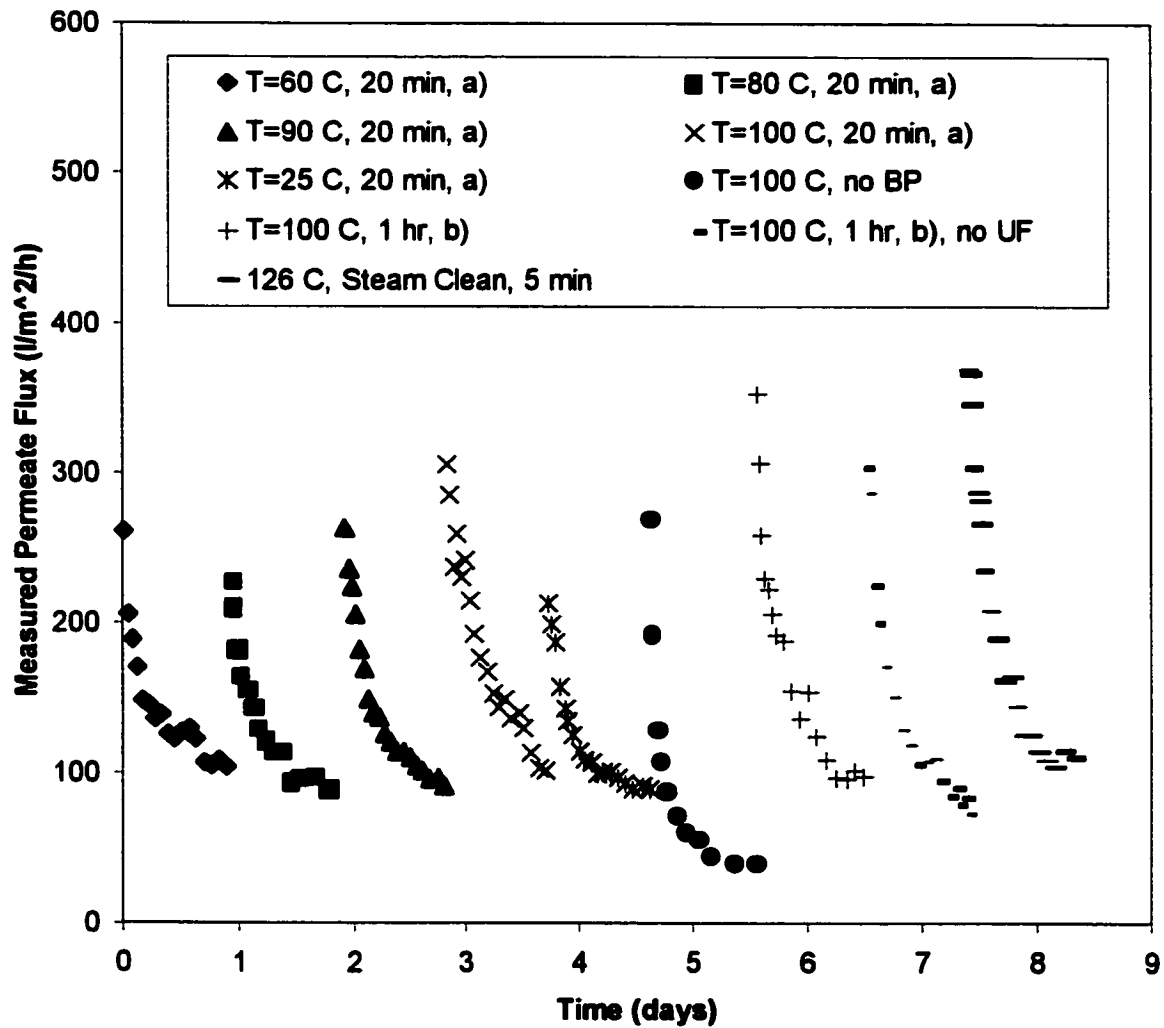


Figure 5.30: Plot of the measured permeate flux vs. time in days. Heating was performed by circulating hot water on the permeate side of the membrane: a) with feed solution inside MF loop, and b) with feed side of MF loop empty. Steam cleaning runs were performed by applying steam on permeate side of the MF membrane while the feed side was open to atmosphere. All runs were performed with backflushing at 35 psig. Measured permeate flux is for bilge water containing 6 to 8 g/l of Oil and Grease + detergent.

### 5.3 Pore size of tubular membranes

#### 5.3.1 KOCH Carbo-cor tubular membranes

In order to determine the effect of membrane pore size on flux reduction, a series of experiments were conducted with different pore size KOCH Carbo-cor membranes. These tests were performed in the experimental set-up shown in the MF/UF hybrid system (Figure 4.2) without using the UF loop, with standard amount of oils, detergents and surfactants in bilge water (2 g/l). Experimental results are summarized in Figure 5.31. The 0.05, 0.1 and 0.2 micron membranes were tested without backflushing and the 0.5 micron membrane with backflushing for 48 hours then without backflushing for the remainder of the run. The 0.1 and 0.2 micron membranes were washed after the first 24 hours of operation.

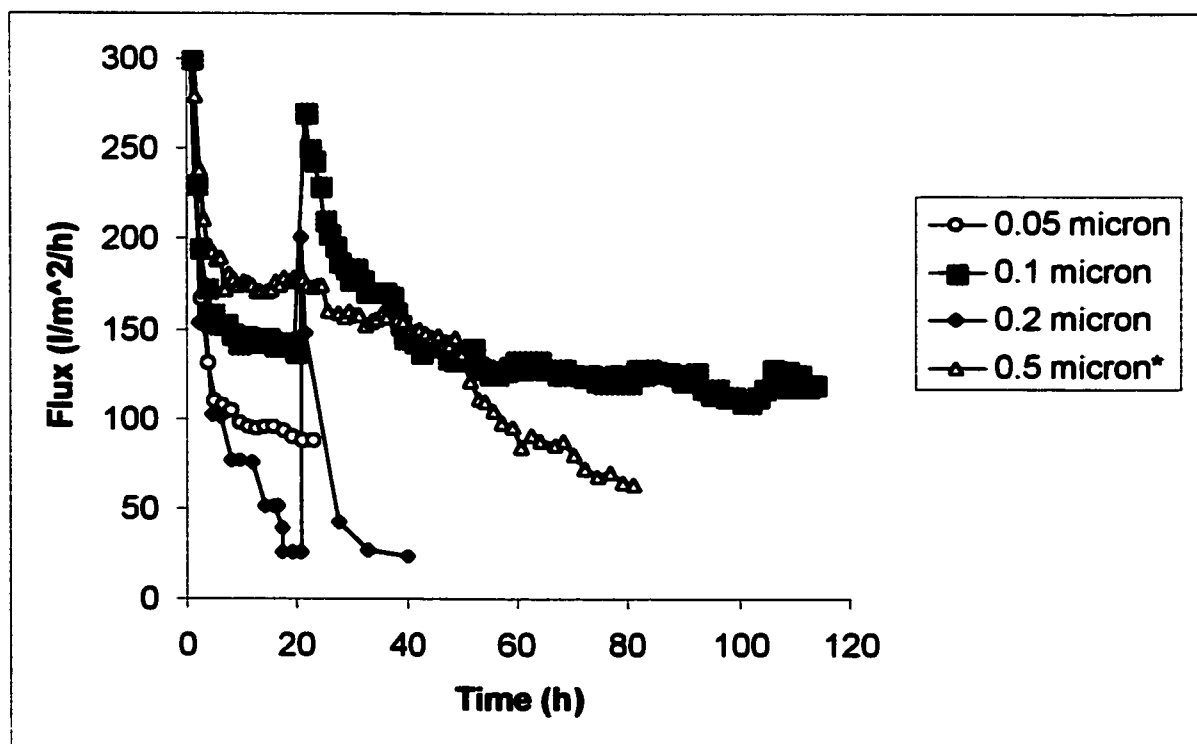


Figure 5.31: Plot of permeate flux vs. time for various KOCH Carbo-cor tubular membranes (Operating pressure 35 psig, 25°C).

\* Backflushing up to 48 hours then no backflushing.

As seen in Figure 5.31, the 0.1 micron membrane had an impressive sustained performance during six days of operation. Permeate flux declined to an unacceptable level for the 0.2 micron membrane after the first day of operation. Flux for the 0.5 micron membrane was 150 l/m<sup>2</sup>/h for the first 2 days with backflushing, when the backflushing stopped, a steep decline in flux was observed. These results show that the 0.2 micron pore size membrane is not a good choice for synthetic bilge water treatment. The results also indicate the effect of particles found in bilge water on the performance of the membranes. Tremblay and Nottegar (2000) studied the particle size distribution in synthetic bilge water. Their findings are shown in Figure 5.32 below. One particle distribution was centered around a size of 0.18 microns (0.089 micron radius) and the larger was centered around 2.68 microns (1.34 micron radius). The lower end of the larger size distribution was 1.8 microns (0.9 micron radius). In the presence of such particles, maximum pore blockage is expected for microfilters with pores falling in the 0.14 to 0.2 micron diameter range. Membranes having a pore size just below the value of 0.14 micron would have the best performance while those within the range are expected to be totally blocked and the larger pore sizes membranes would need backflushing to remove the gradual accumulation of particles within the pores. This is in excellent agreement with what is observed in Figure 5.31 above.

Therefore, membranes with a pore size below or above 0.2 micron should be used for synthetic bilge water treatment. Membranes with pore sizes lower than 0.2 micron do not require backflushing, while membranes with pore sizes higher than 0.2 micron need to be backflushed to remove the accumulated particles within the pores.

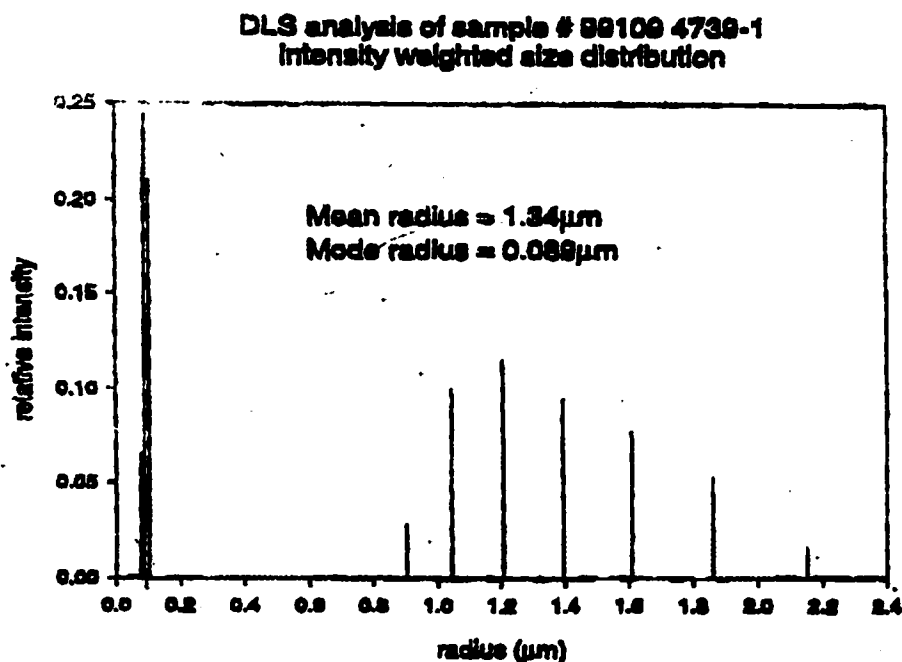


Figure 5.32: Particle size distribution for used oil. DLS measurements. Peaks for the smaller radii are at 0.07, 0.089 and 0.1 microns (Tremblay and Nottegar, 2000).

### 5.3.2 TAMI Céram tubular membranes

Several TAMI membranes were tested to determine their performance in treating bilge water. The 0.8 and 1.4 micron pore size membranes were tested with backflushing. The smaller pore size membranes were tested without backflushing. The steady-state permeate flux data for all the TAMI membranes have been summarized and plotted in Figure 5.33 below, along with the experimental data for KOCH Carbo-cor membranes.

It was found that for the TAMI membranes, below 70 nm pore size, the permeate flux increases gradually with an increase in pore size. The highest flux is for the 70 nm pore size membrane. Above 70 nm pore size, the permeate flux decreases substantially. The largest pore size membrane (1.4 micron) has the lowest permeate flux. The estimated pore sizes for the TAMI 50 kD, 150 kD and 300 kD membranes are 16 nm, 28 nm and 34 nm, respectively. For these membranes and the 70 nm pore size membrane, the 0.18

micron particle found in synthetic bilge water was totally excluded from the membrane pores. Backflushing was applied to both types of larger pore size membranes (0.8 micron and 1.4 micron). The steady-state permeate fluxes for the larger pore KOCH Carbo-cor membrane were found to be higher than those of the TAMI membranes. However, the lower pore sized TAMI membranes had a better performance than the Carbo-cor membranes.

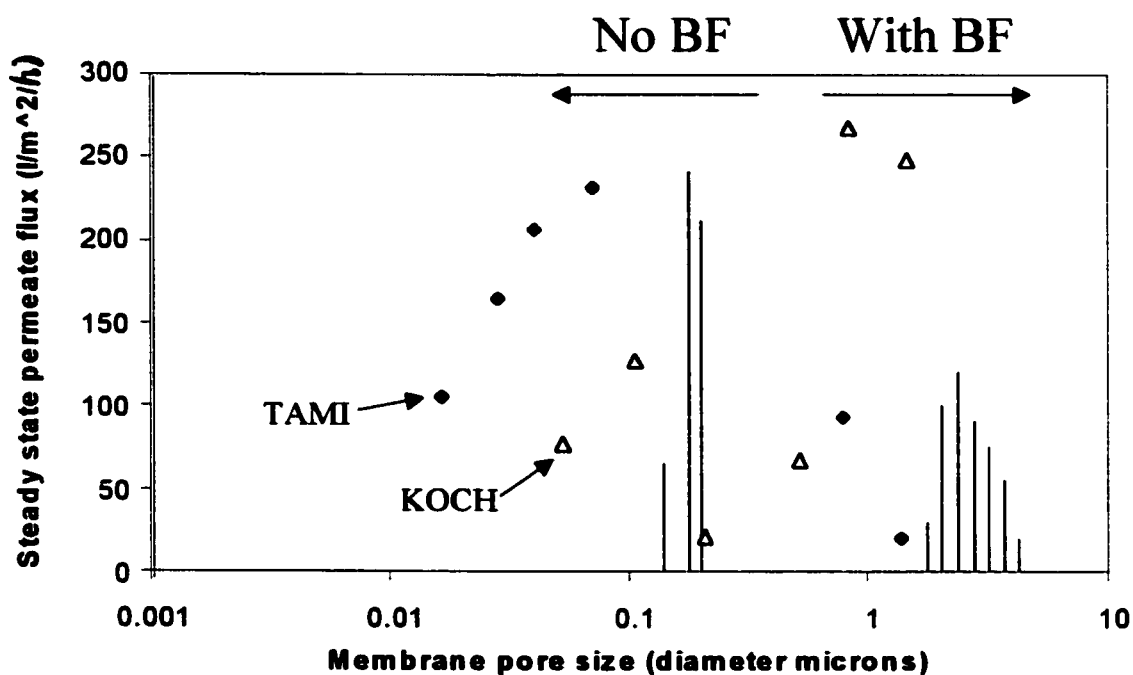


Figure 5.33: Plot of steady-state permeate flux vs. membrane pore size for the various TAMI and KOCH Carbo-cor membranes (TMP=14.67 psig, 35°C).

## 5.4 Modeling and specific cake resistance

### 5.4.1 Modeling of filtration mechanisms

It is important to study the filtration mechanisms of the membranes tested in this work to determine the mechanisms of flux decline. One of these methods is to apply filtration models to the flux decline of these membranes and estimate the filtration characteristics. As described in the theory section, four filtration models were introduced for constant pressure filtration: the complete blocking model, the intermediate blocking model, the pore constriction model and the cake filtration model.

The complete blocking model assumed that each particle reaching the membrane seals the pores and the particles are not superimposed one upon the other. The intermediate blocking model assumed every particle does not block a pore; in this scheme, particles can settle on other particles and block a pore. In the pore constriction model, it is assumed that the pore volume decreases proportionally to filtrate volume by particle deposit on the pore walls. In the cake filtration model, the particles are larger than the pores. It is assumed that the flux decline is due to the accumulation of a cake at the surface of the membrane and that cake thickness increases proportionally with the volume of permeate produced.

These different filtration models have been applied to all the KOCH Carbo-cor and the TAMI Céram membranes tested in this work. All results presented in this section are for the permeation of bilge water without backflushing. Since the objective of this section was to differentiate between pore blocking, constriction and cake formation, modeling analysis focused on the first time the membrane was tested with bilge water. Table 5.4 below shows the operating conditions and the sum of square of residuals defined as the difference between the observed flux and the predicted flux squared for the four models listed in Table 3.1. Table 5.5 shows the filtration constants being used for applying the filtration models. Figures 5.34 to 5.45 show the results of applying the different models to these membranes. The filtration mechanisms of these membranes can be estimated from the modeling results.

For membranes with pore sizes less than 0.2 micron, including the KOCH Carbo-cor 0.05 and 0.1 micron pore size membranes and TAMI Céram 50 kD, 150 kD, 300 kD and 70nm membranes, the filtration mechanism is cake filtration. This is in agreement with the particle size distribution measured using dispersive light scattering (DLS). The 0.18 micron particles are larger than the membrane pores and form a cake on the surface of the membrane. For membranes with pore sizes larger than 0.2 micron, the filtration mechanisms was found to be intermediate blocking or pore constriction. These results are in excellent agreement with previous findings in section 5.3.

**Table 5.4: Operating conditions and sum of squares of residuals for the analysis of various filtration mechanism described in Table 3.1.**

Membrane (New membrane first time tested with bilge water)		Conditions		Sum of square of residuals			
		TMP (psig)	Temperature (°C)	Complete blocking	Intermediate blocking	Pore constriction	Cake filtration
KOCH	0.05 µm	5	35	430	184	287	<u>63</u>
	0.1 µm	5	35	3011	2807	2917	2811
	0.2 µm	35	35	114911	<u>49343</u>	61082	181318
	0.5 µm	10	35	26130	<u>1771</u>	9493	16205
	0.8 µm	10	35	548218	<u>32419</u>	521449	479115
	1.4 µm	10	35	62255	41244	<u>14944</u>	191785
TAMI	50 kD	15	35	4450	3447	3913	<u>2688</u>
	150 kD	7.34	35	1754	1536	1643	1336
	300 kD	7.34	35	23573	15666	19303	<u>9956</u>
	70 nm	15	35	50904	22009	34075	<u>8315</u>
	0.8 µm	5	35	869629	1418630	525043	<u>48702</u>
	1.4 µm	5	35	110365	<u>23372</u>	54784	43426

(Note: Temperature varied from 32 to 40 °C in real runs, the results in the table were corrected to 35 °C)

- The underlined sum of squares of residuals represent the model having the best fit.
- A best fit could not be determined for the 0.1 micron KOCH Carbo-cor membrane and the 150kD TAMI membrane.

**Table 5.5: Operating conditions and different filtration constants for the analysis of various filtration mechanism described in Table 3.1.**

Membrane (New membrane first time tested with bilge water)		Conditions		Filtration constants			
		TMP (psig)	Temperature (°C)	$K_{block}$ (h <sup>-1</sup> )	$K_{inter}$ (h <sup>-1</sup> )	$K_{constriction}$ (h <sup>-1</sup> )	$K_{cake}$ (h <sup>-1</sup> )
KOCH	0.05 µm	5	35	0.066	0.120	0.045	0.418
	0.1 µm	5	35	0.101	0.644	0.057	0.324
	0.2 µm	35	35	1.098	1.911	0.710	7.780
	0.5 µm	10	35	0.427	0.901	0.296	5.199
	0.8 µm	10	35	1.055	3.062	0.835	19.408
	1.4 µm	10	35	0.379	0.733	0.266	4.133
TAMI	50 kD	15	35	0.028	0.035	0.016	0.090
	150 kD	7.34	35	0.024	0.027	0.013	0.060
	300 kD	7.34	35	0.064	0.092	0.038	0.266
	70 nm	15	35	0.147	0.256	0.099	0.795
	0.8 µm	5	35	0.209	2.584	0.132	1.561
	1.4 µm	5	35	1.258	2.584	0.954	10.603

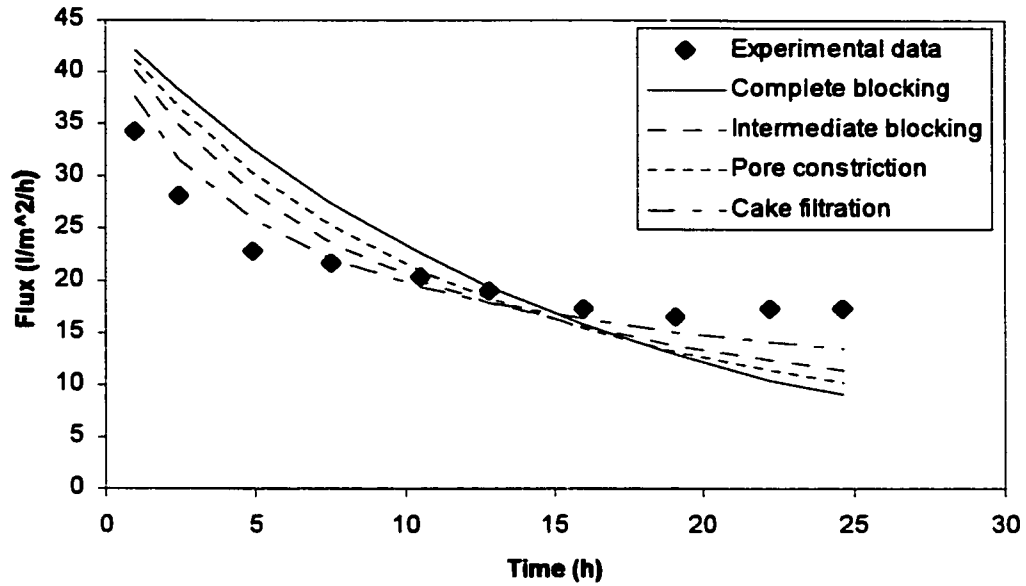


Figure 5.34: Plot of flux vs. time for the KOCH Carbo-cor 0.05 micron membrane (TMP=5psig, 35°C, see Table 5.4 for sum of the square of residuals and Table 5.5 for filtration constants).

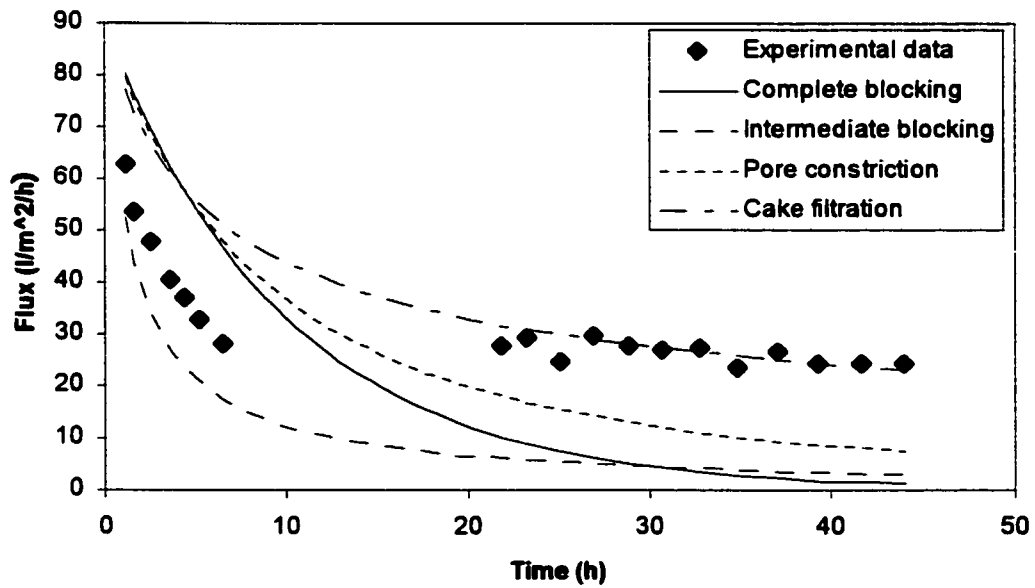


Figure 5.35: Plot of flux vs. time for the KOCH Carbo-cor 0.1 micron membrane (TMP=5psig, 35°C, see Table 5.4 for sum of the square of residuals and Table 5.5 for filtration constants).

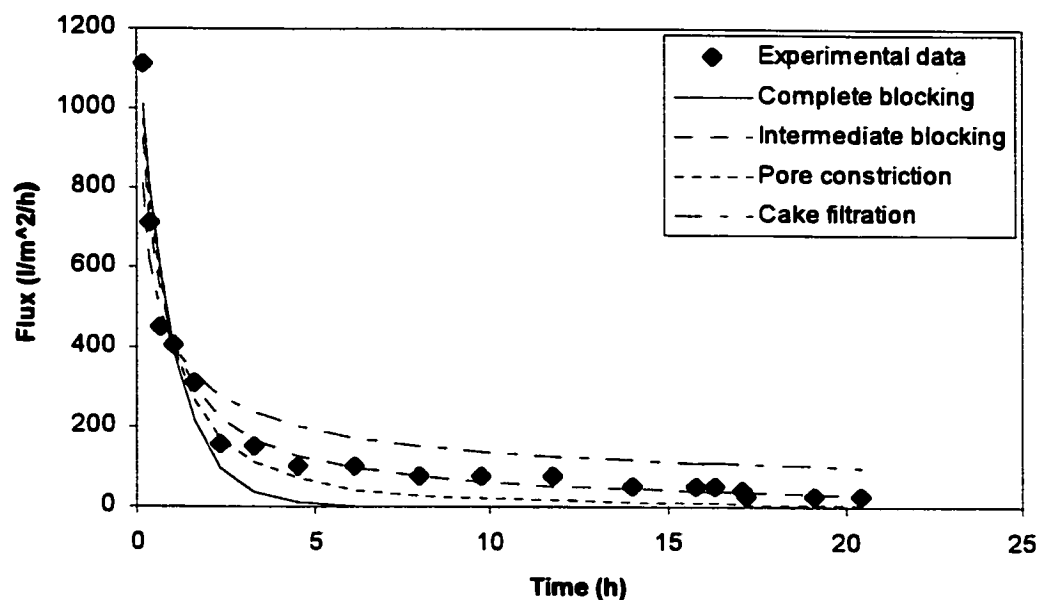


Figure 5.36: Plot of flux vs. time for the KOCH Carbo-cor 0.2 micron membrane (TMP=35psig, 35°C see Table 5.4 for sum of the square of residuals and Table 5.5 for filtration constants).

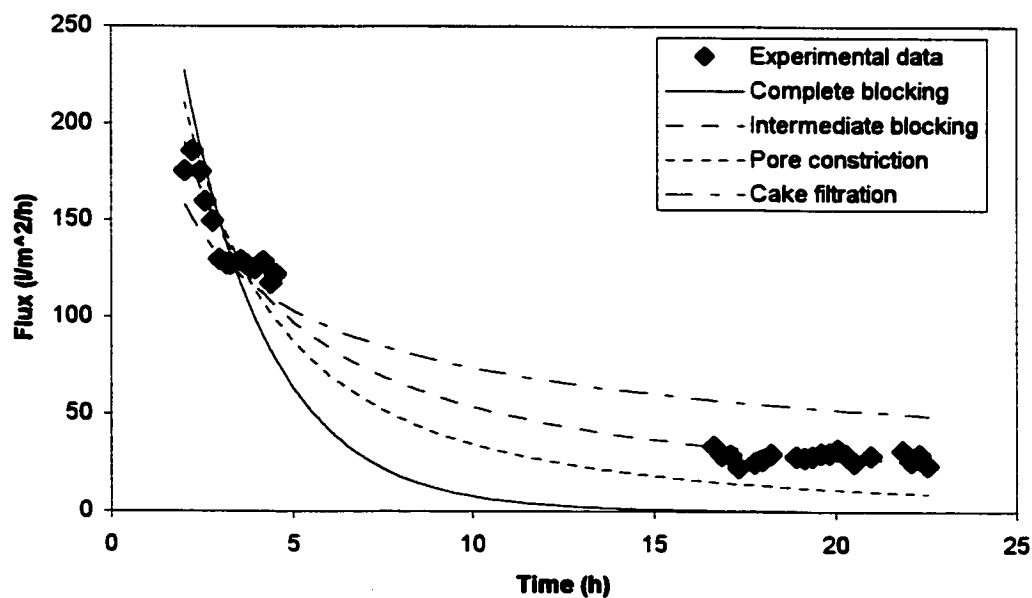


Figure 5.37: Plot of flux vs. time for the KOCH Carbo-cor 0.5 micron membrane (TMP=10psig, 35°C see Table 5.4 for sum of the square of residuals and Table 5.5 for filtration constants).

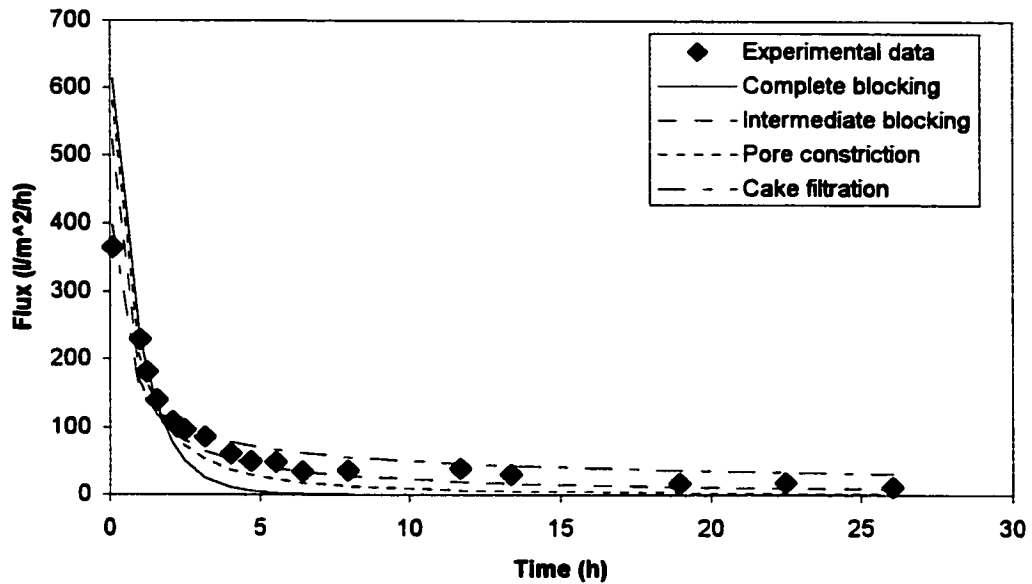


Figure 5.38: Plot of flux vs. time for the KOCH Carbo-cor 0.8 micron membrane (TMP=10psig, 35°C see Table 5.4 for sum of the square of residuals and Table 5.5 for filtration constants).

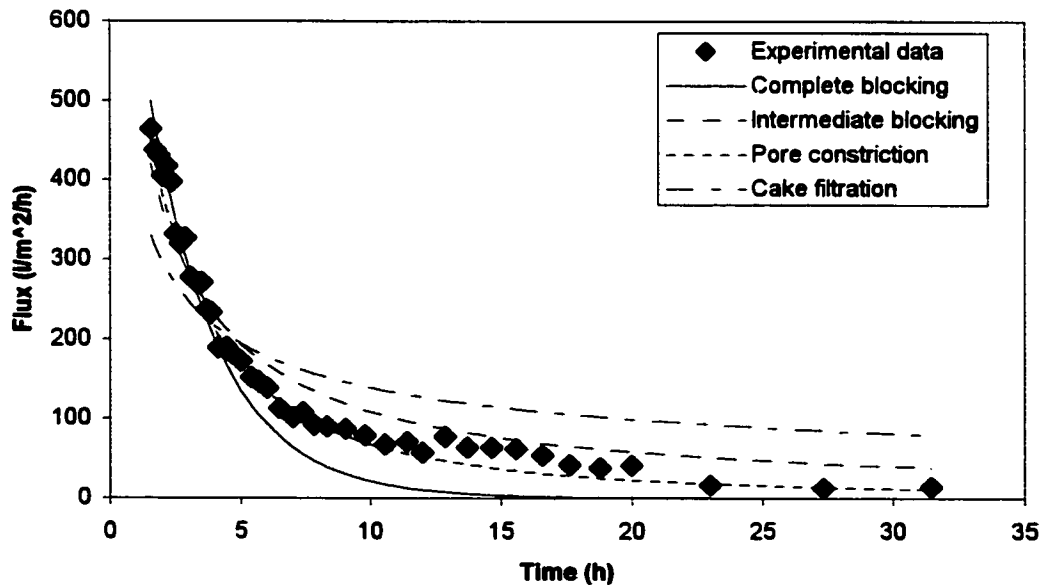


Figure 5.39: Plot of flux vs. time for the KOCH Carbo-cor 1.4micron membrane (TMP=10psig, 35°C, see Table 5.4 for sum of the square of residuals and Table 5.5 for filtration constants).

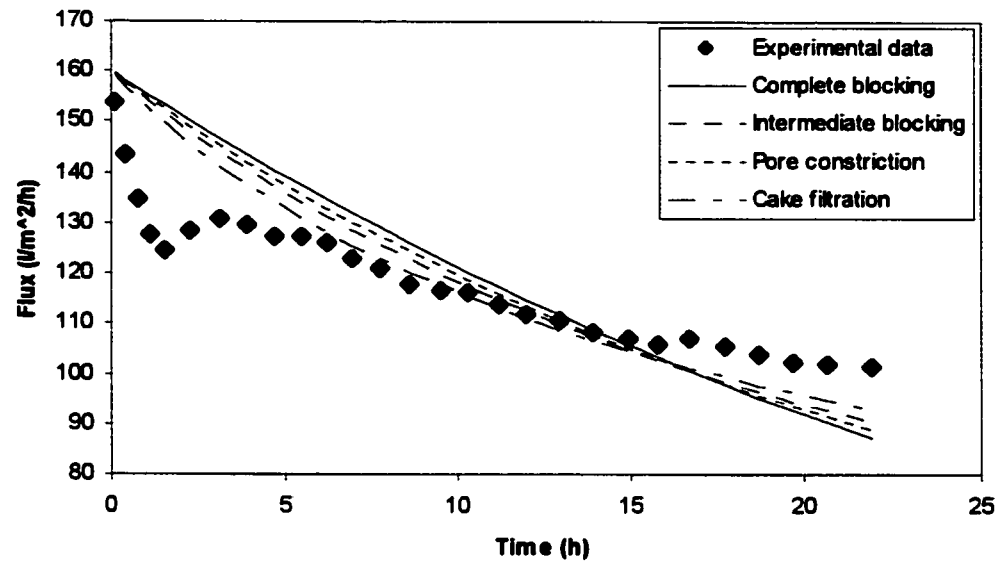


Figure 5.40: Plot of flux vs. time for the TAMI 50kD membrane (TMP=7.34psig, 35°C, see Table 5.4 for sum of the square of residuals and Table 5.5 for filtration constants).

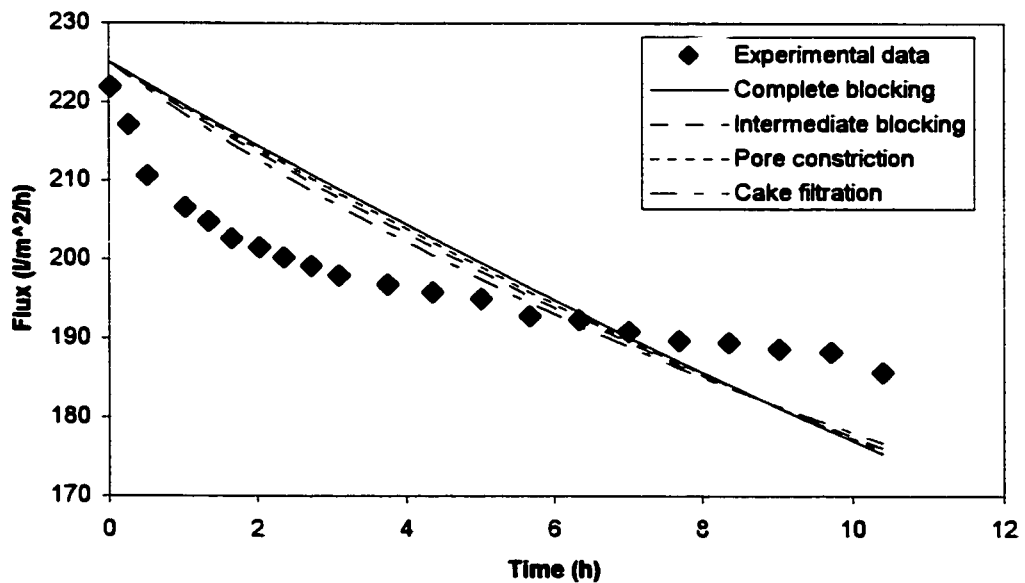


Figure 5.41: Plot of flux vs. time for the TAMI 150kD membrane (TMP=15psig, 35°C, see Table 5.4 for sum of the square of residuals and Table 5.5 for filtration constants).

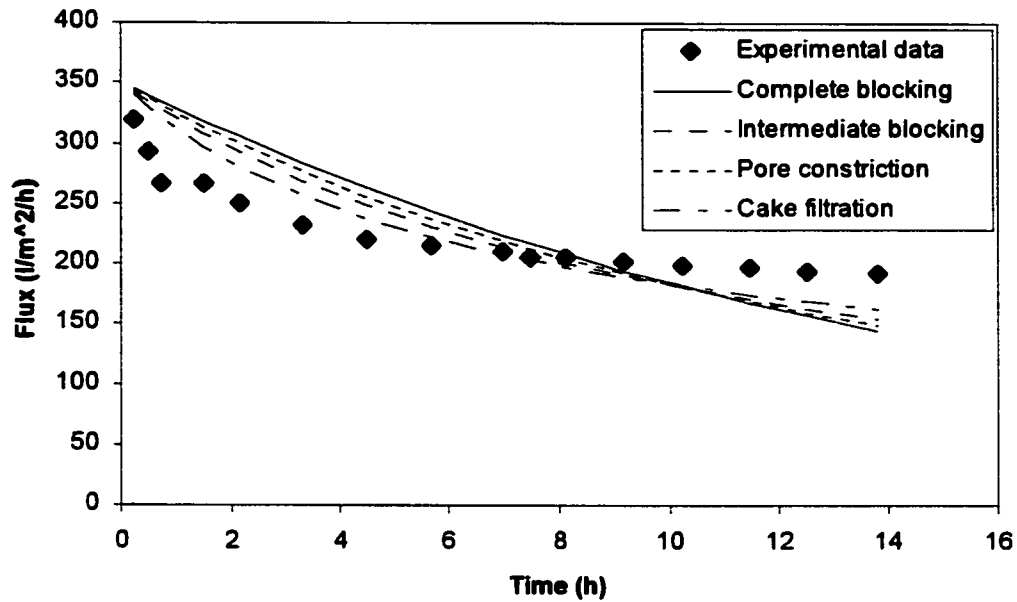


Figure 5.42: Plot of flux vs. time for the TAMI 300kD membrane (TMP=7.34psig, 35°C, see Table 5.4 for sum of the square of residuals and Table 5.5 for filtration constants).

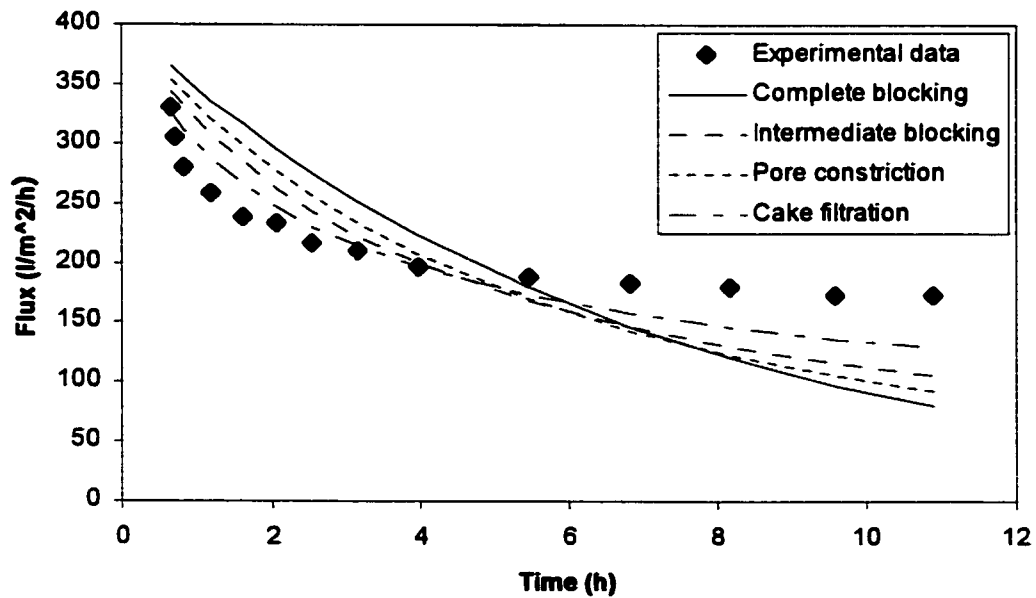


Figure 5.43: Plot of flux vs. time for the TAMI 70nm membrane (TMP=7.34psig, 35°C, see Table 5.4 for sum of the square of residuals and Table 5.5 for filtration constants).

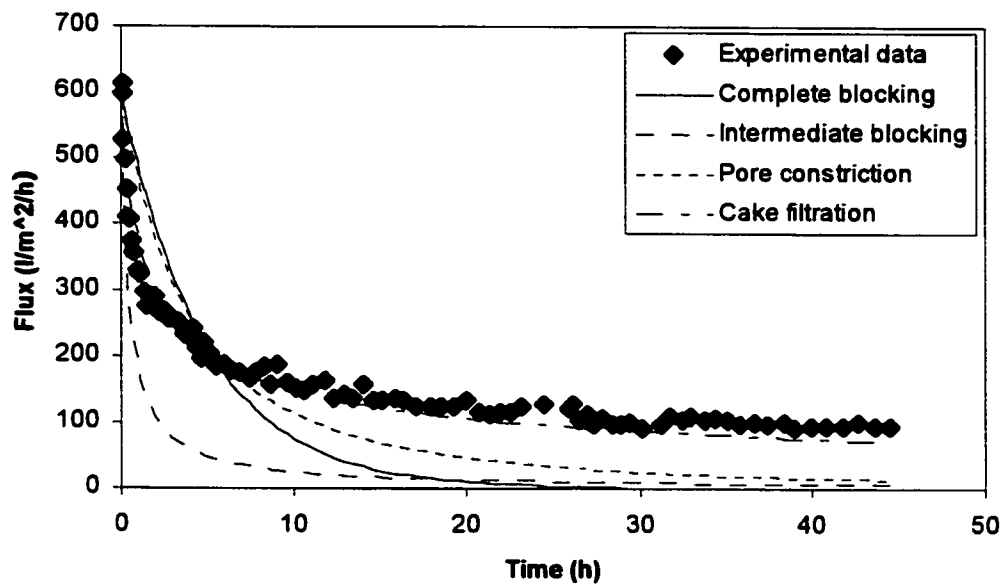


Figure 5.44: Plot of flux vs. time for the TAMI 0.8 micron membrane (TMP=15psig, 35°C, see Table 5.4 for sum of the square of residuals and Table 5.5 for filtration constants).

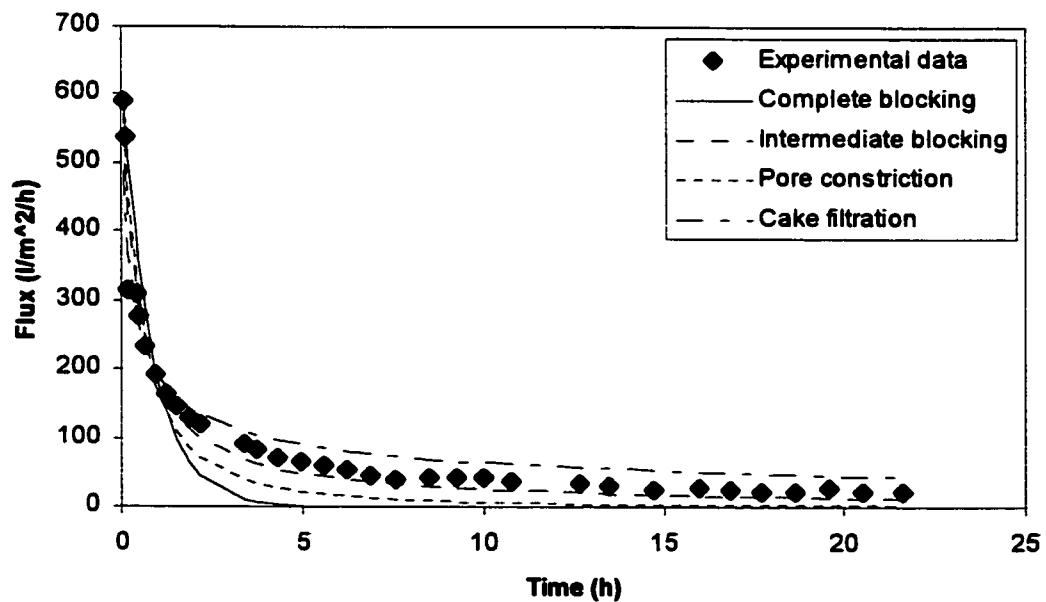


Figure 5.45: Plot of flux vs. time for the TAMI 1.4 micron membrane (TMP=5psig, 35°C, see Table 5.4 for sum of the square of residuals and Table 5.5 for filtration constants).

### 5.4.2 Specific cake resistance

As discussed in the theory section, specific cake resistance  $\alpha_{cake}$  is one of the major characteristics of filter cake formation. Table 5.6 below shows the calculated values of  $\alpha_{cake}$  for the KOCH Carbo-cor 0.05, 0.1, 0.5, 0.8 and 1.4 micron membranes and TAMI Céram 50 kD, 150 kD, 300 kD and 70nm membranes. (See Appendix E for sample calculation). All runs were performed without backflushing. Experimental data can be referred to Figures 5.13 to 5.17.

Table 5.6: Calculated values of specific cake resistance  $\alpha_{cake}$  for various KOCH Carbo-cor and TAMI Céram membranes.

Membrane		TMP (psig)	Specific cake resistance, $\alpha_{cake}$ (m/Kg)	Membrane resistance, $R_m$ (m <sup>-1</sup> )
KOCH	0.05 microm	5	2.38E+15	4.22E+12
		10	1.16E+15	7.73E+12
		15	1.49E+15	9.96E+12
		25	2.36E+15	8.86E+12
	0.1 micron	5	4.97E+14	1.96E+12
		10	9.47E+14	6.06E+12
		15	9.62E+14	1.28E+13
		25	6.35E+14	1.45E+13
	0.5 micron	10	3.33E+14	1.15E+12
		15	8.87E+14	6.64E+12
		20	1.45E+15	2.04E+13
	0.8 micron	10	1.70E+15	
	1.4 micron	10	3.33E+14	
		15	1.68E+16	3.34E+13
20		2.89E+16	5.44E+13	
TAMI	50 kD	7.34	4.52E+14	2.51E+12
		14.67	5.92E+14	2.78E+12
	150 kD	7.34	1.74E+14	1.51E+12
		14.67	3.03E+14	1.81E+12
	300 kD	7.34	2.05E+14	6.53E+11
		14.67	3.76E+14	1.18E+12
	70 nm	7.34	4.27E+14	5.73E+11
		14.67	8.02E+14	1.17E+12

TAMI membranes have cake resistances that are an order of magnitude lower than the KOCH Carbo-cor membranes. This is in agreement with the result discussed in section 5.4.1 where the fouling mechanism for the KOCH Carbo-cor membranes was most likely intermediate blocking and the mechanisms for the TAMI membranes cake filtration.

With the exception of the 150 kD TAMI membrane the specific cake resistance of all other TAMI membranes increased with pressure. The non-descript flux decline of the 150 kD TAMI membrane seen in Figure 5.40 would explain this discrepancy. In most cases, the cake resistance increased with pressure which indicates some degree of cake compressibility. A possible reason for the scatter in these results is related to the difficulty in evaluating the concentration of foulant in the bilge water over a period of 4 days required to span the entire range of pressures.

### **5.5 Oil and grease content of the permeate**

Table 5.7 shows the results for the KOCH membranes. These results are based on the original two loop design where feed is first fed to the MF membrane and the permeate treated by a UF membrane. The base case XM 50 data in the first row of Table 5.7 is for the case where feed solution is allowed to enter into the UF circulation loop. This represents a feed concentration for the UF membrane of 4 g/l of O & G. The second row is the analysis for the MF permeate. This permeate was fed to the UF loop and the UF permeate reported in the third row. The results indicate excellent separation for this mode of operation where the use of two membranes in cascade provided a 12 times reduction in the O & G content in the permeate.

Table 5.7: Oil and grease recovery and rejection of the KOCH Carbo-cor 1.4 micron membrane in a MF/UF hybrid system. Base case is for the UF membrane exposed directly to the feed solution containing 4 g/l of O & G.

Membrane	Recovery of oil & grease (mg/l)
XM 50 (Base case UF loop exposed to 4 g/l O & G)	6.4±0.5
Carbo-cor 1.4 micron (MF loop)	21.9±0.5
XM 50 (UF loop containing MF permeate)	0.53±0.5

The oil and grease content of permeates produced by the TAMI Céram 50 kD, 150 kD, 300 kD, 70nm and 0.8 micron are all below the discharge regulation of 15 mg/l oil and grease. As seen in Figure 5.46 below, even at very high level of feed concentration (100 g/l), the concentration of O & G in permeate were still much lower than the allowable discharge limit. These results show that the TAMI ceramic membranes have excellent oil/grease rejection producing permeate that can be readily discharged overboard.

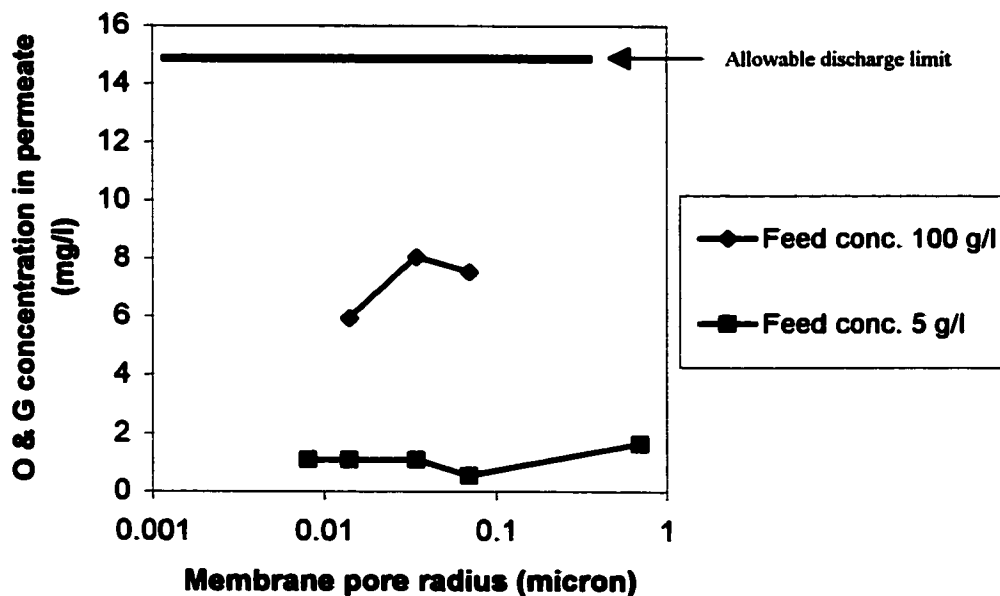


Figure 5.46: Plot of O & G concentration vs. membrane pore radius for the TAMI membranes (35°C, TMP=1 barg).

### 5.6 Effect of feed concentration on permeate flux and oil retention

Feed volume reduction runs were performed for the TAMI 50 kD, 150 kD, 300 kD and 70nm membranes. The feed concentration runs were performed at the end of one week of operation in a total recirculation mode. Volume reduction runs were performed without backflushing. The permeate was discharged to drain and the feed tank emptied from its initial volume of 90 litres. At the end of the volume reduction run, 8 litres of concentrated feed solution remained in the circulation loop. Experimental results have been plotted in Figure 5.47 below. As seen from Figure 5.47, the permeate flux for all the membranes remained at the same level although the oil and grease concentration increased from 5.5 g/l to 90-100 g/l. The results indicate that, as in the CLEANBREAK experiments above, the concentration of the feed solution does not affect permeate flux.

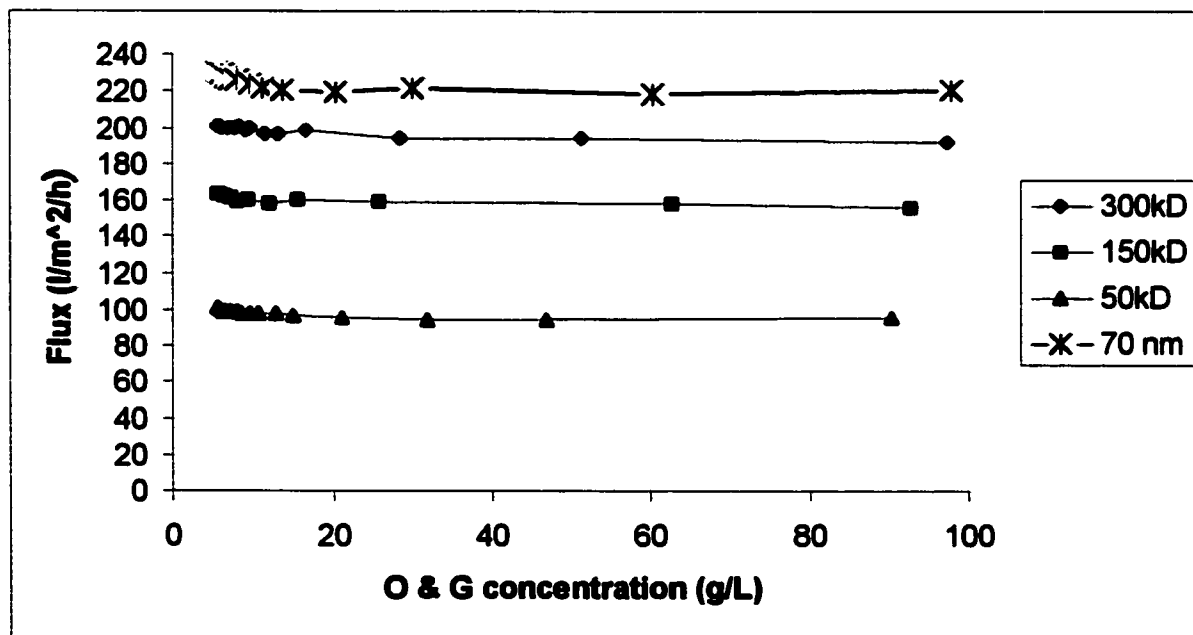


Figure 5.47: Plot of actual flux vs. O & G concentration in the feed loop for the TAMI membranes with different MWCOs. Operating temperature 35°C. TMP= 1 barg (14.67 psig).

In this study, EPA Method 1664 was used to analyze for oil and grease in the permeate. The procedure for n-Hexane extractable material in water (HEM; oil and grease) involves acidifying a water sample to pH 2 followed by a serial extraction with n-Hexane. (See Appendix F for detailed procedure and standardization).

Table 5.8 below shows the results for different TAMI membranes. The results indicate that these ceramic membranes have excellent oil and grease rejection. The 50, 150 and 300 kD membranes had very low permeate concentrations of O & G. The results for the 1.4 micron membrane reflect the low permeate rate for the 1.4 micron membrane. Even with backflushing, the 1.4 micron membrane had very low permeation indicating severe pore plugging. This plugging reduced the pore size of the membrane increasing the selectivity of the membrane.

**Table 5.8: Oil and grease concentration in the permeate of various TAMI membranes after 1 hour in a permeation run at 4 g/l O & G feed concentration.**

Membrane	Conc. of oil & grease in permeate (mg/l)
TAMI 50kD	1.1±0.5
TAMI 150kD	1.1±0.5
TAMI 300kD	1.1±0.5
TAMI 70 nm	0.53±0.5
TAMI 1.4 micron	1.6±0.5

The relation between the feed concentration and permeate concentration was explored by performing volume reduction runs on 150 kD, 300 kD and 70nm membranes. The membrane system was operated in a batch mode where feed was circulated back to the feed tank and permeate from the membrane discarded. The feed tank was emptied from an initial volume of 90 litres. Permeate flux was not affected by feed concentration during these runs, as seen in Figure 5.47 above. However, the feed concentration had a significant effect on permeate concentration as seen in Figure 5.48 below. The 150 kD

membrane having a slightly better performance at higher concentrations than the 300 kD membrane. The 100g/l concentration was the limit achievable with 100 l of bilge water, given the size of the circulation loop. This relation implies that different strategies should be applied to treat dilute versus concentrated bilge water in order to be well below the 15 mg/l discharge limit at all times during the volume reduction process.

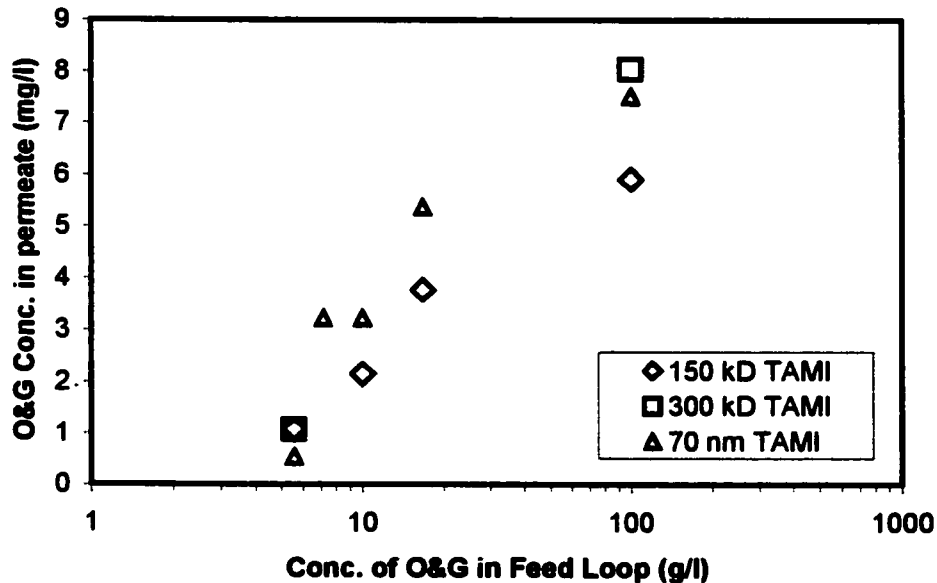


Figure 5.48: Plot of the O & G concentration in the permeate vs. the concentration of O & G in the feed solution. Operating temperature 35°C, TMP=1 barg (14.67 psig).

## **6. CONCLUSIONS**

The research conducted on various membranes in this study provided insight into the effect of bilge water components, membrane cleaning methods and system operational parameters for the treatment of bilge water using a membrane based treatment system.

### **6.1 Effect of bilge water components**

The presence of different salts in synthetic bilge water have an effect on the performance of the membrane. CLEANBREAK formed a filter cake on the membrane surface and caused flux decline. However, high concentrations of CLEANBREAK (10 times that found in synthetic bilge water) had little effect on the performance of the membrane. This was attributed to the hardness of the half seawater mixture. The addition of CLEANBREAK softened the half seawater mixture which mitigated further flux reductions.

### **6.2 Effect of membrane pore size**

Membranes with a 0.2 micron pore size are not suitable in this application. TAMI Céram membranes with pore size less than 0.07 micron and KOCH Carbo-cor membranes with pore size 1.4 microns followed by UF membrane with backflushing had best performance.

### **6.3 Membrane cleaning**

Environmentally friendly cleaning methods, such as hot water heating, air backflushing and steam cleaning were found effective in regenerating membrane flux for large pore KOCH Carbo-cor membranes. KOCH Carbo-cor membranes retained their flux for several months with proper cleaning.

#### **6.4 Effect of trans-membrane pressure (TMP)**

Increasing of TMP offers improvement for smaller pore size but was detrimental for larger pore size membranes. For the KOCH Carbo-cor membranes, permeate flux increased with the increase of TMP for the 0.05 and 0.1 micron pore size membranes but not for the larger pore size membranes. For the TAMI Céram membranes, permeate flux increased with the increase of TMP for pore size below 0.07 micron but not for those above 0.07 micron.

#### **6.5 Effect of backflushing**

Backflushing is a technically feasible and effective method for membrane flux enhancement. Backflushing offered flux improvements for single tube KOCH Carbo-cor membranes but not for multilumen TAMI Céram membranes. Membrane materials and support structure were found to be critical in backflushing.

#### **6.6 Cake vs. blocking**

The filtration mechanisms for membranes with pore size less than 0.2 micron were found to be cake filtration. For those membranes with pore size larger than 0.2 micron, the filtration mechanisms were found a mixture of intermediate blocking and pore constriction.

#### **6.7 Oil and grease concentration**

Oil and grease concentration does not affect permeate flux but affects permeate concentration. The oil and grease content of the permeate was found to be proportional to the logarithm of the oil and grease content of the feed solution.

## **7. RECOMMENDATIONS**

**A number of recommendations can be provided for the treatment of oily bilge water using membrane based treatment system.**

- 1. Tubular membranes with large channels should be used in this application.**
- 2. Further work should include the study of the relationship between the feed concentration and permeate concentration and the study of the effect of temperature in the system.**
- 3. Study the use of membranes having smaller pore diameters after the MF membrane or membranes with MWCO less than 50 kD and NF membranes.**

## **8. REFERENCES**

- ASTM D1141-90, "Standard Specification for Substitute Ocean Water", *Dod Index of Specifications and Standards, Canada*, (November 1992).
- Bhattacharyya, D., A.B.Jumawan, R.B.Grieves and L.R.Harris, "Ultrafiltration Characteristics of Oil-Detergent-Water Systems: Membrane Fouling Mechanisms", *Journal of Separation Science and Technology*, **14(6)**, 529-549 (1979).
- Bhave, R.R., "Inorganic Membranes Synthesis, Characteristics and Applications", *Van Nostrand Reinhold, New York* (1991), pp.83-88, 139-140
- Carman, P.C., "Fundamental Principle of Industrial Filtration", *Trans. Inst. Chem. Eng.*, **16**, 168-187 (1938).
- Cheryan, M., "Ultrafiltration Handbook", *Technomic Publishing Company, Lancaster, Pennsylvania, U.S.A.* (1986), pp.250-256.
- Cheryan, M. and N. Rajagopalan, "Membrane Processing of Oily Streams. Wastewater Treatment and Waste Reduction", *Journal of Membrane Science*, **151**, 13-28, (1998).
- Department of National Defence (DND), "Technical Statement of Requirements for an Oily Water Separator System", *Ottawa, Canada* (July 1996).
- EPA. Method 1664 Revision A: n-Hexane Extractable Material (HEM; Oil and Grease) and Silica Gel Treated n-Hexane Extractable Material (SGT-HEM; Nonpolar Material) by Extraction and Gravimetry. EPA-821-R-93-009. EPA Office of Water. 1999.

- Harris, L.R., D.F. Jackson, and P. Schatzberg, "Oily Bilge Water Treatment With a Tubular Ultrafiltration System", *Journal of Engineering for Industry*, 1215-1220 (November, 1976).
- Héran M. and S.Elmaleh, "Cross-flow Microfiltration With High Frequency Reverse Flow", *Water Science Technology*, **41(10-11)**, 337-343 (2000).
- Hermia, J., "Constant Pressure Blocking Filtration Laws: Applications to Power-law Non-newtonian Fluids", *Journal of Transactions of the Institute of Chemical Engineers*, **60**, 183-187 (1982).
- Hyun, S.H and G. T. Kim, "Synthesis of Ceramic Microfiltration Membrane for Oil/Water Separation", *Separation Science and Technology*, **32(18)**, 2927-2943 (1997).
- Kennedy, M., S.M.Kim, I.Mutenyo, L.Broens and J.Schippers, "Intermittent Crossflushing of Hollow Fiber Ultrafiltration Systems", *Desalination*, **118**, 175-188 (1998).
- Kim, B.S. and H.N. Chang, "Effects of Periodic Backflushing on Ultrafiltration Performance", *Bioseparation*, **2**, 23-29, (1991).
- Kong, J. and K.Li, "Oil Removal From Oil-in-Water Emulsions Using PVDF Membranes", *Separation and Purification Technology*, **16**, 83-93 (1999).
- Kuberkar, V.T. and R.H.Davis, "Microfiltration of Protein-cell Mixtures With Crossflushing or Bachflushing", *Journal of Membrane Science*, **183**, 1-14 (2001).
- Leon, M., S. L. Michaels, V. Goel and R. Kaiser, "Crossflow Microfiltration: Applications, Design and Cost", in "Membrane Handbook", edited by W.S.Winston Ho and K.K.Sirkar, Van Nostrand Reinhold, New York (1992), pp.577-578.

- Levesley, J.A. and M.Hoare, "The Effect of High Frequency Backflushing on The Microfiltration of Yeast Homogenate Suspensions for The Recovery of Soluble Proteins", *Journal of Membrane Science*, **158**, 29-39 (1999).
- Matsuura, T., "Synthetic Membranes and Membrane Separation Processes", CRC Press, Inc., (1994), pp.305-315.
- Mueller, J., Y. Cen and R. H. Davis, "Crossflow Microfiltration of Oily Water", *Journal of Membrane Science*, **129**, 221-235 (1997).
- Mulder, M.; "Basic Principles of Membrane Technology", Kluwer Academic Publishers, 1991, pp.305-307.
- Natasuka S., I. Nakate and T.Miyano, "Drinking Water Treatment by Using Ultrafiltration Hollow Fiber Membranes", *Desalination*, **106**, 55-61 (1996).
- Nottegar, M., "The Effects of Particulates on The Ultrafiltration of Bilge (Oily) Wastewater Containing New or Used Lubricating Oil", M.A.Sc. Thesis, Department of Chemical Engineering, University of Ottawa, Ottawa (2000).
- Pialipp, C.H.Lee, A.G.Fane and C.J.D.Fell, "A Fundamental Study of The Ultrafiltration of Oil-Water Emulsions", *Journal of Membrane Science*, **36**, 161-177 (1988).
- Porter, M.C., "Handbook of Industrial Membrane Technology", Noyes Publications, Park Ridge, New Jersey, U.S.A. (1990), pp.224, 214-216.
- Ramirez, J.A. and R.H.Davis, "Application of Cross-flow Microfiltration With Rapid Backpulsing to Wastewater Treatment", *Journal of Hazardous Materials*, **B: 36**, 179-197 (1998).

- Resera, A., "Oily Water Pollution Abatement Systems – Course Notes: EO 412.08", Naval Engineering Test Establishment (NETE), LaSalle, Canada (November, 1992).
- Resera, A., "Bilge Water Characterization Study and Bilge Fluid Production Estimates", NETE – Project Number IT 1082, Report Number 14/95, LaSalle, Canada (June, 1995).
- Rodgers, V.G.J. and R.E. Sparks, "Effect of Transmembrane Pressure Pulsing on Concentration Polarization", *Journal of Membrane Science*, **68**, 149-168 (1992).
- Rodgers, V.G.J. and R.E. Sparks Sparks, "Effect of Solution Properties on Polarization Redevelopment and Flux in Pressure Pulsed Ultrafiltration", *Journal of Membrane Science*, **78**, 163-180 (1993).
- Sondhi, R., Y.S.Lin and F.Alvarez, "Crossflow Filtration of Chromium Hydroxide Suspension by Ceramic Membranes: Fouling and Its Minimization by Backpulsing", *Journal of Membrane Science*, **174**, 111-122 (2000).
- Srijaroonrat P., E.Julien and Y.Aurelle, "Unstable Secondary Oil/Water Emulsion Treatment Using Ultrafiltration: Fouling Control by Backflushing", *Journal of Membrane Science*, **159(1)**, 11-20 (1999).
- Ting, J. and J. Wu, "Cross-flow Ultrafiltration of Oil/Water Emulsions Using Porous Ceramic Membranes", *Journal of The Chinese Institute of Chemical Engineers*, **30(3)**, 207-214 (1999).
- Transport Canada; "Canada Sipping Act", Ottawa, Canada (2001).
- Tremblay,A.Y. and M. Nottegar, "Bilge Water Membrane Treatment Phenomena Study", Contract W7707-7-5321, DND, Canada (2000).
- Vigneswarne, S., S.Boonthanon and H.Prasanthi, "Filtration Backwash Recycling Using Crossflow Microfiltration", *Desalination*, **106**, 31-38 (1996).

**Wakeman, R.J. and E.S. Tarleton, "Filtration: Equipment Selection, Modeling, and Process Simulation", Elsevier Advanced Technology, Kidlington, UK (1999), pp.56-60.**

**Zeman L.J. and A.L. Zydney, "Microfiltration and Ultrafiltration, Principles and Applications", Marcel Dekker, Inc., (1996), pp. 331-341, 380-381, 575-576.**

## Appendix A

### Langelier Saturation Index Calculation for Half Seawater Solution

The Langelier Saturation Index (LSI; also called Langelier Stability Index) is a calculated number used to predict the calcium carbonate stability in water; that is, whether the solution conditions will precipitate, dissolve, or be in equilibrium with calcium carbonate. The LSI is expressed as the difference between the actual system pH and the saturation  $pH_s$ .

$$LSI = pH - pH_s$$

where pH is the measured water pH,  $pH_s$  is the pH at saturation in calcite or calcium carbonate. If the actual pH of the water is below the calculated saturation  $pH_s$ , the LSI is negative and the water has a very limited scaling potential. If the actual pH exceeds  $pH_s$ , the LSI is positive, and being supersaturated with  $CaCO_3$ , the water has a tendency to form scale. At increasing positive index values, the scaling potential increases. This was noticed first hand, in laboratory experiments where for high LSI values, scale formed readily on the surface of all wetted metal parts exposed to the test solution. This eventually destroyed a vane pump and caused serious delays in the project. The relationship between LSI and scale potential is shown in Table A1 below.

Table A-1: Relationship between Langelier Saturation Index (LSI) and scale potential

LSI	Scale Potential
- negative less than zero	No scale potential. Water will dissolve $CaCO_3$ .
+ positive greater than zero	Scale can form. $CaCO_3$ precipitation may occur.
close to zero	Borderline scale potential. Water quality and temperature changes, or evaporation could change the index.

$pH_s$  is defined as

$$pH_s = (9.3 + A + B) - (C + D)$$

where  $A = (\log_{10} [\text{TDS}] - 1) / 10$

$$B = -13.12 \times \log_{10} (^\circ\text{C} + 273) + 34.55$$

$$C = \log_{10} [\text{Ca}^{2+} \text{ as CaCO}_3] - 0.4$$

$$D = \log_{10} [\text{alkalinity as CaCO}_3]$$

In order to calculate the LSI, it is necessary to know the alkalinity (mg/l as  $\text{CaCO}_3$ ), the calcium hardness (mg/l  $\text{Ca}^{2+}$  as  $\text{CaCO}_3$ ), the total dissolved solids (mg/l TDS), the actual pH, and the temperature of the water ( $^\circ\text{C}$ ). For half seawater solution described in Table 1, these values are:

When  $\text{pH} = 7.5$ , at  $25^\circ\text{C}$ ,

TDS = 20964 mg/L

Calcium = mg/L (or ppm) as  $\text{CaCO}_3$

$$= \frac{[\text{CaCl}_2]}{MW_{\text{CaCl}_2}} MW_{\text{CaCO}_3} = \frac{579 \text{ mg/L}}{111 \text{ g/mole}} 100 \text{ g/mole} = 522 \text{ mg/L}$$

Alkalinity = mg/L (or ppm) as  $\text{CaCO}_3$

$$= \frac{[\text{NaHCO}_3]}{MW_{\text{NaHCO}_3}} MW_{\text{CaCO}_3} = \frac{100.5 \text{ mg/L}}{84 \text{ g/mole}} 100 \text{ g/mole} = 120 \text{ mg/L}$$

(Note: The total alkalinity is the sum of  $\text{HCO}_3^-$ ,  $\text{CO}_3^{2-}$  and  $\text{OH}^-$  ions. The amount of each of the compounds varies with pH. In general, as the pH increases, the shift will be from  $\text{HCO}_3^-$  to  $\text{CO}_3^{2-}$ . The formation of  $\text{CO}_3^{2-}$  is most between 10-11pH. In water having near neutral pH almost all the alkalinity will be the form of  $\text{HCO}_3^-$ .)

$$A = (\log_{10} [\text{TDS}] - 1) / 10 = 0.33$$

$$B = -13.12 \times \log_{10} (^\circ\text{C} + 273) + 34.55 = -13.12 \times \log_{10} (25 + 273) + 34.55 = 2.09$$

$$C = \log_{10} [\text{Ca}^{2+} \text{ as CaCO}_3] - 0.4 = \log_{10} (522) - 0.4 = 2.72 - 0.4 = 2.68$$

$$D = \log_{10} [\text{alkalinity as CaCO}_3] = \log_{10} (120) = 2.08$$

$$\text{pH}_s = (9.3 + A + B) - (C + D) = (9.3 + 0.33 + 2.09) - (2.68 + 2.08) = 6.96$$

$$\text{LSI} = \text{pH} - \text{pH}_s = 7.5 - 6.96 = 0.54$$

## Appendix B

### Raw Data and Sample Calculation of Flat Sheet Tests

Raw Data of QW, P707 & QX Membrane Run at 10 psig (10/14.67\*101 barg)

Date: July 5, 2001

Feed solution: 50 L half seawater + CLEANBREAK with 10 times concentration  
(July 2-5 500-50 L volume reduction run)

Membrane: QW, P707 & QX (Table 3.3 giving details on membranes)

Membrane surface area: 0.045 m<sup>2</sup>

Pressure in: 12 psig

Pressure out: 2 psig

Flowrate: 10 L/min

Table B-1: QW, P707 & QX Membrane Run at 10 psig Experimental Data, Dated July 5, 2001

Operating Time (h)	Membrane	Sample Weight (g)	Sample Time (min)	Temperature (°C)	Flux (l/m <sup>2</sup> /h)	Flux @ 25°C (l/m <sup>2</sup> /h)	Flux @ 10psig (l/m <sup>2</sup> /h)
0	P707	35.286	3	27.1	443.73	415.77	346.48
	QX	12.373	3	27.1	155.59	145.79	182.24
	QW	8.196	3	27.1	103.07	96.57	241.43
1	P707	27.676	3	28.3	348.03	313.58	261.31
	QX	8.843	3	28.3	111.20	100.19	125.24
	QW	7.566	3	28.3	95.14	85.72	214.31
2	P707	18.330	3	28.6	230.50	205.61	171.34
	QX	6.130	3	28.6	77.09	68.76	85.95
	QW	6.769	3	28.6	85.12	75.93	189.82
3	P707	15.048	3	28.6	189.23	168.79	140.66
	QX	5.393	3	28.6	67.82	60.49	75.62
	QW	6.351	3	28.6	79.87	71.24	178.10
4	P707	13.689	3	28.6	172.14	153.55	127.96
	QX	5.019	3	28.6	63.11	56.30	70.37
	QW	6.114	3	28.6	76.88	68.58	171.45

#### Sample Calculation:

For P707 with 35.286 g permeate,

$$\begin{aligned}
 \text{Flux} &= \frac{\text{permeate volume}}{\text{membrane area} * \text{sample time}} \text{ (l/m}^2\text{/h)} \\
 &= (35.286/1000) / (\pi * (0.045/2)^2) / (3/60) \\
 &= 443.73 \text{ (l/m}^2\text{/h)}
 \end{aligned}$$

$$\text{Flux at 25°C} = (\text{Flux @ Temp.}) * (1 + (25 - \text{Temp.}) * 0.03)$$

$$= 443.73 * (1 + (25 - 27.1) * 0.03) = 415.77 \text{ (l/m}^2\text{/h)}$$

The membrane flux recorded for each cell was normalized to the 10 psig pressure by the following formula:

$$\text{Cell 1 (P707) flux @ 10psig} = (\text{flux measure for cell 1}) * 10/12$$

$$= 415.77 * 10/12$$

$$= 346.48 \text{ (l/m}^2\text{/h)}$$

$$\text{Cell 2 (QX) flux @ 10psig} = (\text{flux measure for cell 2}) * 10/12$$

$$= 145.79 * 10/12$$

$$= 182.24 \text{ (l/m}^2\text{/h)}$$

$$\text{Cell 3 (QW) flux @ 10psig} = (\text{flux measure for cell 3}) * 10/12$$

$$= 96.57 * 10/12$$

$$= 241.43 \text{ (l/m}^2\text{/h)}$$

**Raw Data of QW, P707 & QX Membrane Run at 20 psig**

Date: July 6, 2001

Feed solution: 50 L half seawater + CLEANBREAK with 10 times concentration  
(July 2-5 500-50 L volume reduction run)

Membrane: QW, P707 & QX (Table 3.3 giving details on membranes)

Membrane surface area: 0.045 m<sup>2</sup>

Pressure in: 24 psig

Pressure out: 12 psig

Flowrate: 10 L/min

**Table B-2: QW, P707 & QX Membrane Run at 20 psig Experimental Data, Dated July 6, 2001**

Operating Time (h)	Membrane	Sample Weight (g)	Sample Time (min)	Temperature (°C)	Flux (l/m <sup>2</sup> /h)	Flux @ 25°C (l/m <sup>2</sup> /h)	Flux @ 20psig (l/m <sup>2</sup> /h)
4.1	P707	14.288	5	23.4	107.80	112.98	102.71
	QX	10.973	5	23.4	82.79	86.77	96.41
	QW	8.838	5	23.4	66.68	69.88	99.84
5	P707	22.974	5	28.6	173.34	154.62	140.56
	QX	7.761	5	28.6	58.56	52.23	58.04
	QW	9.041	5	28.6	68.22	60.85	86.93
6	P707	22.237	5	29.3	167.78	146.14	132.85
	QX	7.917	5	29.3	59.73	52.03	57.81
	QW	8.762	5	29.3	66.11	57.58	82.26
7	P707	21.657	5	29.4	163.4	141.84	128.94
	QX	7.557	5	29.4	57.02	49.49	54.99
	QW	8.411	5	29.4	63.46	55.09	78.69

The membrane flux recorded for each cell was normalized to the 20 psig pressure by the following formula:

Cell 1(P707) flux @ 20psig = (flux measure for cell 1)\*20/22

Cell 2 (QX) flux @ 20psig = (flux measure for cell 2)\*20/18

Cell 3 (QW) flux @ 20psig = (flux measure for cell 3)\*20/14

**Raw Data of QW, P707 & QX Membrane Run at 30 psig**

Date: July 6, 2001

Feed solution: 50 L half seawater + CLEANBREAK with 10 times concentration  
(July 2-5 500-50 L volume reduction run)

Membrane: QW, P707 & QX (Table 3.3 giving details on membranes)

Membrane surface area: 0.045 m<sup>2</sup>

Pressure in: 34 psig

Pressure out: 25 psig

Flowrate: 10 L/min

**Table B-3: QW, P707 & QX Membrane Run at 30 psig Experimental Data, Dated July 6, 2001**

Operating Time (h)	Membrane	Sample Weight (g)	Sample Time (min)	Temperature (°C)	Flux (l/m <sup>2</sup> /h)	Flux @ 25°C (l/m <sup>2</sup> /h)	Flux @ 30psig (l/m <sup>2</sup> /h)
7.1	P707	26.762	5	29.4	201.92	175.27	161.79
	QX	20.031	5	29.4	151.14	131.19	133.41
	QW	14.756	5	29.4	111.34	96.64	109.40
8	P707	25.227	5	29.5	190.34	164.64	151.98
	QX	15.466	5	29.5	116.69	100.94	102.65
	QW	14.769	5	29.5	111.43	96.39	109.12
9	P707	24.356	5	29.5	183.77	158.96	146.73
	QX	14.734	5	29.5	111.17	96.16	97.79
	QW	14.672	5	29.5	110.70	95.76	108.40
10	P707	23.399	5	29.3	176.55	153.77	141.94
	QX	13.807	5	29.3	104.18	90.74	92.27
	QW	14.416	5	29.3	108.77	94.74	107.25

The membrane flux recorded for each cell was normalized to the 30 psig pressure by the following formula:

Cell 1 (P707) flux @ 30psig = (flux measure for cell 1)\*30/32.5

Cell 2 (QX) flux @ 30psig = (flux measure for cell 2)\*30/29.5

Cell 3 (QW) flux @ 30psig = (flux measure for cell 3)\*30/26.5

**Raw Data of QW, P707 & QX Membrane Run at 40 psig**

Date: July 6, 2001

Feed solution: 50 L half seawater + CLEANBREAK with 10 times concentration  
(July 2-5 500-50 L volume reduction run)

Membrane: QW, P707 & QX (Table 3.3 giving details on membranes)

Membrane surface area: 0.045 m<sup>2</sup>

Pressure in: 44 psig

Pressure out: 35 psig

Flowrate: 10 L/min

**Table B-4: QW, P707 & QX Membrane Run at 30 psig Experimental Data, Dated July 6, 2001**

Operating Time (h)	Membrane	Sample Weight (g)	Sample Time (min)	Temperature (°C)	Flux (l/m <sup>2</sup> /h)	Flux @ 25°C (l/m <sup>2</sup> /h)	Flux @ 40psig (l/m <sup>2</sup> /h)
10.1	P707	27.322	5	29.4	206.15	178.94	168.41
	QX	22.060	5	29.4	166.45	144.47	146.30
	QW	18.477	4	29.4	174.26	151.26	165.77
11	P707	21.019	4	29.1	198.24	173.86	163.63
	QX	16.810	4	29.1	158.54	139.04	140.80
	QW	16.420	4	29.1	154.86	135.82	148.84
12	P707	25.379	5	29.0	191.49	168.51	158.60
	QX	20.249	5	29.0	152.78	134.45	136.15
	QW	20.314	5	29.0	153.27	134.88	147.81
13	P707	24.940	5	29.0	188.18	165.59	155.85
	QX	19.954	5	29.0	150.56	132.49	134.17
	QW	20.269	5	29.0	152.93	134.58	147.49

The membrane flux recorded for each cell was normalized to the 40 psig pressure by the following formula:

Cell 1(P707) flux @ 40psig = (flux measure for cell 1)\*40/42.5

Cell 2 (QX) flux @ 40psig = (flux measure for cell 2)\*40/39.5

Cell 3 (QW) flux @ 40psig = (flux measure for cell 3)\*40/36.5

Date: June 02-07, 2001

Feed solution: 100 L Half seawater (Salts added after 24 hours)

pH of Feed: 8.2

Membrane surface area: 0.045 m<sup>2</sup>

Pressure in: 50 psig

Pressure out: 44 psig

Flowrate: 10 L/min

Table B-5: GN, M100 & QW Membrane Experimental Data, Dated June 2-7, 2001

Operating Time (h)	Membrane	Sample Weight (g)	Sample Time (min)	Temperature (°C)	Flux (l/m <sup>2</sup> /h)	Flux @ 25°C (l/m <sup>2</sup> /h)	Flux @ 50psig (l/m <sup>2</sup> /h)
0	GN	21.618	10	25.4	81.56	80.58	82.22
	M100	33.702	2	25.4	635.71	628.09	668.18
	QW	40.602	2	25.4	765.87	756.68	840.75
1	GN	21.645	10	25	81.66	81.66	83.32
	M100	26.424	2	25	498.43	498.43	530.25
	QW	37.278	2	25	703.17	703.17	781.30
24	GN	21.702	10	25	81.87	81.87	83.54
	M100	22.273	3	25	280.09	280.09	297.97
	QW	37.401	3	25	470.33	470.33	522.58
25	GN	21.718	10	25	81.93	81.93	83.60
	M100	17.888	3	25	224.95	224.95	239.30
	QW	33.743	3	25	424.33	424.33	471.47
49	GN	21.867	10	25	82.49	82.49	84.18
	M100	20.841	5	25	157.25	157.25	167.29
	QW	24.694	3	25	310.53	310.53	345.04
73	GN	21.577	10	25	81.40	81.40	83.06
	M100	22.073	6	25	138.79	138.79	147.64
	QW	40.742	6	25	256.17	256.17	284.63
97	GN	21.346	10	25.9	80.53	78.35	79.95
	M100	23.941	7	25.9	129.03	125.54	133.56
	QW	41.943	7	25.9	226.05	219.94	244.38
121	GN	23.576	10	29.6	88.94	76.67	78.23
	M100	17.243	5	29.6	130.10	112.15	119.30
	QW	28.518	5	29.6	215.17	185.48	206.09

Sample Calculation:

Cell 1(GN) flux @ 50psig = (flux measure for cell 1)\*50/49

Cell 2(M100) flux @ 50psig = (flux measure for cell 1)\*50/47

Cell 3(QW) flux @ 50psig = (flux measure for cell 1)\*50/45

Date: May 26-June 01, 2001

Feed solution: 150 L seawater (Salts added after 24 hours)

pH of Feed: 8.2

Membrane surface area: 0.045 m<sup>2</sup>

Pressure in: 50 psig

Pressure out: 44 psig

Flowrate: 10 L/min

Table B-6: GN, M100 & QW Membrane Experimental Data, Dated May 26 - June1, 2001

Operating Time (h)	Membrane	Sample Weight (g)	Sample Time (min)	Temperature (°C)	Flux (l/m <sup>2</sup> /h)	Flux @ 25°C (l/m <sup>2</sup> /h)	Flux @ 50psig (l/m <sup>2</sup> /h)
0	GN	19.637	10	25	74.08	74.08	75.59
	M100	28.373	2	25	535.19	535.19	569.36
	QW	37.22	2	25	702.07	702.07	780.08
1	GN	18.344	10	25	69.20	69.20	70.62
	M100	21.662	2	25	408.61	408.61	434.69
	QW	35.099	2	25	662.07	662.07	735.63
2	GN	17.549	10	25	66.204	66.204	67.56
	M100	19.888	2	25	375.14	375.14	399.09
	QW	33.151	2	25	625.32	625.32	694.80
24	GN	17.488	10	25	65.97	65.97	67.32
	M100	21.405	3	25	269.17	269.17	286.35
	QW	37.756	3	25	474.79	474.79	527.54
25	GN	20.044	10	25	75.62	75.62	77.16
	M100	17.85	3	25	224.47	224.47	238.80
	QW	36.327	3	25	456.82	456.82	507.58
49	GN	20.432	10	25	77.08	77.08	78.65
	M100	13.793	3	25	173.45	173.45	184.52
	QW	28.911	3	25	363.56	363.56	403.96
72	GN	20.267	10	25	76.46	76.46	78.02
	M100	20.452	5	25	154.31	154.31	164.16
	QW	25.23	3	25	317.27	317.27	352.52
79	GN	20.168	10	25	76.09	76.09	77.64
	M100	19.652	5	25	148.28	148.28	157.74
	QW	25.286	3	25	317.98	317.98	353.31
96	GN	20.115	10	25	75.89	75.89	77.43
	M100	19.578	5	25	147.72	147.72	157.15
	QW	23.038	3	25	289.71	289.71	321.90
120	GN	19.734	10	25	74.45	74.45	75.97
	M100	17.761	5	25	134.01	134.01	142.56
	QW	20.39	3	25	256.41	256.41	284.90
143	GN	19.525	10	25	73.66	73.66	75.16
	M100	16.923	5	25	127.69	127.69	135.84
	QW	18.411	3	25	231.52	231.52	257.25

Date: May 07-May 17, 2001

Feed solution: 150 L seawater ( Salts added after 24 hours; 30.15g NaHCO<sub>3</sub> added after 28 hours)

pH of Feed: 8.2

Membrane surface area: 0.045 m<sup>2</sup>

Pressure in: 50 psig

Pressure out: 44 psig

Flowrate: 10 L/min

Table B-7: GN, M100 & QW Membrane Experimental Data, Dated May 07-17, 2001

Operating Time (h)	Membrane	Sample Weight (g)	Sample Time (min)	Temperature (°C)	Flux (l/m <sup>2</sup> /h)	Flux @ 25°C (l/m <sup>2</sup> /h)	Flux @ 50psig (l/m <sup>2</sup> /h)
0.5	GN	21.978	10	25	82.91	82.91	84.69
	M100	30.839	2	25	581.71	581.71	619.15
	QW	31.395	2	25	592.19	592.19	657.78
24	GN	22.555	10	25	85.09	85.09	86.73
	M100	12.212	2	25	230.35	230.35	244.68
	QW	14.545	2	25	274.36	274.36	304.44
25	GN	23.078	10	25	87.06	87.06	88.78
	M100	10.266	2	25	193.65	193.65	206.38
	QW	13.824	2	25	260.76	260.76	290.00
26.5	GN	23.394	10	25	88.26	88.26	89.80
	M100	13.989	3	25	175.91	175.91	186.17
	QW	18.895	3	25	237.61	237.61	264.44
28	GN	23.061	10	25	86.99	86.99	88.78
	M100	12.752	3	25	160.36	160.36	170.21
	QW	17.379	3	25	218.54	218.54	242.22
28.5	GN	27.991	12	25	87.99	87.99	89.80
	M100	13.54	3	25	170.27	170.27	180.85
	QW	18.283	3	25	229.91	229.91	247.78
55	GN	22.852	10	25	86.21	86.21	87.76
	M100	15.655	5	25	118.12	118.12	125.53
	QW	22.774	5	25	171.83	171.83	191.11
80	GN	20.041	10	25	75.61	75.61	76.53
	M100	12.455	5	25	93.97	93.97	98.94
	QW	14.7	5	25	110.91	110.91	122.22
124	GN	19.378	10	25	73.10	73.10	74.49
	M100	8.805	5	25	66.43	66.43	70.21
	QW	8.756	5	25	66.07	66.07	73.33
151	GN	18.586	10	25	70.12	70.12	71.43
	M100	16.021	10	25	60.44	60.44	63.83
	QW	15.523	10	25	58.56	58.56	65.56
178	GN	17.749	10	25	66.96	66.96	68.37
	M100	14.1	10	25	53.19	53.19	56.38
	QW	13.574	10	25	51.21	51.21	56.67
202	GN	17.749	10	25	66.96	66.96	68.37
	M100	14.1	10	25	53.19	53.19	56.38
	QW	13.574	10	25	51.21	51.21	56.67

226	GN	16.919	10	25	63.83	63.83	65.30
	M100	10.62	10	25	40.06	40.06	42.55
	QW	11.17	10	25	42.14	42.14	46.67

**Raw Data of QW, P707 & QX Membrane Run With Different solutions**

Date: June 16-18, 2001

Feed solution: 100 L distilled water

pH of Feed: 6.5

Membrane surface area: 0.045 m<sup>2</sup>

Pressure in: 35 psig

Pressure out: 26 psig

Flowrate: 10 L/min

**Table B-8: QW, P707 & QX Membrane Experimental Data, Dated June 16-18, 2001**

Operating Time (h)	Membrane	Sample Weight (g)	Sample Time (min)	Temperature (°C)	Flux (l/m <sup>2</sup> /h)	Flux @ 25°C (l/m <sup>2</sup> /h)	Flux @ 30psig (l/m <sup>2</sup> /h)
0	QW	20.271	1	24.3	764.74	780.80	699.22
	P707	28.308	1	24.3	1067.94	1090.36	1072.49
	QX	39.014	1	24.3	1471.83	1502.74	1639.35
16	QW	23.968	2	25.0	452.10	452.10	404.87
	P707	21.783	1.5	25.0	547.85	547.85	538.87
	QX	27.258	1.5	25.0	685.55	685.55	747.87
41	QW	17.776	3	25.0	223.54	223.54	342.95
	P707	16.681	3	25.0	209.77	209.77	549.34
	QX	20.181	3	25.0	253.78	253.78	642.21

**Sample Calculation:**

Cell 1(QW) flux @ 30psig = (flux measure for cell 1)\*30/33.5

Cell 2(P707) flux @ 30psig = (flux measure for cell 1)\*30/30.5

Cell 3(QX) flux @ 30psig = (flux measure for cell 1)\*30/27.5

Date: June 18-19, 2001

Feed solution: 100 L distilled water + 45 g CLEANBREAK

pH of Feed: 8.2

Membrane surface area: 0.045 m<sup>2</sup>

Pressure in: 35 psig

Pressure out: 26 psig

Flowrate: 10 L/min

Table B-9: QW, P707 & QX Membrane Experimental Data, Dated June 18-19, 2001

Operating Time (h)	Membrane	Sample Weight (g)	Sample Time (min)	Temperature (°C)	Flux (l/m <sup>2</sup> /h)	Flux @ 25°C (l/m <sup>2</sup> /h)	Flux @ 30psig (l/m <sup>2</sup> /h)
42	QW	27.185	3	25	341.86	341.86	306.14
	P707	32.587	3	25	409.79	409.79	403.07
	QX	34.030	3	25	427.93	427.93	466.84
43	QW	25.820	3	26.0	324.69	314.95	282.05
	P707	29.181	3	26.0	366.96	355.95	350.11
	QX	30.152	3	26.0	379.17	367.80	401.23
44	QW	25.115	3	26.6	315.83	300.67	269.25
	P707	27.090	3	26.6	340.66	324.31	318.99
	QX	28.309	3	26.6	355.99	338.90	369.71
45	QW	24.259	3	27.1	305.06	285.84	255.98
	P707	25.812	3	27.1	324.59	304.14	299.16
	QX	27.072	3	27.1	340.44	318.99	347.99
47	QW	23.069	3	26.1	290.10	280.52	251.22
	P707	23.652	3	26.1	297.43	287.61	282.90
	QX	25.014	3	26.1	314.56	304.18	331.83
49	QW	21.368	3	25.0	268.71	268.71	240.63
	P707	21.533	3	25.0	270.78	270.78	266.34
	QX	23.041	3	25.0	289.75	289.75	316.09
64	QW	18.998	3	25.6	238.90	234.60	210.09
	P707	18.416	3	25.6	231.59	227.42	223.69
	QX	20.563	3	25.6	258.58	253.93	277.01

Date: June 19-20, 2001

Feed solution: 100 L distilled water + 45g CLEANBREAK + Salt group 1

(MgCl<sub>2</sub>·6H<sub>2</sub>O 555.6g, CaCl<sub>2</sub> 57.9g, SrCl<sub>2</sub>·6H<sub>2</sub>O 2.1g, Na<sub>2</sub>SO<sub>4</sub> 204.7g)

pH of Feed: 8.2

Membrane surface area: 0.045 m<sup>2</sup>

Pressure in: 35 psig

Pressure out: 26 psig

Flowrate: 10 L/min

Table B-10: QW, P707 & QX Membrane Experimental Data, Dated June 19-20, 2001

Operating Time (h)	Membrane	Sample Weight (g)	Sample Time (min)	Temperature (°C)	Flux (l/m <sup>2</sup> /h)	Flux @ 25°C (l/m <sup>2</sup> /h)	Flux @ 30psig (l/m <sup>2</sup> /h)
65	QW	14.581	3	25.5	183.36	180.61	161.74
	P707	13.450	3	25.5	169.14	166.60	163.87
	QX	16.376	3	25.5	205.93	202.84	221.28
66	QW	13.385	3	25.4	168.32	166.30	148.93
	P707	13.178	3	25.4	165.72	163.73	161.04
	QX	16.344	3	25.4	205.53	203.06	221.52
67	QW	12.468	3	25.4	156.79	154.91	138.72
	P707	13.126	3	25.4	165.06	163.08	160.41
	QX	16.389	3	25.4	206.10	203.62	222.13
68	QW	11.950	3	25.4	150.27	148.47	132.96
	P707	12.977	3	25.4	163.19	161.23	158.59
	QX	16.188	3	25.4	203.57	201.12	219.41
70	QW	18.474	5	25.5	139.39	137.30	122.95
	P707	21.720	5	25.5	163.88	161.42	158.78
	QX	27.202	5	25.5	205.24	202.16	220.54
72	QW	17.516	5	25.6	132.16	129.78	116.22
	P707	21.678	5	25.6	163.56	160.62	157.99
	QX	21.167	5	25.6	204.98	201.29	219.59
88	QW	15.258	5	26.0	115.12	111.67	100.00
	P707	21.484	5	26.0	162.10	157.24	154.66
	QX	27.180	5	26.0	205.08	198.92	217.01

Date: June20-21, 2001

Feed solution: 100 L distilled water + 45g CLEANBREAK + Salt group 1 + Salt group 2 (KCl 34.7g, KBr 5.03g, H<sub>3</sub>BO<sub>3</sub> 1.36g, NaHCO<sub>3</sub> 10.05g, NaF 0.15g)

pH of Feed: 8.2

Membrane surface area: 0.045 m<sup>2</sup>

Pressure in: 35 psig

Pressure out: 26 psig

Flowrate: 10 L/min

Table B-11: QW, P707 & QX Membrane Experimental Data, Dated June 20-21, 2001

Operating Time (h)	Membrane	Sample Weight (g)	Sample Time (min)	Temperature (°C)	Flux (l/m <sup>2</sup> /h)	Flux @ 25°C (l/m <sup>2</sup> /h)	Flux @ 30psig (l/m <sup>2</sup> /h)
89	QW	15.209	5	25.7	114.75	112.34	100.61
	P707	21.270	5	25.7	160.49	157.11	154.54
	QX	26.839	5	25.7	202.50	198.25	216.27
91	QW	14.939	5	25.4	112.72	111.36	99.729
	P707	20.791	5	25.4	156.87	154.99	152.45
	QX	26.600	5	25.4	200.70	198.29	216.32
93	QW	14.769	5	25.5	111.43	109.76	98.29
	P707	20.521	5	25.5	154.83	152.51	150.01
	QX	26.426	5	25.5	199.39	196.40	214.25
96	QW	14.973	5	25.6	112.97	110.94	99.35
	P707	21.132	5	25.6	159.44	156.57	154.01
	QX	26.130	5	25.6	197.15	193.61	221.21
112	QW	14.519	5	26.0	109.55	106.26	95.16
	P707	20.233	5	26.0	152.66	148.08	145.65
	QX	26.320	5	26.0	198.59	192.63	210.14

Date: June 21, 2001

Feed solution: 100 L distilled water + 45 g CLEANBREAK + Salt group 1 + Salt group 2 + Salt group 3 (NaCl 1226.7g)

pH of Feed: 8.2

Membrane surface area: 0.045 m<sup>2</sup>

Pressure in: 35 psig

Pressure out: 26 psig

Flowrate: 10 L/min

Table B-12: QW, P707 & QX Membrane Experimental Data, Dated June 21, 2001

Operating Time (h)	Membrane	Sample Weight (g)	Sample Time (min)	Temperature (°C)	Flux (l/m <sup>2</sup> /h)	Flux @ 25°C (l/m <sup>2</sup> /h)	Flux @ 30psig (l/m <sup>2</sup> /h)
113	QW	14.084	5	25.7	106.27	104.03	93.16
	P707	26.601	5	25.7	155.44	152.17	149.68
	QX	26.361	5	25.7	198.90	194.72	212.42
115	QW	14.155	5	25.5	106.80	105.20	94.21
	P707	20.524	5	25.5	154.86	152.53	150.03
	QX	26.333	5	25.5	198.69	195.71	213.50
118	QW	13.682	5	25.5	103.23	101.68	91.06
	P707	19.478	5	25.5	146.96	144.76	142.39
	QX	26.159	5	25.5	197.37	194.41	212.09

### Raw Data of GN, M100 & QW Membrane Run With Different Solutions

Date: June 21-23, 2001  
 Feed solution: 100 L distilled water  
 pH of Feed: 6.3-6.5  
 Membrane surface area: 0.045 m<sup>2</sup>  
 Pressure in: 50 psig  
 Pressure out: 44 psig  
 Flowrate: 10 L/min

**Table B-13: GN, M100 & QW Membrane Experimental Data, Dated June 21-23, 2001**

Operating Time (h)	Membrane	Sample Weight (g)	Sample Time (min)	Temperature (°C)	Flux (l/m <sup>2</sup> /h)	Flux @ 25°C (l/m <sup>2</sup> /h)	Flux @ 50psig (l/m <sup>2</sup> /h)
0	GN	10.912	5	25.8	82.33	80.36	81.99
	M100	34.419	2	25.8	649.24	633.66	674.10
	QW	39.661	2	25.8	748.12	730.16	811.29
1	GN	9.844	5	26.6	74.27	70.71	72.15
	M100	25.49	2	26.6	480.81	457.73	486.95
	QW	33.239	2	26.6	626.98	596.89	663.21
15	GN	9.342	5	25.3	70.49	69.85	71.28
	M100	16.336	2	25.3	308.14	305.37	324.86
	QW	25.429	2	25.3	479.66	475.35	528.16
24	GN	10.152	5	25	76.60	76.60	78.16
	M100	15.965	2	25	301.14	301.14	320.37
	QW	25.233	2	25	475.97	475.97	528.85
40	GN	10.151	5	25	76.59	76.59	78.15
	M100	14.253	2	25	268.85	268.85	286.01
	QW	24.58	2	25	463.65	463.65	515.16

**Sample Calculation:**

Cell 1(GN) flux @ 50psig = (flux measure for cell 1)\*50/49

Cell 2(M100) flux @ 50psig = (flux measure for cell 1)\*50/47

Cell 3(QW) flux @ 50psig = (flux measure for cell 1)\*50/45

Date: June 23-24, 2001

Feed solution: 100 L distilled water + 45g CLEANBREAK

pH of Feed: 8.2

Membrane surface area: 0.045 m<sup>2</sup>

Pressure in: 50 psig

Pressure out: 44 psig

Flowrate: 10 L/min

Table B-14: GN, M100 & QW Membrane Experimental Data, Dated June 23-24, 2001

Operating Time (h)	Membrane	Sample Weight (g)	Sample Time (min)	Temperature (°C)	Flux (l/m <sup>2</sup> /h)	Flux @ 25°C (l/m <sup>2</sup> /h)	Flux @ 50psig (l/m <sup>2</sup> /h)
41	GN	9.746	5	25	73.53	73.53	75.04
	M100	13.754	2	25	259.44	259.44	275.99
	QW	23.613	2	25	445.41	445.41	494.90
42	GN	9.663	5	25	72.91	72.91	74.40
	M100	13.664	2	25	257.74	257.74	274.19
	QW	23.669	2	25	446.46	446.46	496.07
63	GN	9.687	5	25	73.09	73.09	74.58
	M100	12.606	2	25	237.78	237.78	252.96
	QW	20.691	2	25	390.29	390.29	433.66
64	GN	9.65	5	25	72.81	72.81	74.30
	M100	12.679	2	25	239.16	239.16	254.43
	QW	20.665	2	25	389.80	389.80	433.11

Date: June 24-25, 2001

Feed solution: 100 L distilled water + 45g CLEANBREAK + Salt group 1

pH of Feed: 8.2

Membrane surface area: 0.045 m<sup>2</sup>

Pressure in: 50 psig

Pressure out: 44 psig

Flowrate: 10 L/min

Table B-15: GN, M100 & QW Membrane Experimental Data, Dated June 24-25, 2001

Operating Time (h)	Membrane	Sample Weight (g)	Sample Time (min)	Temperature (°C)	Flux (l/m <sup>2</sup> /h)	Flux @ 25°C (l/m <sup>2</sup> /h)	Flux @ 50psig (l/m <sup>2</sup> /h)
65	GN	8.91	5	25	67.23	67.23	68.60
	M100	12.485	3	25	157.00	157.00	167.02
	QW	28.356	3	25	356.58	356.58	396.20
66	GN	8.889	5	25	67.07	67.07	68.44
	M100	12.322	3	25	154.95	154.95	164.84
	QW	27.989	3	25	351.97	351.97	391.07
87	GN	8.935	5	25.1	67.42	67.21	68.59
	M100	10.628	3	25.1	133.65	133.25	141.75
	QW	24.723	3	25.1	310.90	309.96	344.40
88	GN	8.625	5	25.1	65.08	64.88	66.21
	M100	10.531	3	25.1	132.43	132.03	140.46
	QW	24.045	3	25.1	302.37	301.46	334.96

Date: June 25-26, 2001

Feed solution: 100 L distilled water + 45g CLEANBREAK + Salt group 1 + 2

pH of Feed: 8.2

Membrane surface area: 0.045 m<sup>2</sup>

Pressure in: 50 psig

Pressure out: 44 psig

Flowrate: 10 L/min

Table B-16: GN, M100 & QW Membrane Experimental Data, Dated June 25-26, 2001

Operating Time (h)	Membrane	Sample Weight (g)	Sample Time (min)	Temperature (°C)	Flux (l/m <sup>2</sup> /h)	Flux @ 25°C (l/m <sup>2</sup> /h)	Flux @ 50psig (l/m <sup>2</sup> /h)
89	GN	8.042	5	25.1	60.68	60.50	61.73
	M100	10.733	3	25.1	134.97	134.56	143.15
	QW	23.909	3	25.1	300.66	299.76	333.07
91	GN	7.999	5	25	60.35	60.35	61.59
	M100	10.557	3	25	132.76	132.76	141.23
	QW	23.843	3	25	299.83	299.83	333.15
94	GN	7.793	5	25	58.80	58.80	59.99
	M100	10.586	3	25	133.12	133.12	141.62
	QW	23.559	3	25	296.26	296.26	329.18
111	GN	7.664	5	26	57.83	56.09	57.24
	M100	10.391	3	26	130.67	126.75	134.84
	QW	22.892	3	26	287.87	279.24	310.26

Date: June 26, 2001

Feed solution: 100 L distilled water + 45g CLEANBREAK + Salt group 1 + 2 +3

pH of Feed: 8.2

Membrane surface area: 0.045 m<sup>2</sup>

Pressure in: 50 psig

Pressure out: 44 psig

Flowrate: 10 L/min

Table B-17: GN, M100 & QW Membrane Experimental Data, Dated June 26, 2001

Operating Time (h)	Membrane	Sample Weight (g)	Sample Time (min)	Temperature (°C)	Flux (l/m <sup>2</sup> /h)	Flux @ 25°C (l/m <sup>2</sup> /h)	Flux @ 50psig (l/m <sup>2</sup> /h)
112	GN	7.912	5	25.8	59.70	58.26	59.45
	M100	10.493	3	25.8	131.95	128.78	137.01
	QW	22.679	3	25.8	285.19	278.35	309.28
115	GN	7.872	5	25.7	59.40	58.15	59.33
	M100	10.411	3	25.7	130.92	128.17	136.35
	QW	22.611	3	25.7	284.34	278.37	309.30
120	GN	7.831	5	26.4	59.09	56.60	57.76
	M100	10.305	3	26.4	129.59	124.14	132.07
	QW	22.52	3	26.4	283.19	271.30	301.44

## Appendix C

### Raw Data and Sample Calculation of the KOCH XM50 Hollow Fiber Membrane Tests

Date: July 2-5, 2001

Feed solution: 1. Distilled water

2. Half seawater + CLEANBREAK

Membrane: KOCH XM50 Hollow Fiber

Surface area: 0.092416 m<sup>2</sup>

Inlet pressure: 20 psig

Outlet pressure: 0 psig

Flowrate: 13 L/min

Table C-1: KOCH XM50 Hollow Fiber Membrane Experimental Data, Dated July 2-5, 2001

Operating Time (h)	Feed & Volume (L)	Permeate Volume (L or g)	Permeate Time (second)	Temperature (°C)	Flux (l/m <sup>2</sup> /h)	Flux @ 25°C (l/m <sup>2</sup> /h)
0	1; 100L	1 L	113	26.2	344.73	332.32
0	2; 150L	1 L	140	25.4	278.24	274.91
0.25		1 L	198	26.1	196.74	190.25
0.5		1 L	230	26.5	169.37	161.75
0.75		1 L	250	26.8	155.82	147.40
1.25		1 L	289	27.2	134.79	125.89
1.75		1 L	312	27.4	124.85	115.86
2.75		1 L	353	27.7	110.35	101.41
3.75		1 L	370	27.9	105.28	96.12
4	2; 50L added	1 L	348	24.1	111.94	114.96
4.5		1 L	366	25.6	106.43	104.52
5.5		1 L	384	26.6	101.44	96.57
7.5		1 L	405	26.5	96.18	91.86
9		1 L	406	27.0	95.95	90.19
9.25	2; 100L added	1 L	375	25.1	103.88	103.57
10		1 L	388	25.4	100.40	99.19
12		1 L	410	25.9	95.01	92.45
16	2; 50 L added	46.03 g	20	25.3	89.65	88.85
27		43.07 g	20	27.0	83.88	78.85
29		40.66 g	20	27.0	79.18	74.43
31	2; 100L added	41.79 g	20	26.1	81.40	78.71
33		41.03 g	20	26.1	79.92	77.29
36		40.26 g	20	26.2	78.42	75.59
37	2; 50 L added	42.20 g	20	25.5	82.20	80.97
52		36.51 g	20	27.7	71.12	65.36
54		36.42 g	20	27.9	70.93	64.76

**Sample Calculation:**

1. For pure water with 1 L permeate,

$$\begin{aligned} \text{Flux} &= \frac{\text{permeate volume}}{\text{membrane area} * \text{sample time}} \text{ (l/m}^2\text{/h)} \\ &= 1 / 0.092416 / (113/3600) \\ &= 344.73 \text{ (l/m}^2\text{/h)} \end{aligned}$$

$$\begin{aligned} \text{Flux at 25}^\circ\text{C} &= (\text{Flux @ Temp.}) * (1 + (25 - \text{Temp.}) * 0.03) \\ &= 344.73 * (1 + (25 - 26.2) * 0.03) \\ &= 332.32 \text{ (l/m}^2\text{/h)} \end{aligned}$$

2. For Feed 2 with 46.03 g permeate at 16 hours,

$$\begin{aligned} \text{Flux} &= \frac{\text{permeate volume}}{\text{membrane area} * \text{sample time}} \text{ (l/m}^2\text{/h)} \\ &= (46.03/1000) / 0.092416 / (20/3600) \\ &= 89.65 \text{ (l/m}^2\text{/h)} \end{aligned}$$

$$\begin{aligned} \text{Flux at 25}^\circ\text{C} &= (\text{Flux @ Temp.}) * (1 + (25 - \text{Temp.}) * 0.03) \\ &= 89.65 * (1 + (25 - 25.3) * 0.03) \\ &= 88.85 \text{ (l/m}^2\text{/h)} \end{aligned}$$

Date: July 16, 2001

Feed solution: 100L Distilled water + 1 x CLEANBREAK (45 g)

pH of feed: 8.2

Membrane: KOCH XM50 Hollow Fiber

Surface area: 0.092416 m<sup>2</sup>

Inlet pressure: 20 psig

Outlet pressure: 0 psig

Flowrate: 10 L/min

**Table C-2: KOCH XM50 Hollow Fiber Membrane Experimental Data, Dated July 16, 2001**

Operating Time (h)	Volume of Feed (L)	Permeate Volume (L)	Permeate Time (second)	Temperature (°C)	Flux (l/m <sup>2</sup> /h)	Flux @ 25°C (l/m <sup>2</sup> /h)
0	100	1 L	290	24.9	134.33	134.73
0.25	90	1 L	280	27.7	139.12	127.85
1.75	80	1 L	280	29.5	139.12	120.34
2.5	70	1 L	281	30.4	138.63	116.17
3.25	60	1 L	282	30.7	138.14	114.51
4	50	1 L	284	30.8	137.16	113.30

Date: July 17, 2001

Feed solution: 100 L half seawater + 1 x CLEANBREAK (45 g)

pH of feed: 8.2

Membrane: KOCH XM50 Hollow Fiber

Surface area: 0.092416 m<sup>2</sup>

Inlet pressure: 20 psig

Outlet pressure: 0 psig

Flowrate: 10 L/min

**Table C-3: KOCH XM50 Hollow Fiber Membrane Experimental Data, Dated July 17, 2001**

Operating Time (h)	Volume of Feed (L)	Permeate Volume (L)	Permeate Time (second)	Temperature (°C)	Flux (l/m <sup>2</sup> /h)	Flux @ 25°C (l/m <sup>2</sup> /h)
0	100	1 L	246	26.4	158.35	151.70
0.75	90	1 L	282	27.9	138.14	126.12
1.5	80	1 L	317	29.3	122.88	107.03
2.5	70	1 L	346	29.7	112.58	96.71
3.75	60	1 L	271	29.9	104.99	89.56
4.75	50	1 L	386	29.9	100.92	86.08

Date: July 18, 2001

Feed solution: 100 L half seawater + 2 x CLEANBREAK (90 g)

pH of feed: 8.2

Membrane: KOCH XM50 Hollow Fiber

Surface area: 0.092416 m<sup>2</sup>

Inlet pressure: 20 psig

Outlet pressure: 0 psig

Flowrate: 10 L/min

**Table C-4: KOCH XM50 Hollow Fiber Membrane Experimental Data, Dated July 18, 2001**

Operating Time (h)	Volume of Feed (L)	Permeate Volume (L)	Permeate Time (second)	Temperature (°C)	Flux (l/m <sup>2</sup> /h)	Flux @ 25°C (l/m <sup>2</sup> /h)
0	100	1 L	252	25.4	154.58	152.72
0.75	90	1 L	304	27.9	128.14	116.99
1.5	80	1 L	347	28.7	122.26	99.80
2.5	70	1 L	380	29.0	102.51	92.21
3.75	60	1 L	398	29.4	97.88	84.96
4.75	50	1 L	416	29.3	93.64	81.56

Date: July 19, 2001

Feed solution: 100 L half seawater + 4 x CLEANBREAK (180 g)

pH of feed: 8.2

Membrane: KOCH XM50 Hollow Fiber

Surface area: 0.092416 m<sup>2</sup>

Inlet pressure: 20 psig

Outlet pressure: 0 psig

Flowrate: 10 L/min

**Table C-5: KOCH XM50 Hollow Fiber Membrane Experimental Data, Dated July 19, 2001**

Operating Time (h)	Volume of Feed (L)	Permeate Volume (L)	Permeate Time (second)	Temperature (°C)	Flux (l/m <sup>2</sup> /h)	Flux @ 25°C (l/m <sup>2</sup> /h)
0	100	1 L	237	24.9	164.36	164.86
0.75	90	1 L	283	27.9	137.65	125.67
1.5	80	1 L	343	29.3	113.57	98.92
2.5	70	1 L	385	29.8	101.18	86.61
3.75	60	1 L	398	30.0	97.88	83.19
4.75	50	1 L	410	30.1	95.01	80.47

Date: August 28, 2001

Feed solution: 100 L half seawater + 10 x CLEANBREAK (450 g)

pH of feed: 8.2

Membrane: KOCH XM50 Hollow Fiber

Surface area: 0.092416 m<sup>2</sup>

Inlet pressure: 20 psig

Outlet pressure: 0 psig

Flowrate: 10 L/min

**Table C-6: KOCH XM50 Hollow Fiber Membrane Experimental Data, Dated August 28, 2001**

Operating Time (h)	Volume of Feed (L)	Permeate Volume (L)	Permeate Time (second)	Temperature (°C)	Flux (l/m <sup>2</sup> /h)	Flux @ 25°C (l/m <sup>2</sup> /h)
0	100	1 L	242	24.2	160.9682	164.83139
0.75	90	1 L	276	27.9	141.1387	128.85967
1.5	80	1 L	322	29.6	120.9761	104.28137
2.5	70	1 L	356	29.8	109.4222	93.66538
3.75	60	1 L	381	30.9	102.2422	84.145364
4.75	50	1 L	390	31	99.8828	81.903899

## Appendix D

### Raw Data and Sample Calculation of KOCH Carbo-cor Membranes Testing

Date: March 28, 2001

Feed: 100L bilge water

Membrane pore size: 0.05  $\mu\text{m}$

Operating conditions: Pressure 35 psig; no backflushing; with concentration

Temperature: 25  $^{\circ}\text{C}$

Table D-1: KOCH Carbo-cor 0.05  $\mu\text{m}$  Experimental Data, Dated March 28, 2001

Accumulated Time (h)	Time interval dt (h)	Permeate tank level difference dv(mV)	Permeate flowrate dv/dt*150(ml/h)	Permeate flux ( $\text{l}/\text{m}^2/\text{h}$ )
1.007	0.413	19.9	7214	327.93
1.669	0.414	14	5072	230.55
2.535	0.419	10.2	3648	165.85
3.634	0.413	7.9	2864	130.20
4.970	0.414	6.7	2422	110.12
6.420	0.417	6.6	2368	107.66
7.903	0.420	6.4	2285	103.89
9.401	0.426	6.1	2147	97.61
11.037	0.436	6.1	2097	95.32
12.614	0.442	6.1	2068	94.01
14.184	0.446	6.2	2084	94.73
15.835	0.450	6.3	2096	95.28
17.552	0.463	6.3	2039	92.68
19.256	0.464	6.1	1971	89.59
20.994	0.462	5.9	1915	87.05
22.8109	0.484	6.2	1918	87.18

Date: March 21-22, 2001

Feed: 100L bilge water

Membrane pore size: 0.1  $\mu\text{m}$

Operating conditions: Pressure 35 psig; no backflushing

Temperature: 25  $^{\circ}\text{C}$

Table D-2: KOCH Carbo-cor 0.1  $\mu\text{m}$  Experimental Data, Dated March 21-22, 2001

Accumulated Time (h)	Time interval dt (h)	Permeate tank level difference dv(mV)	Permeate flowrate dv/dt*150(ml/h)	Permeate flux (l/m <sup>2</sup> /h)
0.628	0.464	20.4	6591	299.61
1.385	0.464	15.7	5066	230.29
2.306	0.465	13.3	4282	194.66
3.328	0.469	11.9	3800	172.73
4.455	0.472	11	3488	158.57
5.668	0.484	10.9	3371	153.23
6.844	0.492	11	3353	152.41
8.055	0.491	10.6	3234	147.01
9.305	0.494	10.3	3124	142.01
10.53	0.502	10.8	3222	146.47
11.803	0.510	10.7	3146	143.01
13.112	0.513	10.9	3186	144.84
14.429	0.517	11	3186	144.82
15.651	0.524	10.8	3091	140.51
16.913	0.534	11.1	3116	141.67
18.159	0.535	11.2	3136	142.56
19.450	0.537	10.8	3013	136.98

Date: March 22-23, 2001  
 Feed: 100L bilge water  
 Membrane pore size: 0.1  $\mu\text{m}$   
 Operating conditions: Pressure 35 psig; no backflushing  
 Temperature: 25  $^{\circ}\text{C}$

**Table D-3: KOCH Carbo-cor 0.1  $\mu\text{m}$  Experimental Data, Dated March 22-23, 2001**

Accumulated Time (h)	Time interval dt (h)	Permeate tank level difference dv(mV)	Permeate flowrate dv/dt*150(ml/h)	Permeate flux ( $\text{l}/\text{m}^2/\text{h}$ )
21.479	0.386	15.3	5931	269.61
22.333	0.389	14.3	5511	250.50
23.088	0.388	13.9	5367	243.95
23.898	0.392	13.2	5048	229.47
24.762	0.391	12.1	4636	210.73
25.681	0.391	11.6	4445	202.04
26.624	0.402	11.6	4320	196.38
27.617	0.312	8.6	4126	187.54
28.552	0.311	8.4	4038	183.58
29.532	0.311	8.1	3895	177.05
30.589	0.312	8.4	4031	183.25
31.601	0.312	8.1	3890	176.83
32.636	0.312	7.8	3741	170.06
34.772	0.312	7.8	3745	170.26
35.872	0.311	7.8	3753	170.59
36.951	0.311	7.7	3702	168.29
37.892	0.312	7.3	3506	159.38

Date: March 24-25, 2001

Feed: 100L bilge water

Membrane pore size: 0.1  $\mu\text{m}$

Operating conditions: Pressure 35 psig; no backflushing

Temperature: 25  $^{\circ}\text{C}$

Table D-4: KOCH Carbo-cor 0.1  $\mu\text{m}$  Experimental Data, Dated March 24-25, 2001

Accumulated Time (h)	Time interval dt (h)	Permeate tank level difference dv(mV)	Permeate flowrate dv/dt*150(ml/h)	Permeate flux (l/m <sup>2</sup> /h)
38.737	0.445	10	3369	153.16
39.211	0.451	9.6	3190	145.03
40.210	0.445	9.5	3197	145.34
41.302	0.445	9.3	3131	142.34
42.339	0.447	9	3016	137.11
43.341	0.445	9.3	3131	142.32
44.375	0.445	9.3	3128	142.21
45.390	0.445	9.2	3096	140.75
46.426	0.446	9.3	3123	141.98
47.509	0.446	8.8	2956	134.40
48.592	0.446	8.7	2925	132.95
49.680	0.446	9	3026	137.58
50.787	0.446	8.7	2924	132.94
51.824	0.448	9.2	3079	139.97
52.915	0.446	8.5	2854	129.72
54.048	0.445	8.4	2828	128.54
55.186	0.447	8.2	2747	124.87
56.315	0.447	8.2	2750	125.04
57.518	0.448	8.4	2809	127.72
58.644	0.446	8.5	2853	129.68
59.728	0.446	8.7	2921	132.81
60.821	0.447	8.4	2818	128.09
61.963	0.445	8.5	2859	129.95

Date: March 25-26, 2001  
 Feed: 100L bilge water  
 Membrane pore size: 0.1  $\mu\text{m}$   
 Operating conditions: Pressure 35 psig; no backflushing  
 Temperature: 25  $^{\circ}\text{C}$

**Table D-5: KOCH Carbo-cor 0.1  $\mu\text{m}$  Experimental Data, Dated March 25-26, 2001**

Accumulated Time (h)	Time interval dt (h)	Permeate tank level difference dv(mV)	Permeate flowrate dv/dt*150(ml/h)	Permeate flux ( $\text{l}/\text{m}^2/\text{h}$ )
62.866	0.452	8.8	2918	132.65
63.946	0.446	8.7	2923	132.90
65.065	0.446	8.4	2824	128.38
66.176	0.445	8.4	2826	128.46
67.331	0.446	8.2	2755	125.24
68.452	0.446	8.4	2823	128.33
69.590	0.446	8.2	2752	125.10
70.747	0.448	8.2	2742	124.67
71.979	0.449	8.2	2737	124.44
73.098	0.447	8.2	2746	124.82
74.247	0.448	8	2677	121.70
75.424	0.448	7.9	2644	120.20
76.578	0.449	8.2	2736	124.39
77.726	0.448	8.2	2744	124.77
78.979	0.448	7.9	2642	120.12
80.159	0.446	7.9	2656	120.74
81.305	0.447	8.4	2813	127.87
82.479	0.446	8.2	2756	125.28
83.604	0.446	8.4	2822	128.27
84.754	0.449	8.4	2801	127.34
85.878	0.451	8.4	2788	126.74
87.046	0.459	8.5	2774	126.09
88.225	0.459	8.4	2741	124.60
89.424	0.459	8.2	2676	121.64
90.624	0.459	8.2	2676	121.65

Date: March 26-27, 2001

Feed: 100L bilge water

Membrane pore size: 0.1  $\mu\text{m}$

Operating conditions: Pressure 35 psig; no backflushing; with concentration

Temperature: 25  $^{\circ}\text{C}$

Table D-6: KOCH Carbo-cor 0.1  $\mu\text{m}$  Experimental Data, Dated March 26-27, 2001

Accumulated Time (h)	Time interval dt (h)	Permeate tank level difference dv(mV)	Permeate flowrate dv/dt*150(ml/h)	Permeate flux ( $\text{l}/\text{m}^2/\text{h}$ )
92.043	0.459	8.5	2773	126.05
93.376	0.459	7.9	2579	117.22
94.719	0.459	7.7	2511	114.17
96.107	0.459	7.9	2579	117.25
97.523	0.459	7.6	2481	112.79
98.913	0.459	7.6	2478	112.66
100.340	0.459	7.4	2413	109.72
101.672	0.461	7.4	2407	109.43
103.091	0.459	7.6	2481	112.77
104.449	0.459	7.9	2577	117.17
105.836	0.461	8.7	2827	128.53
107.009	0.460	8.4	2735	124.33
107.394	0.360	6.4	2660	120.92
108.664	0.355	6.2	2613	118.7
108.570	1.115	20.8	2797	127.14
109.801	1.123	20.7	2763	125.61
111.009	1.114	20.4	2746	124.83
112.294	1.137	19.8	2610	118.64
113.599	1.165	20.4	2625	119.32

Date: March 15-16, 2001

Feed: 100L bilge water

Membrane pore size: 0.2  $\mu\text{m}$

Operating conditions: Pressure 35 psig; 1-20 hours with backflushing 3/58 second; then membrane was cleaned; 20-40 hours without backflushing

Temperature: 25  $^{\circ}\text{C}$

Table D-7: KOCH Carbo-cor 0.2  $\mu\text{m}$  Experimental Data, Dated March 15-16, 2001

Accumulated Time (h)	Time interval dt (h)	Permeate tank level difference dv(mV)	Permeate flowrate dv/dt*150(ml/h)	Permeate flux (l/m <sup>2</sup> /h)
0.155	0.013	2.2	24416	1109.83
0.357	0.013	1.4	15660	711.83
0.638	0.013	0.9	9865	448.41
1.029	0.013	0.8	8922	405.57
1.576	0.013	0.6	6792	308.74
2.317	0.013	0.3	3358	152.66
3.278	0.013	0.3	3316	150.77
4.524	0.013	0.2	2236	101.67
6.107	0.013	0.2	2206	100.30
7.939	0.026	0.3	1686	76.63
9.718	0.026	0.3	1675	76.14
11.78	0.027	0.3	1665	75.72
14.027	0.026	0.2	1114	50.65
16.336	0.026	0.2	1118	50.85
15.799	0.053	0.4	1124	51.13
17.096	0.052	0.3	853	38.78
17.216	0.026	0.1	563	25.63
19.102	0.027	0.1	554	25.19
20.449	0.027	0.1	552	25.10
20.786	0.306	9	4400	200.00
21.457	0.459	9.9	3228	146.76
27.465	0.459	2.8	913	41.53
32.941	0.414	1.6	578	26.29
40.191	0.415	1.4	505	22.95

Date: March 16-19, 2001

Feed: 100L bilge water

Membrane pore size: 0.5  $\mu\text{m}$

Operating conditions: Pressure 35 psig; 1-68 hours with backflushing 3/27 second; then membrane was cleaned; 68-81 hours without backflushing

Temperature: 25  $^{\circ}\text{C}$

Table D-8: KOCH Carbo-cor 0.5  $\mu\text{m}$  Experimental Data, Dated March 16-19, 2001

Accumulated Time (h)	Time interval dt (h)	Permeate tank level difference dv(mV)	Permeate flowrate dv/dt*150(ml/h)	Permeate flux (l/m <sup>2</sup> /h)
1.669	0.493	20.2	6134	278.85
2.273	0.501	17.5	5237	238.07
2.985	0.501	15.5	4636	210.76
3.729	0.500	14.2	4252	193.31
4.485	0.501	14.2	4247	193.06
5.270	0.501	13.8	4128	187.66
6.047	0.500	13.9	4165	189.33
6.876	0.460	11.6	3780	171.86
7.691	0.459	12.2	3978	180.83
8.511	0.459	11.9	3885	176.61
9.342	0.459	11.7	3816	173.48
10.156	0.460	11.9	3877	176.27
10.985	0.460	11.8	3844	174.73
11.816	0.459	11.7	3816	173.48
12.670	0.459	11.5	3753	170.59
13.520	0.459	11.5	3752	170.54
14.388	0.459	11.5	3754	170.64
15.242	0.459	11.6	3786	172.09
16.078	0.459	11.9	3883	176.52
16.915	0.459	11.7	3819	173.60
17.740	0.459	12	3915	177.99
18.572	0.460	11.9	3880	176.37
19.389	0.459	12	3913	177.87
20.229	0.459	11.9	3885	176.63
21.070	0.459	11.9	3888	176.74
21.915	0.459	11.7	3822	173.73
22.768	0.458	11.6	3795	172.52
23.620	0.458	11.7	3827	173.96
24.459	0.458	11.7	3827	173.98
25.617	0.917	21.5	3516	159.83
27.482	0.919	21.4	3492	158.76
28.526	0.919	21	3426	155.74
29.495	0.91	21.5	3510	159.54
30.488	0.919	21.2	3459	157.26
31.491	0.919	21.2	3457	157.13
32.493	0.919	20.4	3327	151.24
33.508	0.918	20.8	3396	154.39

34.501	0.919	20.9	3409	154.98
35.467	0.919	21.4	3489	158.62
36.446	0.919	21.1	3441	156.43
38.404	0.918	20.9	3411	155.07
39.392	0.919	20.7	3377	153.53
40.427	0.919	20	3262	148.31
41.479	0.918	20	3265	148.41
42.509	0.919	20.2	3296	149.81
43.557	0.919	19.9	3247	147.63
44.623	0.918	19.6	3199	145.44
45.671	0.919	19.7	3213	146.07
46.751	0.918	19	3101	140.97
47.844	0.918	18.9	3085	140.26
48.911	0.919	19.6	3197	145.33
50.018	0.918	18.4	3004	136.56
51.622	1.197	21.2	2655	120.69
53.031	1.196	19.4	2431	110.53
54.440	1.196	19.3	2418	109.93
55.886	1.196	18.2	2281	103.70
57.488	1.195	17.1	2144	97.48
59.118	1.196	16.8	2105	95.70
60.881	1.196	14.8	1855	84.34
62.611	0.779	10.4	2000	90.92
64.320	0.680	8.7	1918	87.19
68.550	1.229	15.8	1927	87.62
70.333	1.229	14.4	1756	79.85
72.384	1.229	13	1585	72.08
74.523	1.228	12.2	1489	67.71
76.663	1.229	12.5	1525	69.34
78.980	1.228	11.5	1403	63.81
81.209	1.229	11.3	1378	62.67

Date: March 31, 2001

Feed: 100L bilge water

Membrane pore size: 0.8  $\mu\text{m}$

Operating conditions: Pressure 35 psig; without backflushing; with concentration

Temperature: 25  $^{\circ}\text{C}$

Table D-9: KOCH Carbo-cor 0.8  $\mu\text{m}$  Experimental Data, Dated March 31, 2001

Accumulated Time (h)	Time interval dt (h)	Permeate tank level difference dv(mV)	Permeate flowrate dv/dt*150(ml/h)	Permeate flux (l/m <sup>2</sup> /h)
0.173	0.089	11.6	19352	879.67
0.460	0.091	5.8	9481	430.99
0.999	0.506	21.2	6283	285.61
2.016	0.506	10.1	2989	135.90
3.728	0.509	5.5	1619	73.60
6.296	0.515	4.1	1193	54.27

9.203	0.534	3.6	1010	45.94
12.598	0.546	3.7	1016	46.19
16.096	0.567	3.7	977	44.42
20.100	0.587	3.2	817	37.13

### Sample Calculation:

The following describe how the experimental data listed in Table D1-D9 was obtained. Table D10 lists the original data recorded and stored in the computer during the run of Carbo-cor 0.05 micron membrane on March 28, 2001. It is an abbreviated data set taken as sample explanation.

Table D-10: KOCH Carbo-cor 0.05  $\mu\text{m}$  Experimental Raw Data, Dated March 28, 2001

Time (msecond)	Permeate tank level reading (mV)	Pressure (psig)	Temperature ( $^{\circ}\text{C}$ )
3859707	0.0333	34.6	24.8
3876097	0.0336	35.1	24.8
3892526	0.0339	35.0	24.8
3908987	0.0342	35.1	24.8
3925432	0.0345	35.5	24.9
3941932	0.0346	34.9	24.9
3958448	0.0349	35.3	25.0
3974987	0.0354	35.1	25.0
3991487	0.0356	34.9	24.9
4008042	0.0359	35.2	24.9

.....

5398435	0.0542	35.1	24.9
5414871	0.0543	34.8	24.8
5431387	0.0546	34.8	24.8
5447942	0.0548	34.8	24.8
5464371	0.0549	34.9	24.8
5480926	0.0552	34.9	24.9
5497426	0.0554	34.9	24.9
5513761	0.0557	34.7	24.9
5530316	0.0558	35.1	24.9
5546777	0.0543	34.9	25.0

During the experimental run, the data was recorded by the computer using the LABVIEW software program. The permeate tank's pressure transducer continually fed a signal to the personal computer. At a set point, associated with the low tank level, the discharge valve was closed and the permeate tank began to fill. At a high set point, associated with the high tank level, the discharge valve opened thereby dumping the permeate back to the feed tank. In this manner, the volume of the permeate collected over a given time interval can be determined.

Two points of the permeate tank level (0.0349 & 0.0548) were taken for calculation.

The time interval  $dt = (5447942-3958448)/1000/60/60 = 0.414$  (h)

Permeate tank level reading difference  $dv = (0.0548-0.0349)*1000 = 19.9$  (mV)

Permeate volume  $\Delta$ Tank volume =  $dv * \text{coefficient} = dv * 150$  (mL)

$$\text{Permeate flowrate} = \frac{\Delta \text{Tank volume}}{\Delta \text{Time}} \quad (\text{l/h}) = dv/dt * 150$$

$$= 19.9/0.414 * 150 = 7210 \text{ (mL/h)}$$

$$\text{Permeate flux} = \frac{\text{permeate volume}}{\text{membrane area} * \text{sample time}} \text{ (L/m}^2\text{/h)} = 7210/1000/0.022$$

$$= 327.73 \text{ (L/m}^2\text{/h)}$$

During the run, the operating pressure was well maintained to 35 +/- 0.5 psig, the temperature was 25 +/- 0.1°C. The result of the permeate flux calculated from above was considered at 35 psig and 25 °C.

The coefficient 150 was from the tank level calibration as shown below.

Table D-11: Permeate Tank Level Calibration Data, Dated March 05, 2001

Permeate volume (L)	Permeate tank level reading (mV)
0	0.0533
0.1	0.0539
0.2	0.0545
0.25	0.0548
0.35	0.0555
0.45	0.0562
0.5	0.0566
0.6	0.0572
0.7	0.0578
0.75	0.0583
0.85	0.0589
0.95	0.0595
1	0.0598
1.1	0.0606
1.2	0.0612
1.25	0.0615
1.35	0.0623
1.45	0.0629
1.5	0.0632

The permeate tank level was calibrated by discharging certain amount of permeate from the permeate tank and recorded the corresponding tank level reading in the computer. The data was shown in the table above.

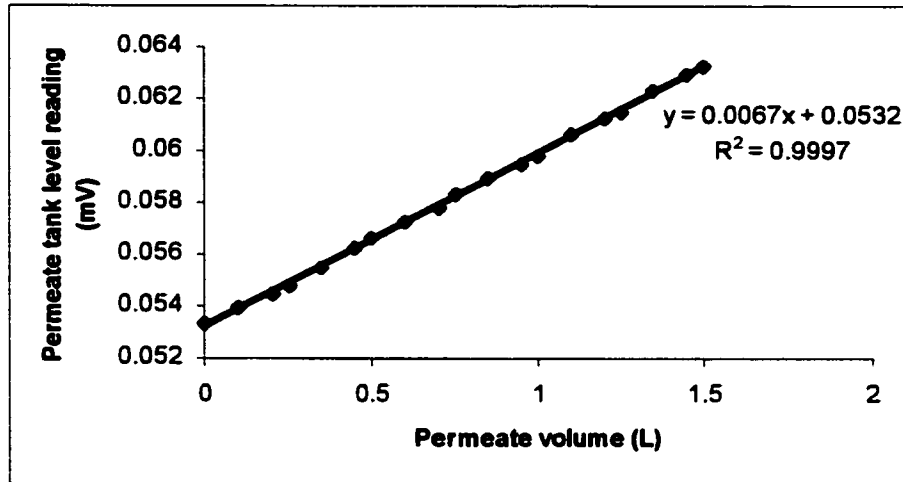


Figure D-1: Plot of Permeate tank level reading vs. Permeate volume

From equation  $y = 0.0067x + 0.0532$ , it is easily seen that

$$\frac{\Delta \text{Permeate tank level}}{\Delta \text{Permeate volume}} = 0.0067$$

$$\text{Therefore, } \Delta \text{ Permeate volume} = \frac{\Delta \text{Permeate tank level}}{0.0067}$$

$$= \Delta \text{ Permeate tank level} * 149.2537$$

In sample calculation, 150 was used instead of 149.2537 as calibration coefficient.

## Appendix E

### Calculation of Specific Cake Resistance for the KOCH Carbo-cor Membranes

As identified in the experimental section, three separation mechanisms have been used to explain the flux decline associated with particle deposition during membrane filtration: pore blockage, pore constriction and cake filtration. Specific cake resistance  $\alpha_{cake}$  is one of the major characteristics of filter cake formation. A plot of  $t/V$  versus  $V$  can be used to determine  $\alpha_{cake}$  and  $R_m$ . The following describes the summarized data and sample calculation of  $\alpha_{cake}$  and  $R_m$  for the KOCH Carbo-cor 0.05, 0.1, 0.5, 0.8 and 1.4 micron membranes.

#### Sample calculation

The following describes how the data in Table E-1 was obtained. These sample calculations are based upon the raw data for the KOCH Carbo-cor 0.05 micron experimental runs from August 21-25, 2001.

Date: August 21-25, 2001

Feed: 100L bilge water with 2 x oils (100L half seawater + 200g diesel fuel, 160g used oil, 40g hydraulic oil, 90g CLEANBREAK & 10g OSTREM Rust Stain Remover)

Membrane pore size: KOCH Carbo-cor 0.05  $\mu\text{m}$

Operating conditions: Inlet pressure 30psig, outlet pressure 20psig, TMP=5, 10, 15 & 25 psig.

Table E-1: KOCH Carbo-cor 0.05  $\mu\text{m}$  Experimental Data, dated August 21-25, 2001

TMP (psig)	Accumulated time, t (h)	Actual flux (L/m <sup>2</sup> /h)	Actual permeate (L/ m <sup>2</sup> )	Accumulated permeate (L/ m <sup>2</sup> )	Accumulated permeate volume, V (m <sup>3</sup> )	t/V (s/ m <sup>3</sup> )
5	1.003	32.58	32.68	32.677	0.001438	2511113
	2.449	26.76	42.92	75.60	0.003326	2651072
	4.898	21.53	59.11	134.71	0.005927	2974720
	7.52	20.76	55.47	190.17	0.008368	3235464
	10.48	19.54	59.58	249.75	0.010989	3432197
	12.81	18.34	44.26	294.01	0.012936	3565789
	15.97	16.82	55.56	349.57	0.015381	3738748
	19.09	16.05	51.14	400.71	0.017631	3897086
	22.29	16.71	52.43	453.14	0.019938	4024231
	24.64	16.67	39.25	492.38	0.021665	4094256
10	0.511	36.58	18.712	18.711	0.000823	2236479
	2.51	33.73	70.247	88.958	0.003914	2308131
	3.9	31.62	45.452	134.41	0.005914	2374309
	5.347	29.93	44.519	178.929	0.007873	2445036
	6.705	30.45	40.982	219.911	0.009676	2494469
	8.711	30.52	61.175	281.086	0.012368	2535718
	10.72	28.73	59.453	340.539	0.014984	2575171
	12.77	27.69	57.872	398.412	0.01753	2622381
	14.79	26.83	55.006	453.417	0.01995	2668355
	16.91	26.36	56.427	509.845	0.022433	2713531

	18.37	26.34	38.414	548.258	0.024123	2740966
	20.49	26.22	55.759	604.017	0.026577	2775346
	22.73	26.35	58.883	662.901	0.029168	2805351
	23.75	26.29	26.943	689.842	0.030353	2817200
15	0.801	41.83	33.518	33.517	0.001475	1956069
	2.289	38.08	59.424	92.941	0.004089	2014806
	3.847	37.5	58.865	151.805	0.006679	2073160
	5.416	36.29	57.882	209.687	0.009226	2113094
	7.096	34.46	59.431	269.118	0.011841	2157265
	8.698	33.36	54.339	323.458	0.014232	2200221
	10.35	33	54.643	378.101	0.016636	2238608
	11.98	31.97	53.148	431.249	0.018975	2273091
	13.65	30.76	52.362	483.611	0.021279	2309400
	15.36	29.35	51.396	535.007	0.02354	2349066
	16.58	29.96	36.299	571.306	0.025137	2375103
	18.33	28.62	51.176	622.482	0.027389	2409486
	20.02	28.86	48.613	671.095	0.029528	2441181
	22.78	28.84	79.514	750.609	0.033027	2483004
25	0.477	74.16	35.395	35.395	0.001557	1103337
	1.59	71.07	80.81	116.205	0.005113	1119617
	2.703	65.9	76.214	192.419	0.008466	1149355
	3.816	60.19	70.148	262.567	0.011553	1189022
	4.992	56.62	68.673	331.241	0.014575	1232949
	6.116	50.58	60.245	391.485	0.017225	1278123
	7.317	47.11	58.704	450.189	0.019808	1329885
	8.464	44.82	52.682	502.871	0.022126	1377045
	10.85	40.8	102.1	604.972	0.026619	1467210
	13.14	39.01	91.325	696.298	0.030637	1543708
	14.34	37.01	45.819	742.116	0.032653	1581308
	15.54	39.79	46.145	788.261	0.034683	1613474
	16.73	38.28	46.19	834.451	0.036716	1640183
	17.93	39.04	46.329	880.780	0.038754	1665223
	19.97	38.73	79.485	960.264	0.042252	1701545
	22.4	38.65	93.996	1054.261	0.046387	1738396
	23.49	39.75	42.895	1097.156	0.048275	1752033

**A) Determination of  $Kp/2$  and  $l/q_0$**

Take the experimental data of TMP=5 psig, accumulated time  $t = 2.449$  h, the actual flux at this point was  $26.76$  (L/m<sup>2</sup>/h)

$$\begin{aligned}
 \text{Actual permeate} &= \text{accumulated time} * \text{actual flux} \\
 &= 2.449 \text{ h} * 26.76 \text{ (L/m}^2\text{/h)} \\
 &= 42.92 \text{ (L/ m}^2\text{)}
 \end{aligned}$$

$$\text{Accumulated permeate} = 42.92 + 32.68 = 75.60 \text{ (L/ m}^2\text{)}$$

$$\begin{aligned} \text{Accumulated permeate volume, } V &= \text{Accumulated permeate} * \text{membrane area} \\ &= 75.60 \text{ L/m}^2 * 1\text{m}^3/1000\text{L} * 0.044\text{m}^2 \\ &= 0.003326 \text{ m}^3 \end{aligned}$$

$$t/V = 2.449 \text{ h}/0.003326 \text{ m}^3 * (3600\text{s/h}) = 2651074 \text{ (s/ m}^3\text{)}$$

Plots of  $t/V$  vs.  $V$  for this membrane at different TMPs can be found from Figure E1 to E4 below.

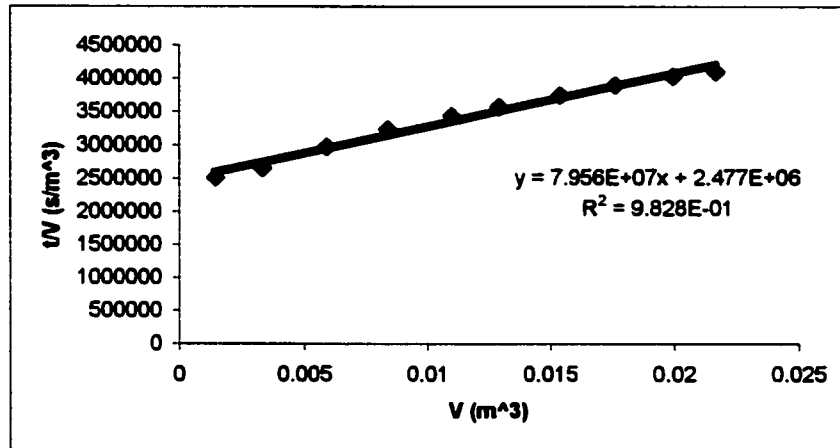


Figure E-1: Plot of  $t/V$  vs.  $V$  for the KOCH Carbo-cor 0.05 micron membrane operating at TMP= 5psig.

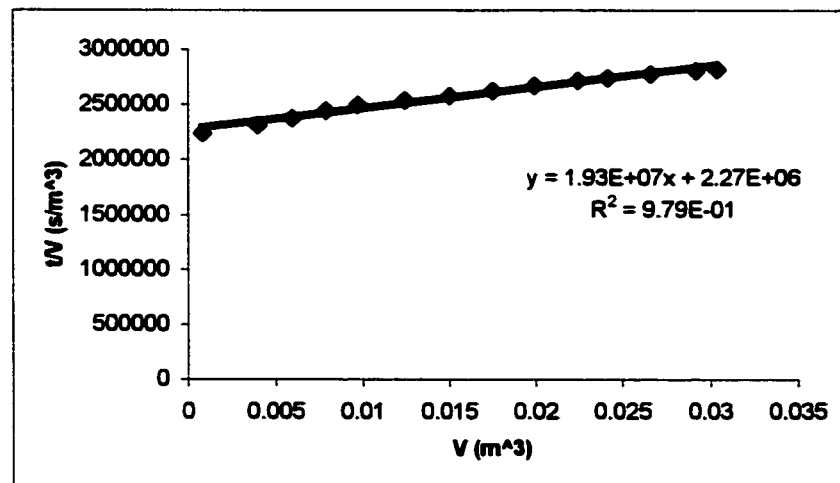


Figure E-2: Plot of  $t/V$  vs.  $V$  for the KOCH Carbo-cor 0.05 micron membrane operating at TMP= 10psig.

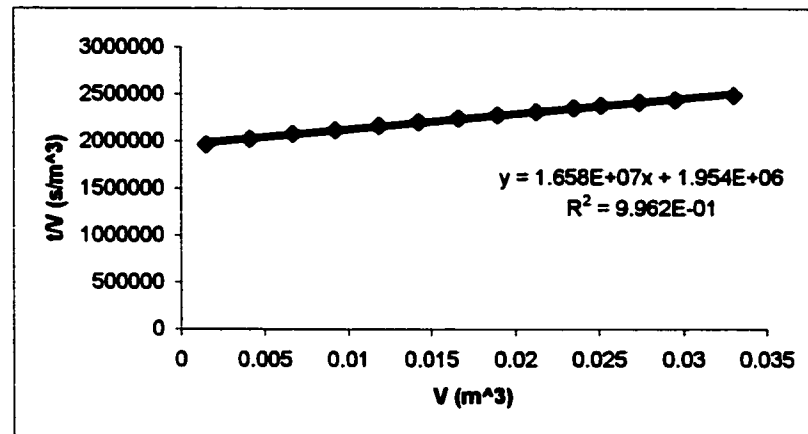


Figure E-3: Plot of  $t/V$  vs.  $V$  for the KOCH Carbo-cor 0.05 micron membrane operating at TMP= 15psig.

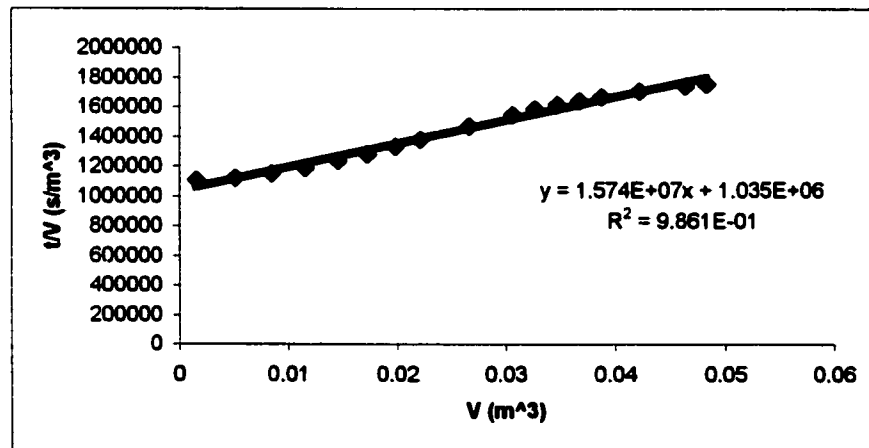


Figure E-4: Plot of  $t/V$  vs.  $V$  for the KOCH Carbo-cor 0.05 micron membrane operating at TMP= 25psig.

Using Equation (3.19):

$$\frac{t}{V} = \left( \frac{K_p}{2} \right) V + \frac{1}{q_0}$$

$\frac{K_p}{2}$  and  $\frac{1}{q_0}$  can be determined from the above plots. Results are shown in Table E-2 below.

Table E-2: Values of  $K_p/2$  and  $1/q_0$  determined from  $t/V$  vs.  $V$  plots for the KOCH Carbo-cor 0.05 micron membrane

	TMP (psig)			
	5	10	15	25
$K_p/2$ (s/m <sup>6</sup> )	7.96E+07	1.93E+07	1.66E+07	1.57E+07
$1/q_0$ (s/m <sup>3</sup> )	2.48E+06	2.27E+06	1.95E+06	1.04E+06

**B) Calculation of  $\alpha_{cake}$**

The specific cake resistance can be calculated using Equation (3.22):

$$\alpha_{cake} = \frac{A^2 \Delta P K_p}{c \mu}$$

Where  $A = 0.044m^2$  (2 membranes tested at the same time)

$$c = \text{Concentration of the feed} = c_{oil+detergent} = \frac{0.5Kg}{100L} = \frac{0.005Kg}{L}$$

$$\mu = 0.00089 \text{ Pa s (viscosity of water at } 25^\circ\text{C)}$$

When  $\Delta P = 5\text{psig} = 34450 \text{ Pa}$ ,

$$\alpha_{cake} = \frac{(0.044m^2)^2 * 34450P_a * 7.96 * 10^7 * 2 \frac{s}{m^6}}{\frac{0.005Kg}{L} * \frac{1000L}{m^3} * 0.00089P_a s} = 2.38E+15 \text{ (m/Kg)}$$

When  $\Delta P = 10\text{psig} = 68900 \text{ Pa}$ ,

$$\alpha_{cake} = \frac{(0.044m^2)^2 * 68900P_a * 1.93 * 10^7 * 2 \frac{s}{m^6}}{\frac{0.005Kg}{L} * \frac{1000L}{m^3} * 0.00089P_a s} = 1.16E+15 \text{ (m/Kg)}$$

When  $\Delta P = 15\text{psig} = 103350 \text{ Pa}$ ,

$$\alpha_{cake} = \frac{(0.044m^2)^2 * 103350P_a * 1.66 * 10^7 * 2 \frac{s}{m^6}}{\frac{0.005Kg}{L} * \frac{1000L}{m^3} * 0.00089P_a s} = 1.49E+15 \text{ (m/Kg)}$$

When  $\Delta P = 25\text{psig} = 172250 \text{ Pa}$ ,

$$\alpha_{cake} = \frac{(0.044m^2)^2 * 172250P_a * 1.57 * 10^7 * 2 \frac{s}{m^6}}{\frac{0.005Kg}{L} * \frac{1000L}{m^3} * 0.00089P_a s} = 2.36E+15 \text{ (m/Kg)}$$

C) Calculation of  $R_m$ 

The membrane resistance can be calculated using Equation (3.23):

$$R_m = \frac{A\Delta P}{\mu q_0}$$

When  $\Delta P = 5\text{psig} = 34450\text{ Pa}$ ,

$$R_m = \frac{0.044\text{m}^2 * 34450P_a * 2.48 * 10^6 (s/m^3)}{0.00089P_a s} = 4.22\text{E}+12 \text{ (m}^{-1}\text{)}$$

When  $\Delta P = 10\text{psig} = 68900\text{ Pa}$ ,

$$R_m = \frac{0.044\text{m}^2 * 68900P_a * 2.27 * 10^6 (s/m^3)}{0.00089P_a s} = 7.73\text{E}+12 \text{ (m}^{-1}\text{)}$$

When  $\Delta P = 15\text{psig} = 103350\text{ Pa}$ ,

$$R_m = \frac{0.044\text{m}^2 * 103350P_a * 1.95 * 10^6 (s/m^3)}{0.00089P_a s} = 9.96\text{E}+12 \text{ (m}^{-1}\text{)}$$

When  $\Delta P = 25\text{psig} = 172250\text{ Pa}$ ,

$$R_m = \frac{0.044\text{m}^2 * 172250P_a * 1.04 * 10^6 (s/m^3)}{0.00089P_a s} = 8.86\text{E}+12 \text{ (m}^{-1}\text{)}$$

## Appendix F

### Oil and Grease Determination Using EPA Method 1664: Procedure and Standards

In June 1999, EPA approved the use of Method 1664 for the analysis of oil and grease, replacing other EPA methods such as Method 413.1. The full text of the method 1664 was published by EPA in Method 1664 Revision A: n-Hexane Extractable Material (HEM; Oil and Grease) and Silica Gel Treated n-Hexane Extractable Material (SGT-HEM; Nonpolar Material) by Extraction and Gravimetry (EPA, 1999).

In this study, oil and grease in the permeate sample were determined by n-Hexane liquid-liquid extraction. The following describes the experimental procedure and standardization being performed in our lab.

#### 1. Procedure

- 1) Collect 1 L of permeate sample;
- 2) Acidify the sample to pH < 2 using H<sub>2</sub>SO<sub>4</sub>;
- 3) Pour the sample into the separatory funnel;
- 4) Add 30 mL of n-Hexane (EM Science, >99.99%) to the sample;
- 5) Extract the sample by shaking the separatory funnel vigorously for 2 minutes;
- 6) Allow the sample to settle for a minimum of 10 minutes;
- 7) Drain the aqueous layer (lower layer);
- 8) Place a filter paper (Fisher Scientific, Diameter: 15 cm, Porosity: medium) in a filter funnel, add approximately 10 g of anhydrous Na<sub>2</sub>SO<sub>4</sub> (BDH, 99%);
- 9) Drain the n-Hexane layer (upper layer) from the separatory funnel through the Na<sub>2</sub>SO<sub>4</sub> into a pre-weighed dish;
- 10) Repeat the extraction with fresh 30 mL of n-Hexane;
- 11) Weigh the dish after the solvent is distilled from the dish. The residue in the dish is defined as oil and grease.

#### 2. Standards

- 1) Materials:
  - Reagent water (reverse osmosis water)
  - n-Hexane (EM Science, >99.99%)
  - Hexadecane (Aldrich Chemical Company, Inc., 99 + %)
  - Stearic acid (Fisher Scientific, purified)
  - Acetone (BDH, 99.5%)
  - Sodium sulfate (Na<sub>2</sub>SO<sub>4</sub>) (BDH, 99%).
- 2) Prepare Hexadecane/ Stearic acid (1:1) spiking solution
  - Place 200 ± 2 mg Hexadecane and 200 ± 2 mg Stearic acid in a 100-mL volumetric flask and fill to the mark with acetone. Store in the dark at room temperature.
- 3) Using a pipet, spike 10.0 ± 0.1 mL of Hexadecane/ Stearic acid spiking solution into 1 L of reagent water to produce approximately 20 mg/L each of Hexadecane and Stearic acid. Perform extraction following the procedures described above.
- 4) Perform extractions of different concentration of Hexadecane and Stearic acid in 1L of standard.

The results are listed in Table F-1 below.

Table F-1: Actual recovery values of different concentration Hexadecane and Stearic acid in 1 L of standard.

Concentration of Hexadecane & stearic acid (mg/L)	Amount of O&G recovered per litre of standard (mg)
40	7.6
30	5.8
20	3.8
15	3.3
10	2.3
0	0.2

The results are plotted in Figure F-1 below. The regression from this calibration plot was used to determine all hexane extractible oil and grease data reported in this study.

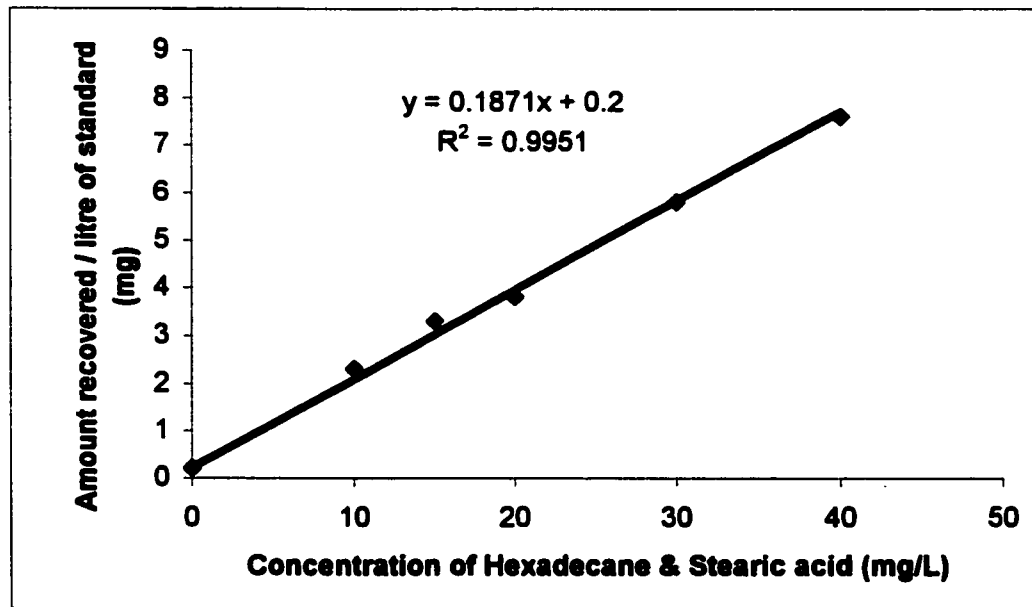


Figure F-1: Calibration curve of n-Hexane liquid-liquid extraction for the determination of oil and grease.